STARDEX

STAtistical and Regional dynamical Downscaling of EXtremes for European regions

EVK2-CT-2001-00115

Deliverable D10

Recommendations on the best predictor variables for extreme events.

FOREWORD

The STARDEX project on STAtistical and Regional dynamical Downscaling of Extremes for European regions is a research project supported by the European Commission under the Fifth Framework Programme and contributing to the implementation of the Key Action "global change, climate and biodiversity" within the Environment, Energy and Sustainable Development.

STARDEX will provide a rigorous and systematic inter-comparison and evaluation of statistical and dynamical downscaling methods for the construction of scenarios of extremes. The more robust techniques will be identified and used to produce future scenarios of extremes for European case-study regions for the end of the 21st century. These will help to address the vital question as to whether extremes will occur more frequently in the future.

For more information about STARDEX, contact the project co-ordinator Clare Goodess (c.goodess@uea.ac.uk) or visit the STARDEX web site:
http://www.cru.uea.ac.uk/projects/stardex/

STARDEX is part of a co-operative cluster of projects exploring future changes in extreme events in response to global warming. The other members of the cluster are MICE and PRUDENCE. This research is highly relevant to current climate related problems in Europe. More information about this cluster of projects is available through the MPS Portal:
http://www.cru.uea.ac.uk/projects/mps/

STARDEX is organised into five workpackages including Workpackage 2 on 'Observational analysis of changes in extremes, their causes and impacts' which was responsible for the production of this deliverable (D9). Workpackage 2 is co-ordinated by András Bárdossy from the Institut für Wasserbau, University of Stuttgart, Germany.

STARDEX PROJECT MEMBERS

UEA	University of East Anglia, UK
KCL	King's College London, UK
FIC	Fundación para la Investigación del Clima, Spain
UNIBE	University of Berne, Switzerland
CNRS	Centre National de la Recherche Scientifique, France
ARPA-SMR	Servizio Meteorologico Regionale, ARPA-SMR Emilia-Romagna, Italy
ADGB	University of Bologna, Italy
DMI	Danish Meteorological Institute, Denmark
ETH	Swiss Federal Institute of Technology, Switzerland
FTS	Fachhochschule Stuttgart – Hochschule für Technik, Germany
USTUTT-IWS	Institut für Wasserbau, Germany
AUTH	University of Thessaloniki, Greece

D10 AUTHORS AND VERSION HISTORY

Lead author:
Panagiotis Maheras, AUTH

Contributing authors:
Christina Anagnostopoulou, AUTH
Konstantia Tolika, AUTH

Final Version: 3 November 2003

CONTENTS

1. Introduction

The frequency and intensity increase of drier conditions over the Greek area during the last twenty years might be related to the dominance of the anticyclonic circulation during the same time period, due to mainly increased atmospheric geopotential heights and decreased cyclone activity over the Greek region (Maheras and Anagnostopoulou, 2003). Concerning temperature, local warming trends observed in some specific cases have been related to urban heat island effects (Bartzokas and Metaxas, 1995; Xoplaki et al., 2002) and in a few cases, changes in the large scale circulation have been invoked to explain winter and summer air temperature trends. For instance, the cooling during the last twenty years has been attributed to the local circulation changes, which favor stronger and more frequent northerly winds in the Aegean region (Bartzokas and Metaxas 1991) or to the increase of the northerly meridional circulation (Kutiel and Maheras 1995), resulting from the frequency increase of anticyclonic continental circulation types (Arseni – Papadimitriou et al., 2000). In spite of these attempts, more work should be done on large, regional and local scale circulation variability that affects Greek climate in order to understand precipitation and temperature variability and trends of extreme events in this area.

The objective of this study is to analyze and to recommend the best predictor variables related to extreme events in Greek area.

2. Data and Method

The following data sets have been used in this study:

- Gridded (2.5x2.5 latitude – longitude resolution) SLP data as well as geopotential heights at different levels (1000hPa, 850hPa, 700hPa, 500hPa and 300hPa) taken from the NCEP/NCAR reanalysis data sets (Kalnay et al., 1996).
- Daily, monthly and seasonal values were computed from the 6-hourly data for the specific area used in this area bounded by latitudes 20^o to 65^o N and longitudes 20o W to 50^o E.
- Thickness fields for the layers 300-500hPa, 500-700hPa, 1000-700hPa and 500-1000hPa were derived from the corresponding geopotential height data.
- Two daily catalogues of 20 (SLP) and 14 (500hPa) circulation types were constructed for the period 1958-2000 using gridded NCEP reanalysis SLP and 500hPa geopotential data.The classification scheme is based on automatic classification using spatial methods of geometry and topology (Maheras et al., 2000). It has already been demonstrated that each of the 20 (SLP) and 14 (500hPa) circulation types has a characteristic underlying synoptic pattern and produces the expected type and direction flow over Greece (Maheras et al., 2000). Mean yearly and seasonal circulation type frequencies for the two catalogues and the corresponding trend (positive or negative) are shown in figures 1 and 2.

In order to investigate the dry or wet character of the circulation types, the ratio (PROPct/PROPtot) has been computed (Goodess and Jones, 2002). The mean percentage precipitation total for each circulation type with reference to the annual and seasonal precipitation total has also been calculated over the study period, as well as the mean annual and seasonal anomalies of the minimum and maximum temperatures.

Within the context of our study, the underlined questions are: a) Does the relationship between the circulation types and the precipitation or the temperature remain constant or change with time? and b) If such changes are observed, can they be correlated to the change of the circulation type frequency or can be the result of the changes of the interior relationship between the weather circulation and climate? To investigate this relationship, the trends of the precipitation amount and frequency, the minimum and maximum temperatures for every station and for every circulation type have been computed. The results of these computations are shown in figures.

Previous studies have shown (Xoplaki et al., 2002) that for the prediction of the temperature fields in summer and precipitation fields in winter for the Mediterranean region, the thickness field 1000-700hPa has given the best results for temperature and the geopotential fields of 700hPa and 500hPa for precipitation. In order to find the best predictor fields for precipitation and temperature, the mean correlation coefficients of every station have been calculated between the minimum and maximum temperature as well as the precipitation and the geopotential height fields (original and thickness). Useful comparative results can be derived from tables (1-3) indicating the maximum values of the positive and negative correlation coefficients

3. Results

The anticyclonic circulation types show statistically significant positive trends for the classification of the 500hPa (figure1). On the contrary, the cyclonic types of the same classification present negative trends. The circulation types for the classification of the SLP (figure 2) are characterized by similar behavior (positive trends for the anticyclonic types and negative trends for the cyclonic ones). A very important fact is the positive trend of the MB_2 circulation type (shallow anticyclonic field).

The wettest circulation types are the cyclonic C, Csw, Cs, Cnw Cne and the Cw (figure 3, 5) for the 500hPa classification. On the other hand, for the SLP classification (figure4, 6), type Mt2 can be added in winter and type Dor in summer. All the other types (the anticyclonic, the MB and Cse, Cn, Dsec and Mt1) present a very small percentage of precipitation amounts.

Some of the cyclonic circulation types exhibit scattered statistical significant positive and negative trends, on annual and seasonal basis (figure 7), in their relationship with the amount and the frequency of precipitation. Characteristically, the stations that present positive trend of precipitation or absence of it in some indices, related to extreme precipitation, such as prec90p, 644R5d, 646SDII, 691R90T, appear to have also positive trends of the amount of precipitation in some of the circulation types. For example, Athens (Csw), Naxos (Csw, Cne), Larissa (Csw), Milos (C). Stations that show negative trends for the above indices, present also negative trends and in the amount of precipitation with some of the circulation types, such as Skyros (C, Cs in the case of the year), Rhodes (Csw in the case of winter), Samos (Csw, Cnw, Cne, Cw) etc. Similar results are deduced for the circulation types of the SLP classification (figure 8).

The circulation types (500hPa classification, figure 9) show a different behavior in their relations with the minimum temperature, according to the station and the season. Regularly, during winter period the first four anticyclonic circulation types form negative anomalies of the minimum temperatures, while the other two show positive ones. Positive anomalies are also presented by the cyclonic types C, Csw, Cnw and Cw. The rest of the cyclonic types present negative deviations. During the other seasons almost all anticyclonic types are associated with positive anomalies (the A1 circulation type differs from one station to the other). On the contrary, all cyclonic types, in their total, are characterized by negative anomalies.

The trends of minimum temperature in relation to the circulation types (500hPa) vary from station to station and from season to season (figure 9). In winter for example, most of the stations present negative trend for most of the circulation types. The minimum temperature for the stations of Ierapetra, Naxos and Rhodes tend to increase for the specific circulation types A2, A3, A4, A5 and C. The minimum temperature decreases for the other seasons particularly for the cyclonic types, except for the stations Naxos, Kythira, Samos that occur positive trends for anticyclonic types.

The circulation types SLP (figure 10) show a better behavior in their relationships with the minimum temperatures. Almost all stations present negative anomalies for all seasons for the first 5 anticyclonic types and for the mixed ones (Mt1 and Mt2). On the other hand, these anomalies are positive for all the stations concerning the types A6 and Dsec. The rest of the types vary from station to station and from season to season. The trends of the minimum temperature with the circulation types SLP (figure 10) present significant variability, similarly to the 500hPa classification types.

However, it is possible to form a rule:

In general there are more positive trends than negative during year, while some stations present only positive (Kerkyra) or negative trends (Samos).

The maximum temperatures in their relationships with the circulation types (500hPa) show a more stable behavior (figure 11). The anticyclonic types present positive anomalies while the cyclonic ones negative anomalies almost for all the stations and for all the seasons, except winter. During winter, the circulation types Cw and Cnw present positive anomalies for some stations such as Chania, Alexandroupoli, Herakleio.

Generally, the maximum temperatures form negative trends in winter, spring and autumn (except for the stations of Athens and Chania where their trends are positive). During summer, most of the stations exhibit positive trends for all circulation types, except of Cse, Cn, Cw whose trends are negative.

For the classification of SLP (figure 12) maximum temperatures seem to differ from those of the 500hPa classification. In almost all of the stations and for all seasons, the first three anticyclonic circulation types that can be characterized as cold (Maheras et al., 2000) show negative anomalies whilst the next three anticyclonic types show positive ones. The cyclonic types behavior varies from station to station and from season to season, whereas in summer the circulation types appear to have negative anomalies. The mixed types form comparatively intense negative anomalies and the characteristic types positive anomalies.

With respect to the statistically significant trends of the maximum temperatures, negative trends during winter, spring and autumn seem to be predominant. On the contrary, during summer positive trends are found for almost all stations, except some of the stations in the southern Greek area (Ierapetra, Rhodes, Herakleio, Samos), which show negative trends for the types C, Cnw, Dsec and MB2.

The mean maximum correlation coefficients (maximum positive and negative) between the SLP or geopotential and thickness fields and the seasonal precipitation or minimum and maximum temperature, are summarized in tables 1 to 3. According to table 1, the negative correlation coefficients of precipitation in the case of the year are higher, in absolute value, than the positive ones. The SLP and the 1000hPa field present the greatest absolute values followed by the 500hPa and 300hPa geopotential field and the 1000-700hPa-thickness field. On the contrary, in winter, the greatest absolute values occur in the 700hPa (-0.66), followed by the 500hPa (-0.65), 850hPa, 1000hPa and SLP. During spring, the highest absolute values can be found in 300hPa (-0.55), 500hPa (-0.54) and 700hPa (-0.51). In summer, the condition differentiates. The thickness field 700-500hPa (-0.47) and 1000-500hPa (-0.46) show the greatest absolute negative values of the correlation coefficients. Finally, autumn appears to be characterized by lower values of the correlation coefficient in comparison to the other seasons. Higher coefficients form from the 1000hPa and SLP field (-0.31).

The mean maximum correlation coefficients for the minimum temperatures (table 2) are in absolute value greater than those of the precipitation Without exception, for all seasons, the greatest values of the positive correlation coefficients form from the 1000-700hPa, 1000-500hPa and 700-500hPa thickness field. In autumn and winter, the correlation coefficients show the highest values 0.73(1000-700hPa) and 0.72(1000-700hPa) respectively. Finally, maximum temperature presents greater correlation coefficients (table 3) as compared to minimum temperature. As discussed above, the greatest positive correlation coefficients occur in the 1000-700hPa (0.79 in spring and autumn) and 1000-500hPa thickness fields.

4. Summary and conclusions

The increasing frequency of the anticyclonic circulation types (significant positive trends) combined with the decreasing frequency of the cyclonic types (significant negative trends) can explain the positive trend of the 641CDD index (maximum number of consecutive dry days). The negative trends of the rest of the indices (prec90p, 644R5d, 646SDII, 691R90T and 692R90N) that occur mainly in western and northern Greece can be explained by the decrease of the frequency of the circulation type C and Csw as well as by their negative trends in relation to precipitation in some stations. It is evident that, the extreme rainfall can be attributed mainly to the prevalence of the cyclonic types C and Csw, as well as to the Cs and Mt2 in southern Greece. Comparing the results of the two classifications it seems that the classification of 500hPa is the most skillful predictor in the case of the of extreme rainfall indices.

The decreasing trend of the minimum temperatures in central and southwestern Greek area can be interpreted by the increasing frequency of the cold anticyclonic types of SLP (A1, A2, A3). Similarly, the positive trend of the annual frost days in some continental stations can be explained. It seems that the classification of the SLP is the most skillful predictor for the extreme indices of minimum temperature.

The increase of the frequency of the anticyclonic types, which form positive anomalies, and the positive trends of the most circulation types in the majority of the stations can explain the increasing maximum summer temperatures. The 500hPa classification is a more skillful predictor that the SLP classification.

Finally, concerning geopotential heights and thickness predictors, it appears that the most skillful predictors for precipitation are 500hPa and 300hPa geopotential fields along with SLP, whilst for the minimum and maximum temperature are the 1000-700hPa and 1000-500hPa thickness fields.

5. Referencies:

Arseni – Papadimitriou A, Maheras P, Patrikas I, Anagnostopoulou Chr, 2000: Distribution Géographique des témperatures maximales par type de circulation et leurs tendances, en Grèce. Publication de l'AIC, 13, 347-355.

Bartzokas A and Metaxas D, 1991: Climatic fluctuation of temperature and air circulation in the Mediterranean. Environment and quality of life, Climate and global change. Proc European Scholl of Climatology and Natural Hazards course, France 279-297.

Bartzokas A, Lolis C and Metaxas D, 1995: Factor analysis of some climatological elements in Athens, 1931-1992. *Theor and Appl Climatology*, 52, 195-205.

Goodess C M , Jones P D, 2002: Links between circulation and changes in the characteristics of Iberian Rainfall. *Int. J. Climatol*, 22, 1593-1615.

Kalnay E, Kanamitsou M, Kistler R, Collins W, Deaven D, Gandin L, Irebell M, Saha W, White G, Woolen J, Zhu Y, Leetman A, Reynolds R, Chelliah M, Edisuzaki W, Huggins W, Janowiak J, Mo KC, Ropelewski C, Wang J, Jenne R, Joseph D, 1996: The NCEP/NCAR 40-year Reanalysis project. *Bulletin of American Meteorological Society,* 77, 437-471.

Kutiel H and Maheras , 1998: Variation in the temperature regime across the Mediterranean during the last century and their relationship with circulation indices. *Theor and Appl Climatology*, 61, 39-53.

Maheras P, Patrikas I, Karacostas Th and Anagnostopoulou Chr, 2000a: Automatic classification of circulation types in Greece: Methodology, Description, Frequency, Variability and Trend Analysis *Theor and Appl Climatology*, 65, 205-223.

Maheras P and Anagnostopoulou Chr, 2003: Circulation types and their influence on the interannual variability and Precipitation changes in Greece, *Mediterranean Climate,* Springer-Verlag Berlin Heidelberg, 215-239.

Xoplaki E, González-Rouco J F, Gyalistras D, Luterbacher J, Rickli R, Wanner H, 2003: Interannual summer air temperature variability over Greece and its connection to the large-scale atmospheric circulation and Meidterranean SSTs 1950-1999. *Climate Dynamics (2003) 20*: 537-554.

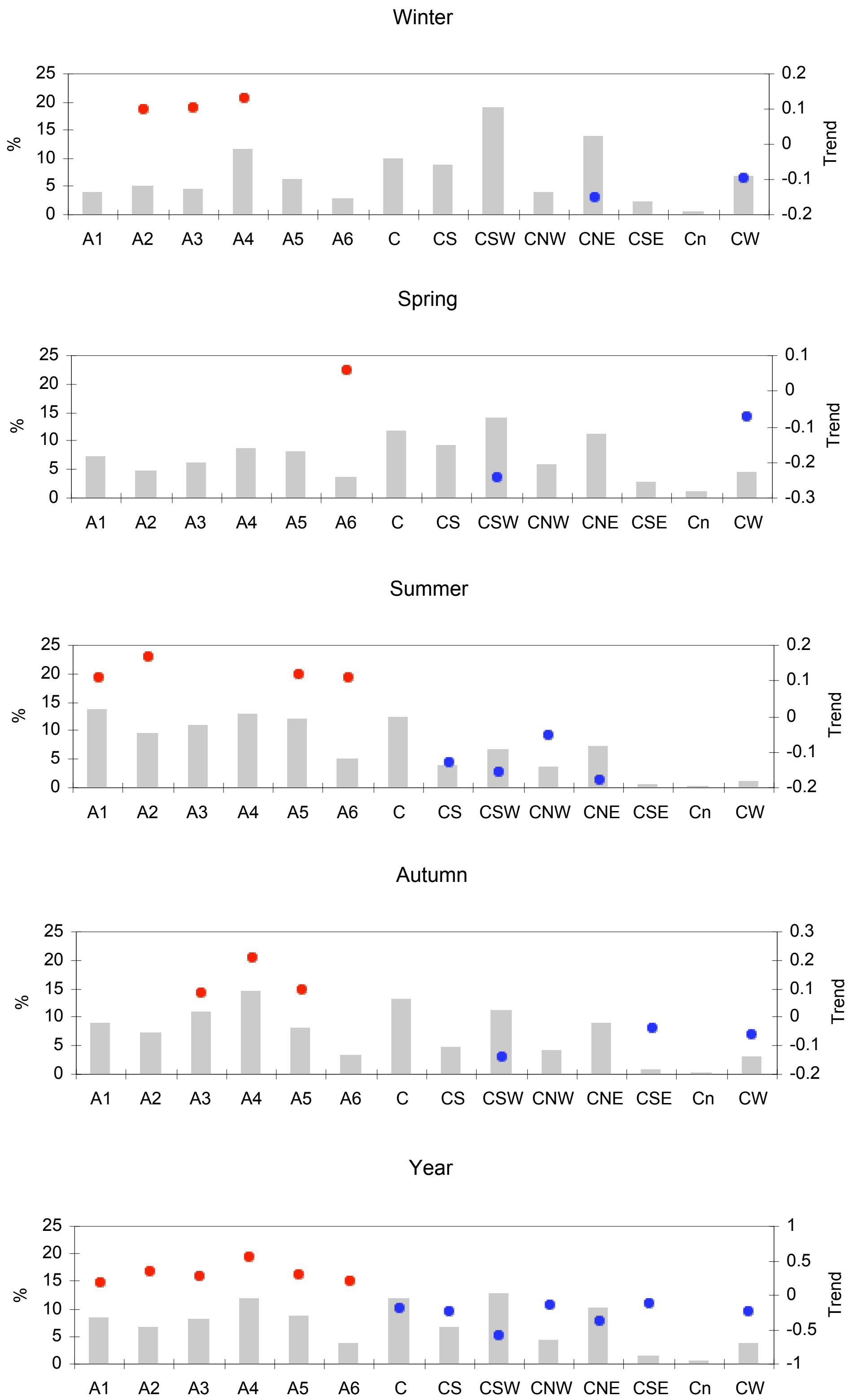

Figure 1: Trends (red circles positive and blue circles negative) and frequencies (bars) of the circulation types in the case of the 4 seasons and the year at 500hPa (1958-2000) Only the stat. signif. ones at a level 0.05 are marked

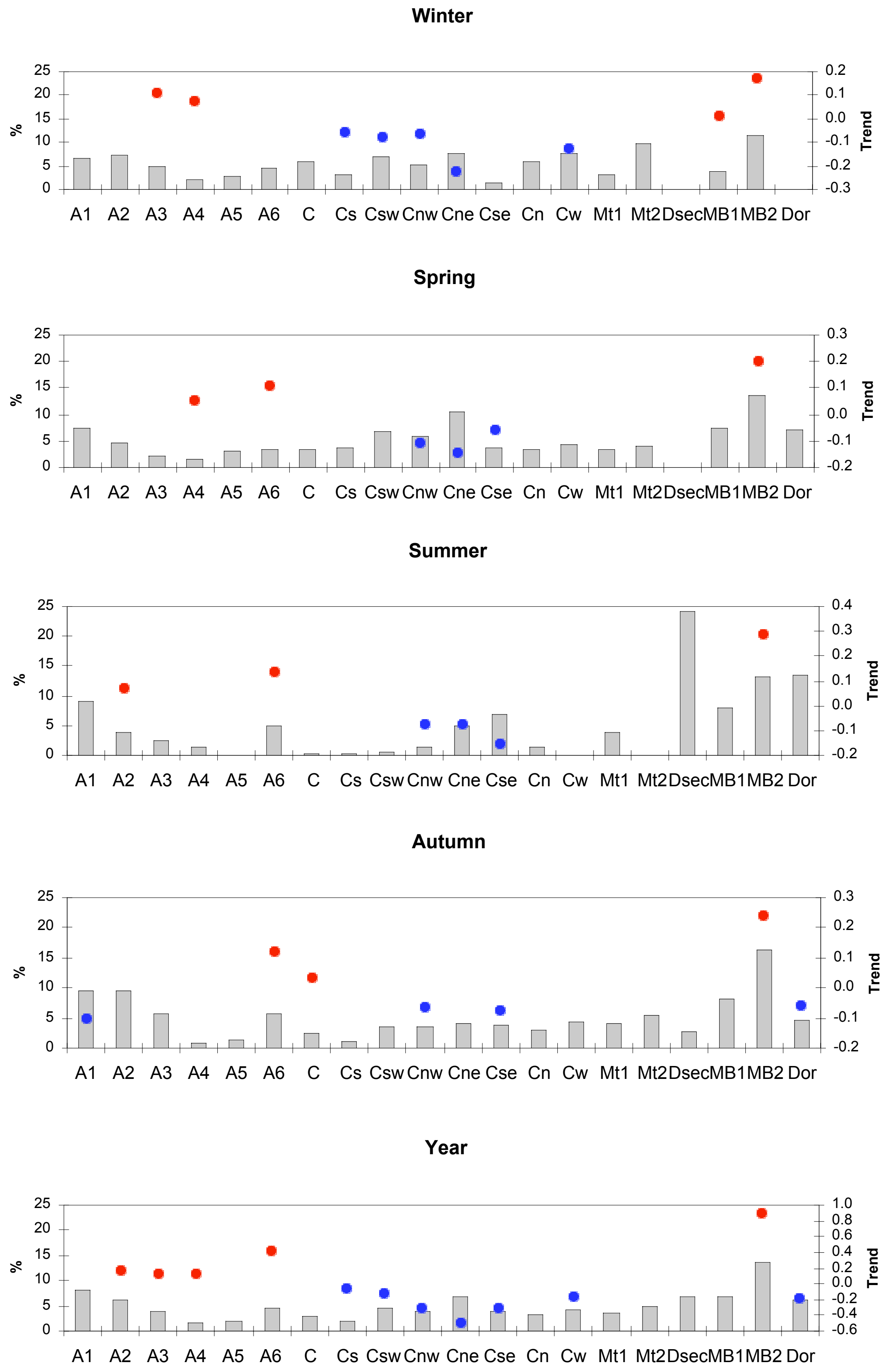

Figure 2: Trends (red circles positive and blue circles negative) and frequencies (bars) of the circulation types in the case of the 4 seasons and the year at SLP (1958-2000) Only the stat. signif. ones at a level 0.05 are marked

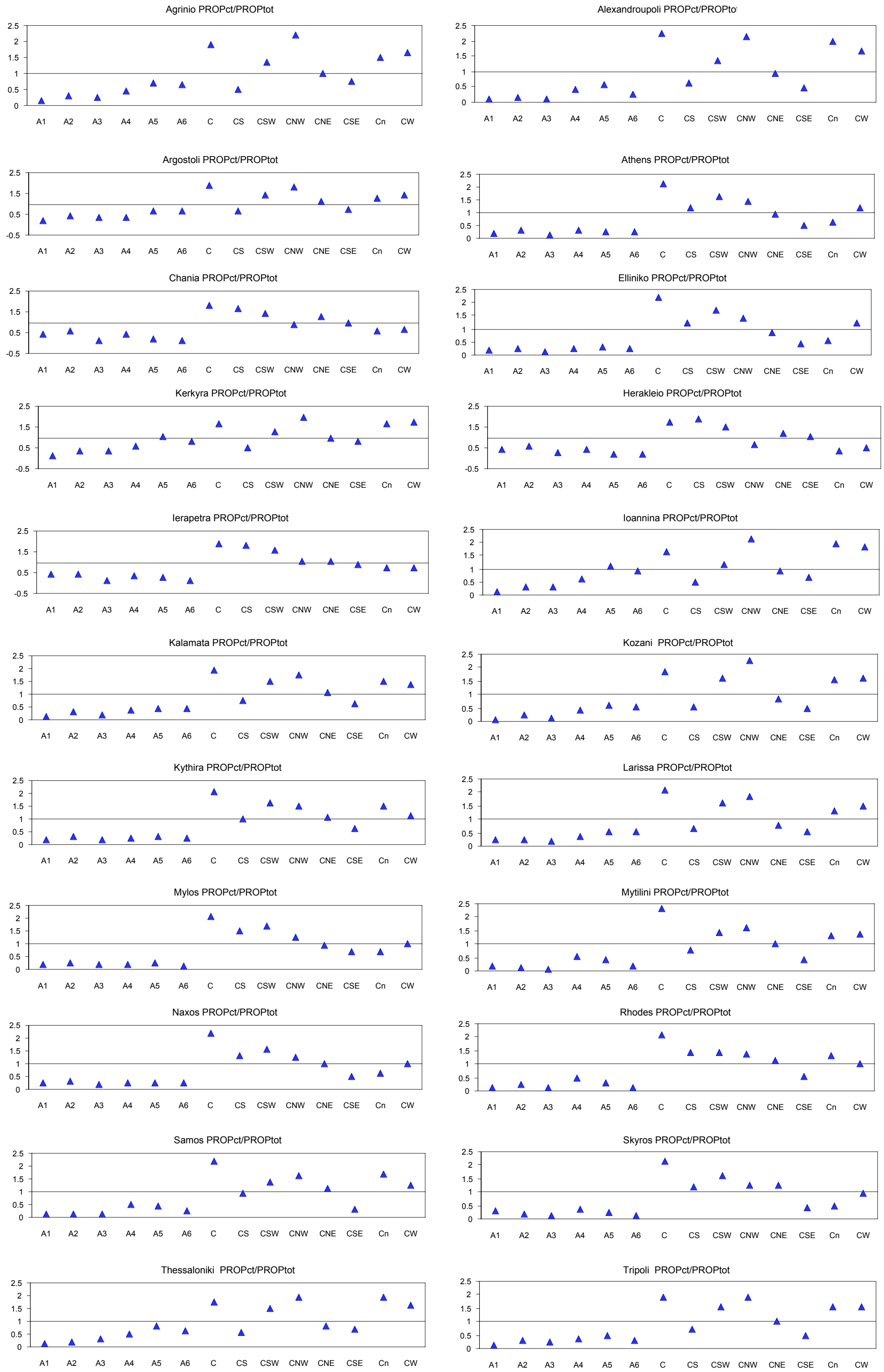

Figure 3a: Winter standardized ratios PROPct/PROPtot for the 14 circulation types and the 22 rainfall stations for the period 1958-2000 at 500hPa

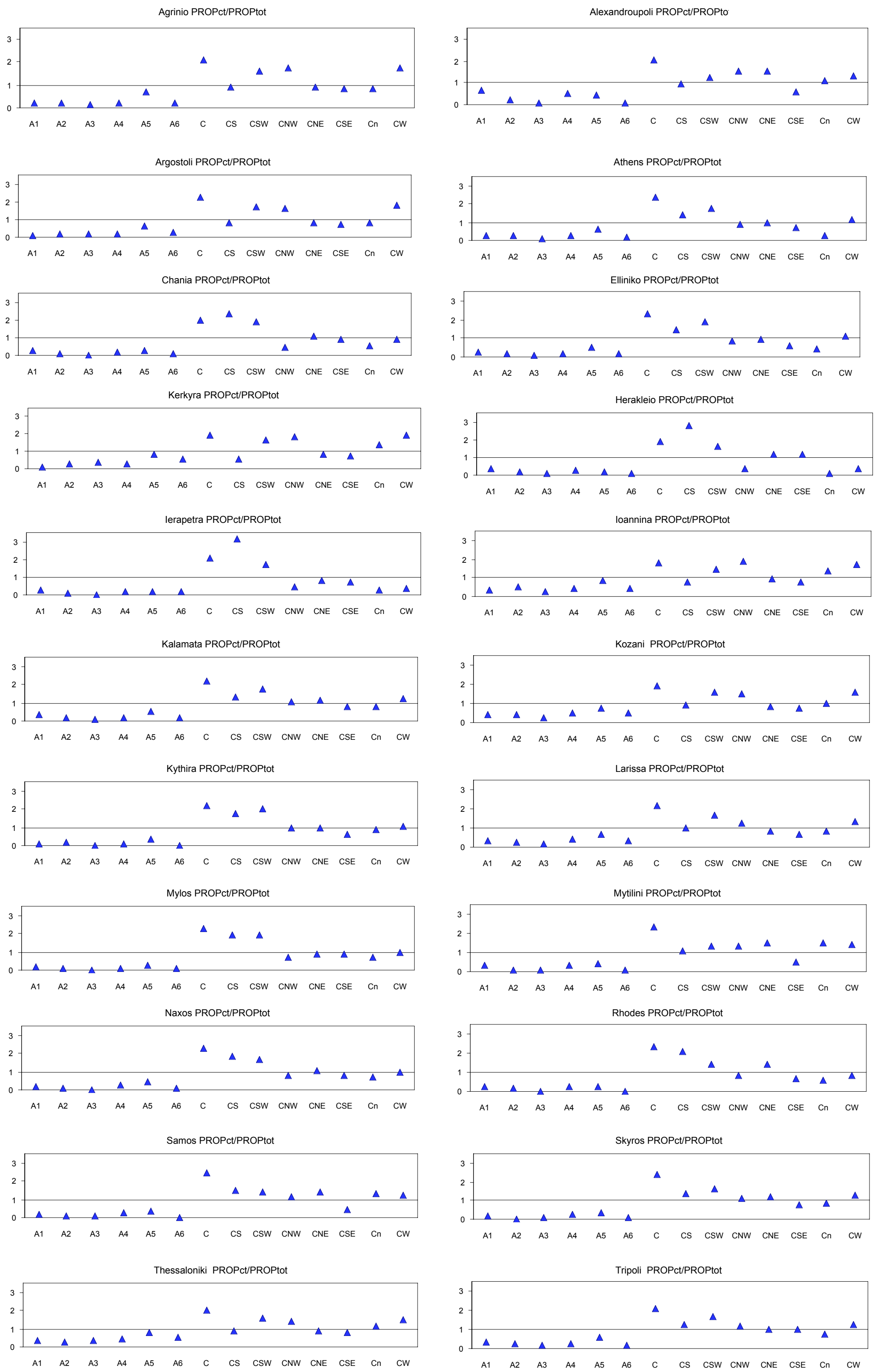

Figure 3b. Spring standardized ratios PROPct/PROPtot for the 14 circulation types and the 22 rainfall stations for the period 1958-2000 at 500hPa

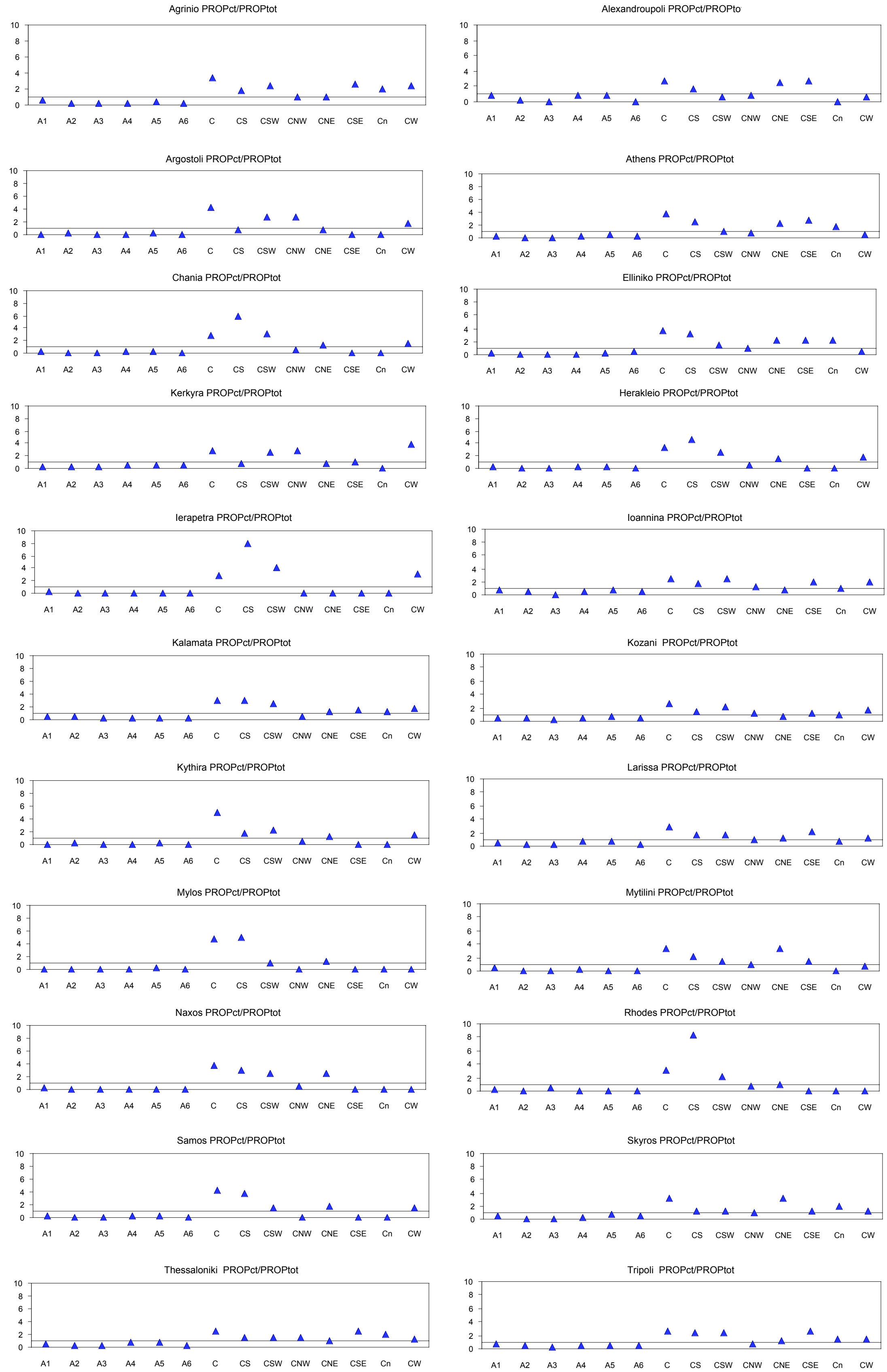

Figure 3c. Summer standardized ratios PROPct/PROPtot for the 14 circulation types and the 22 rainfall stations for the period 1958-2000 at 500hPa

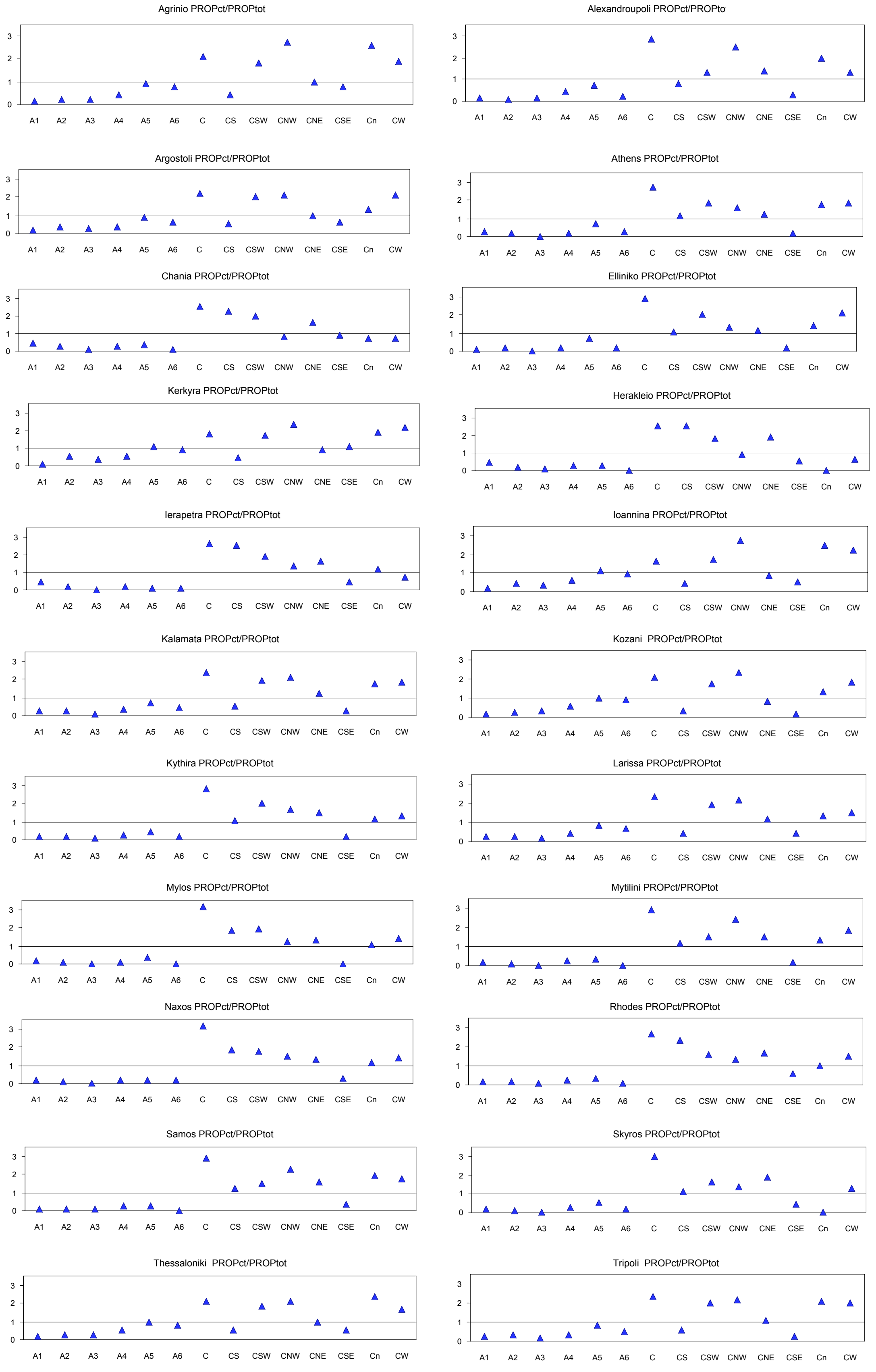

Figure 3d. Autumn standardized ratios PROPct/PROPtot for the 14 circulation types and the 22 rainfall stations for the period 1958-2000 at 500hPa

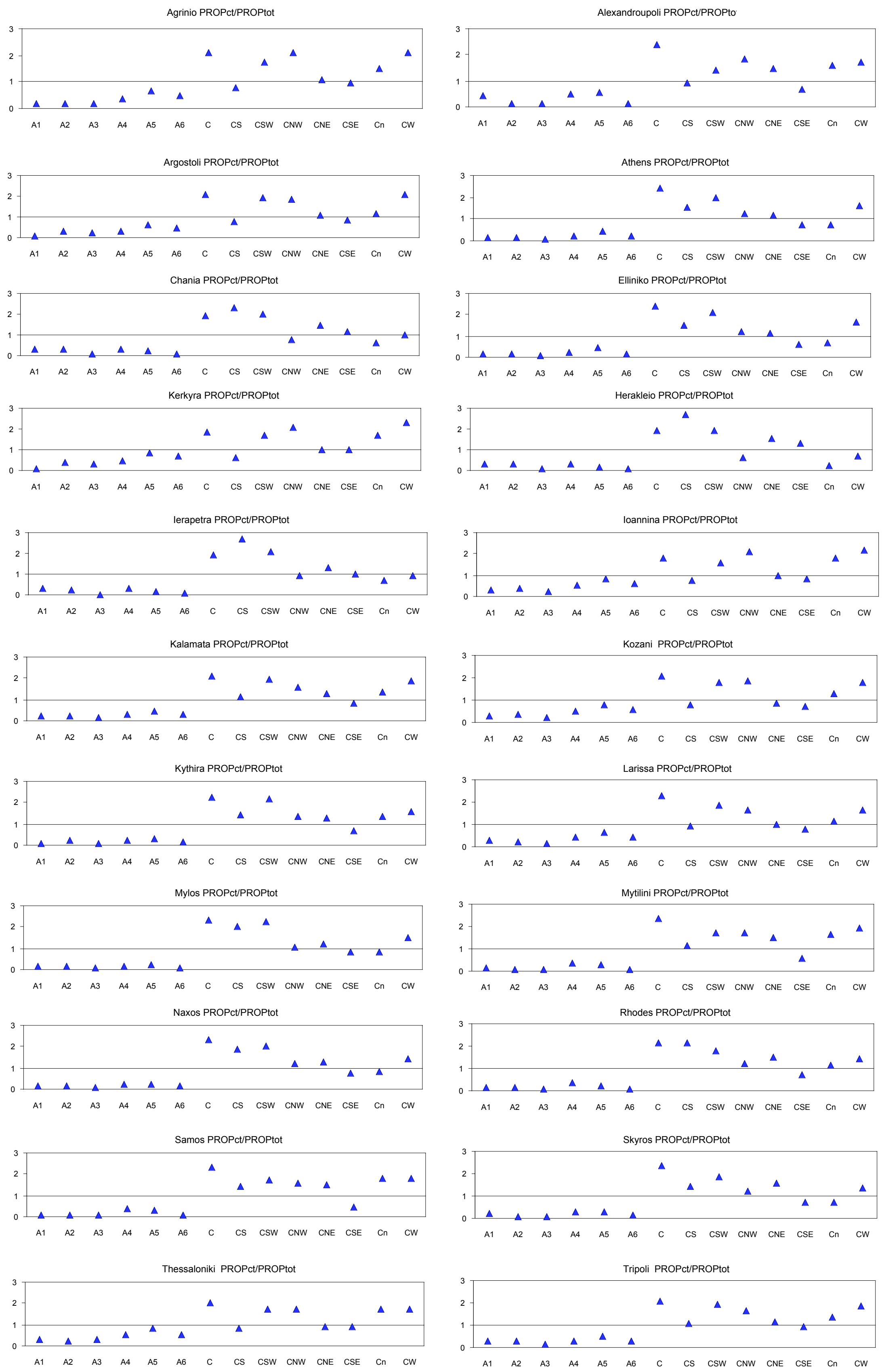

Figure 3e. Annual standardized ratios PROPct/PROPtot for the 14 circulation types and the 22 rainfall stations for the period 1958-2000 at 500hPa

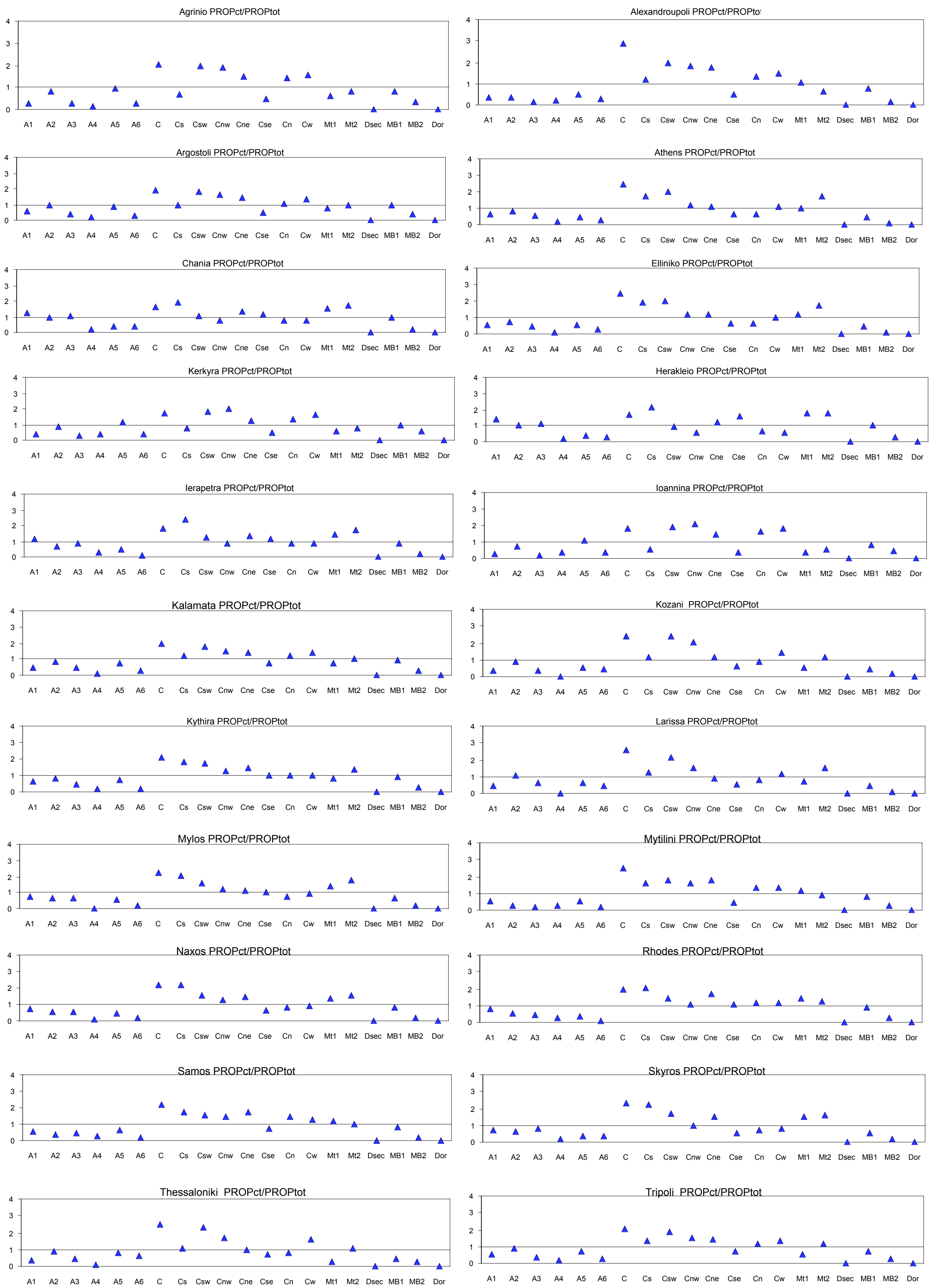

Figure 4a. Winter standardized ratios PROPct/PROPtot for the 20 circulation types and the 22 rainfall stations for the period 1958-2000 at SLP

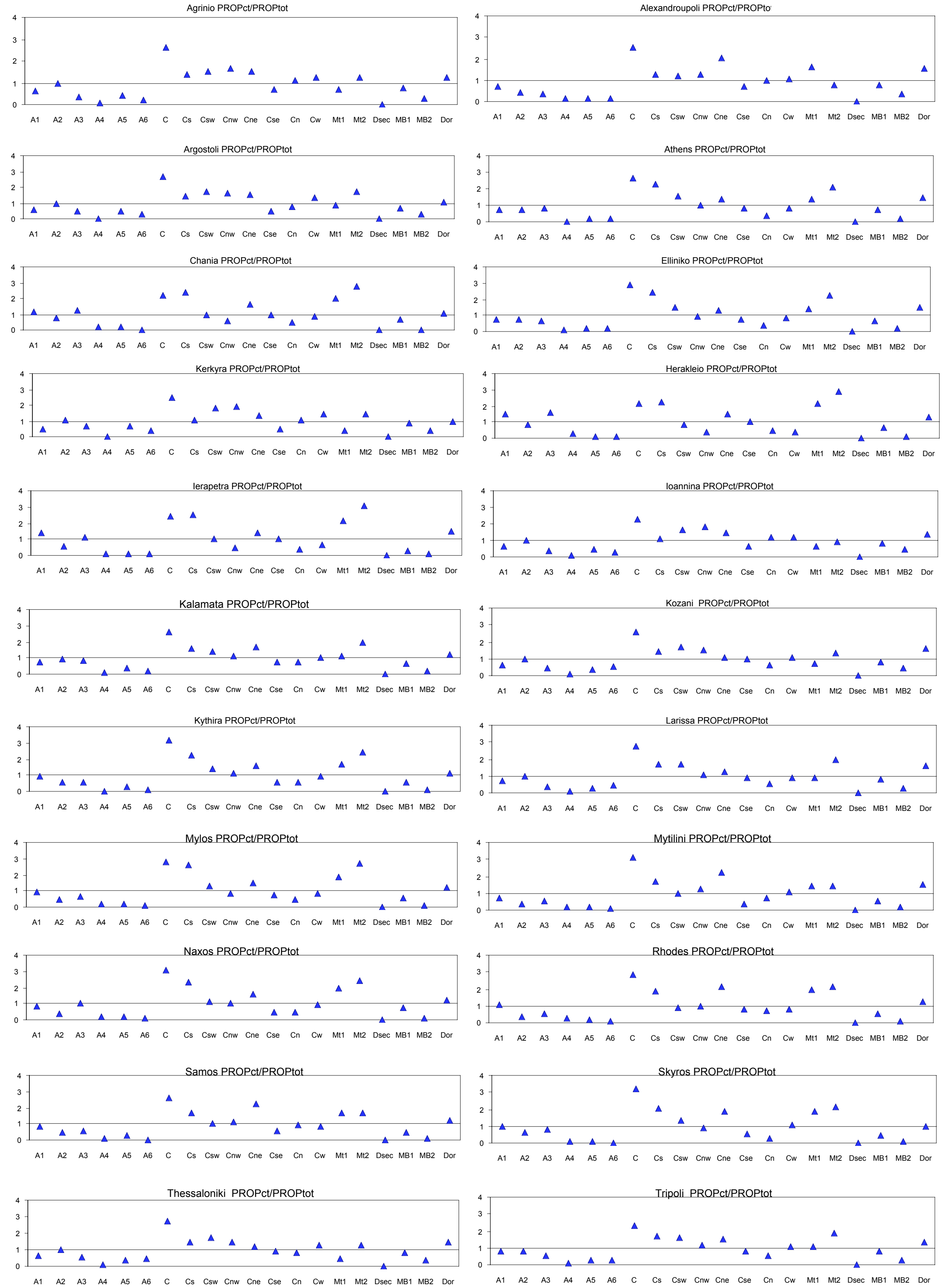

Figure 4b. Spring standardized ratios PROPct/PROPtot for the 20 circulation types and the 22 rainfall stations for the period 1958-2000 at SLP

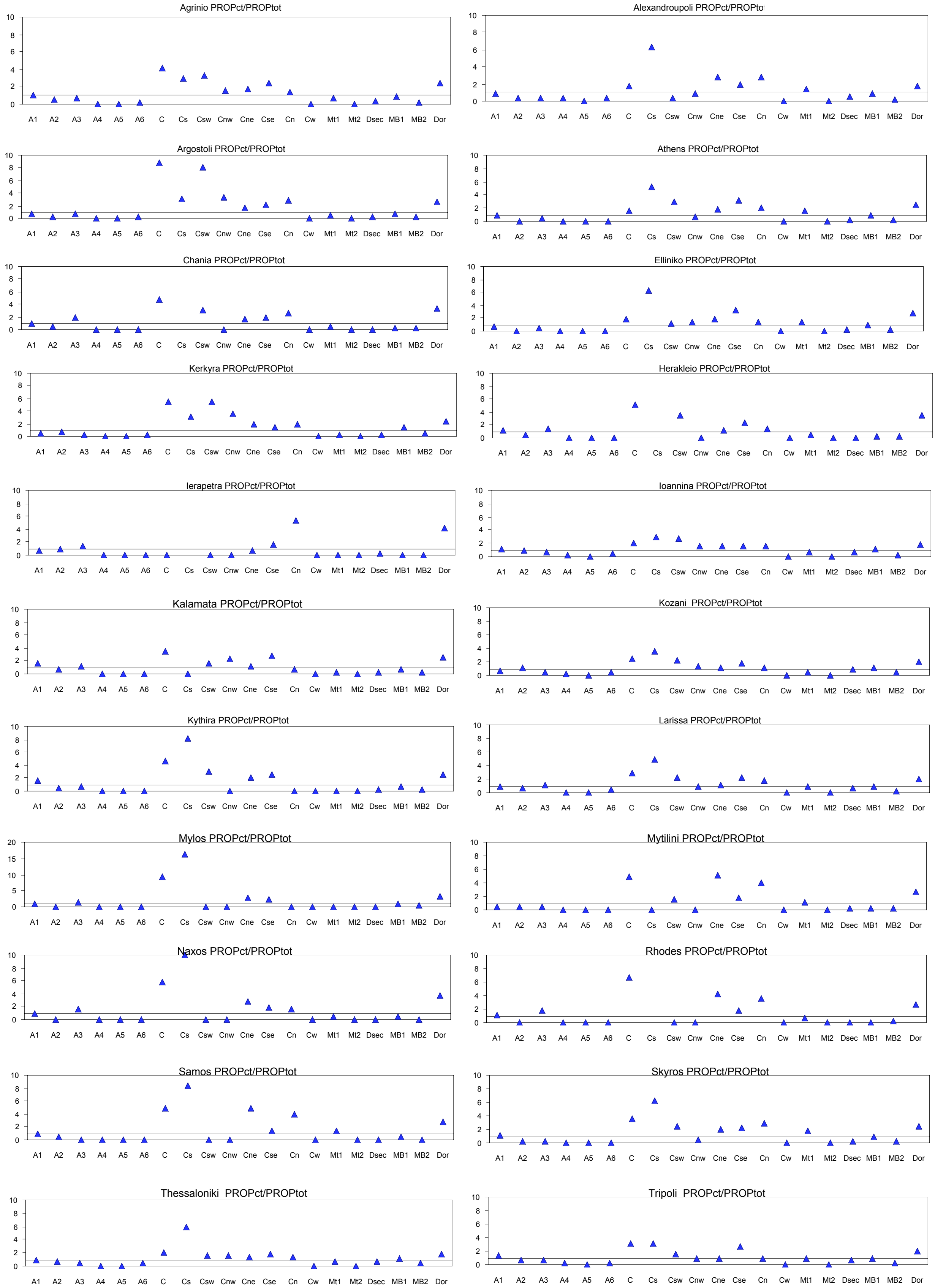

Figure 4c. Summer standardized ratios PROPct/PROPtot for the 20 circulation types and the 22 rainfall stations for the period 1958-2000 at SLP

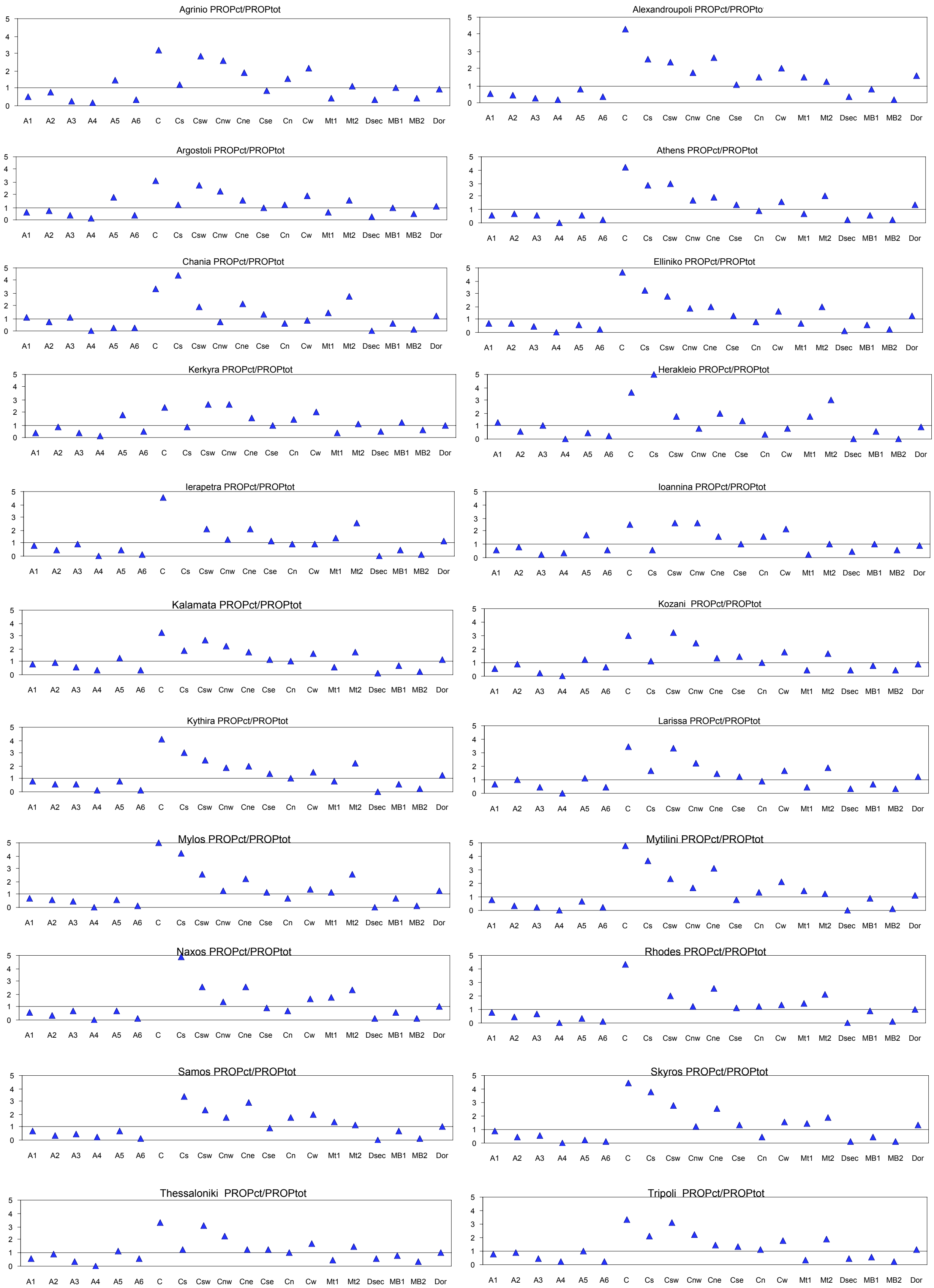

Figure 4d. Autumn standardized ratios PROPct/PROPtot for the 20 circulation types and the 22 rainfall stations for the period 1958-2000 at SLP

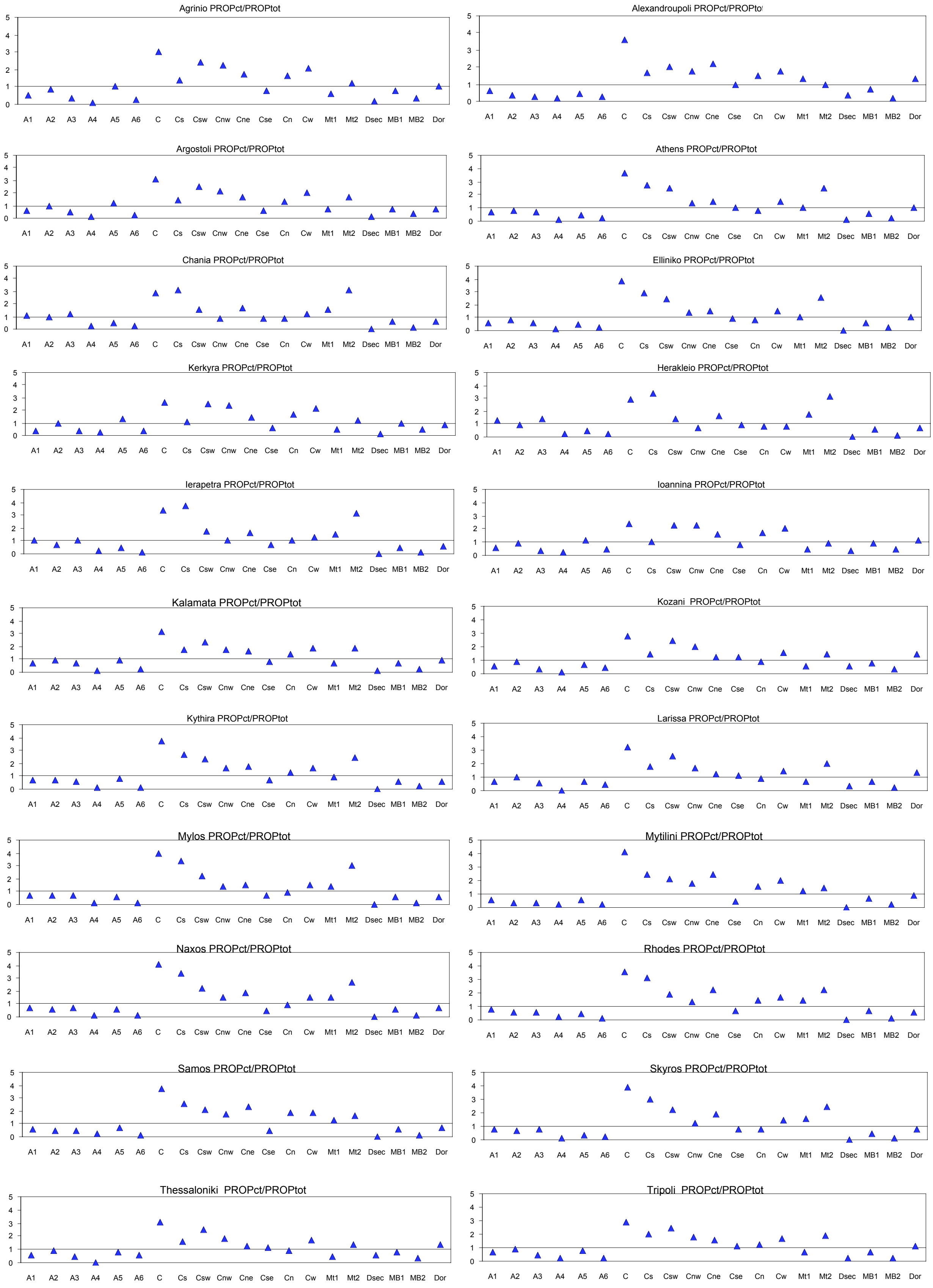

Figure 4e. Annual standardized ratios PROPct/PROPtot for the 20 circulation types and the 22 rainfall stations for the period 1958-2000 at SLP

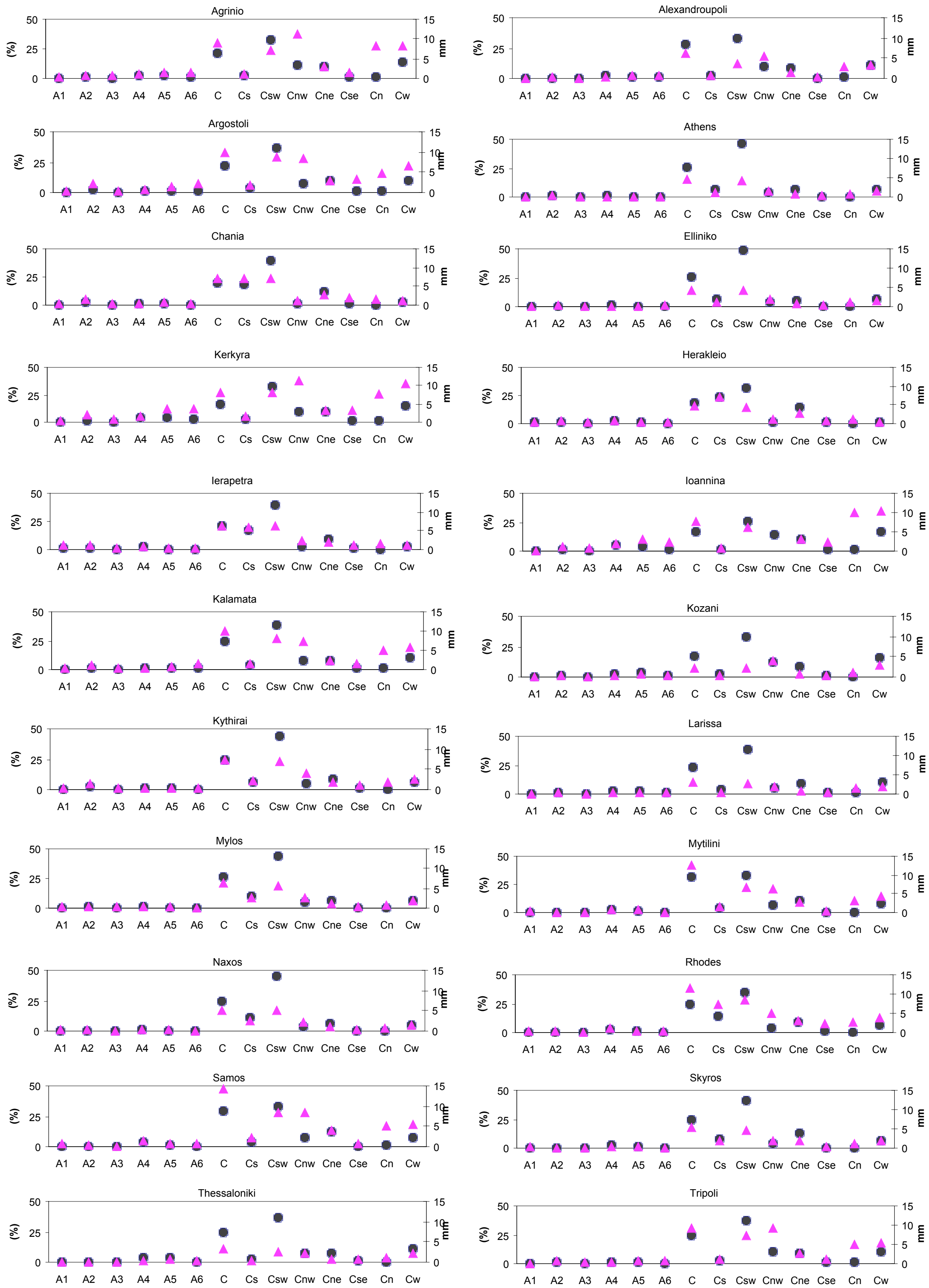

Figure 5a. Winter percentage (%) of precipitation amount (left axis, cycles) and winter standardized ratios PROPct/PROPtot for the 14 circulation types (500hPa) and the 22 rainfall stations (right axis, triangle)

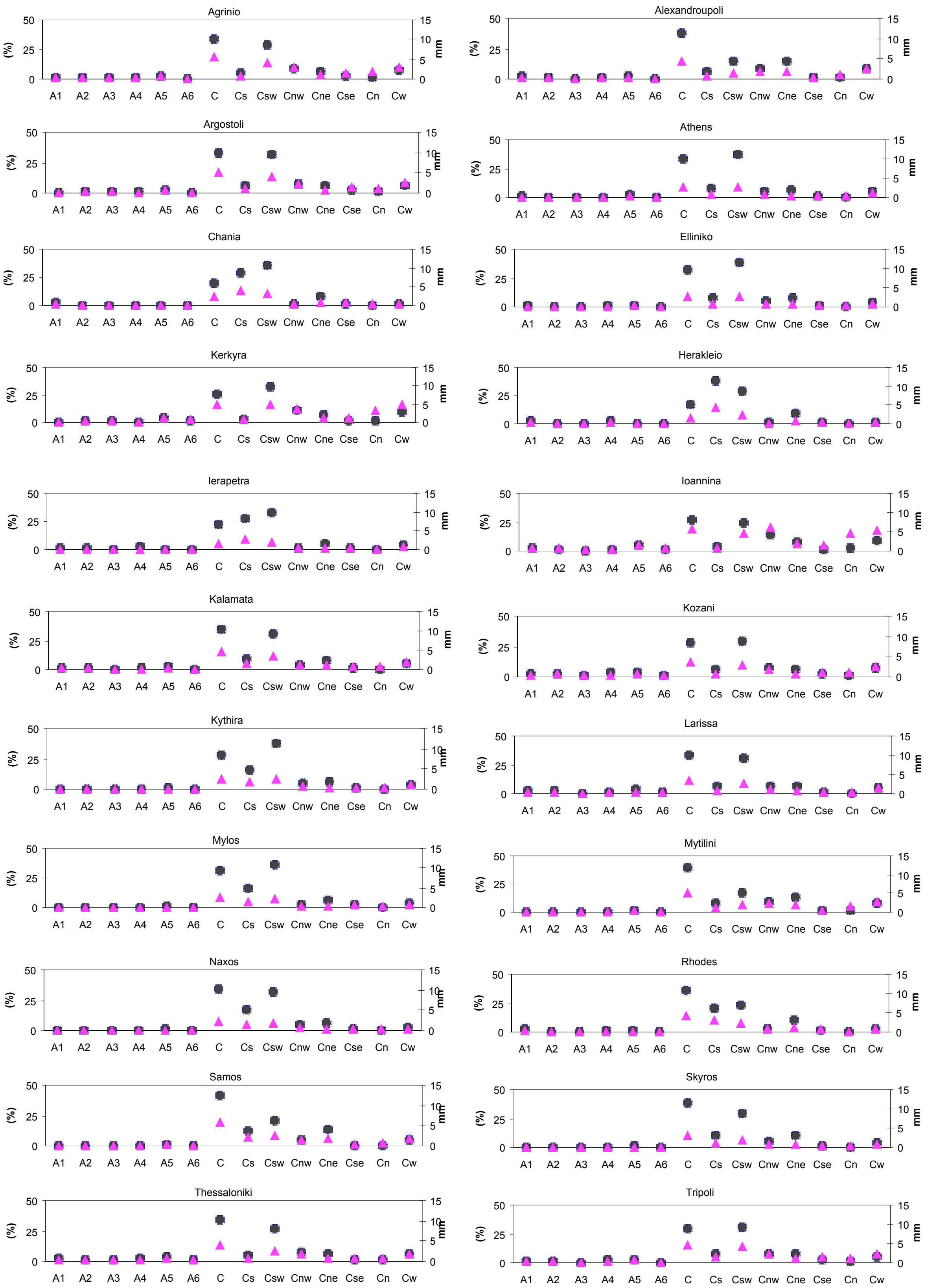

Figure 5b. Spring percentage (%) of precipitation amount (left axis, cycles) and spring standardized ratios PROPct/PROPtot for the 14 circulation types (500hPa) and the 22 rainfall stations (right axis, triangle)

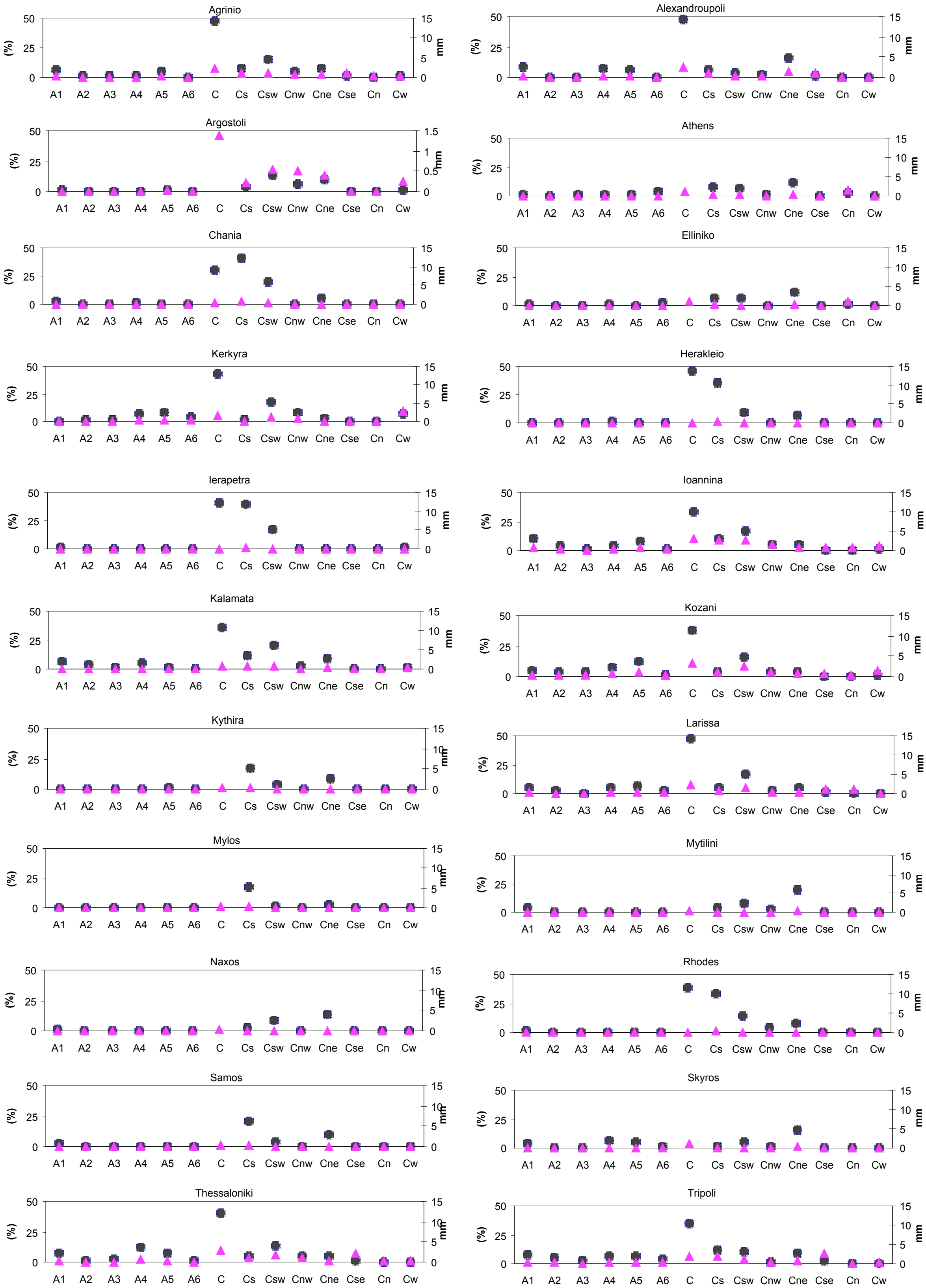

Figure 5c. Summer percentage (%) of precipitation amount (left axis, cycles) summer standardized ratios PROPct/PROPtot for the 14 circulation types (500hPa) and the 22 rainfall stations (right axis, triangle)

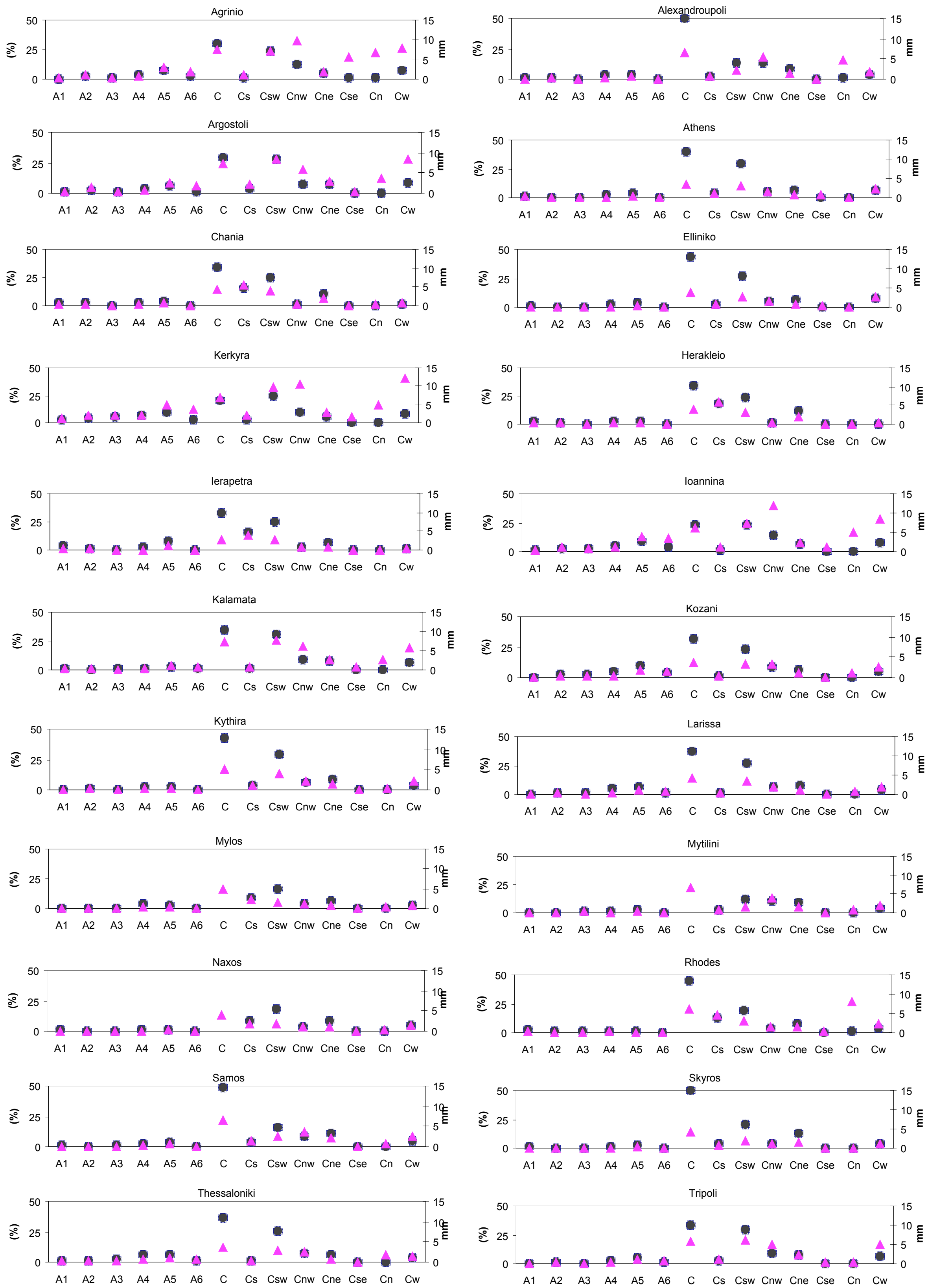

Figure 5d. Autumn percentage (%) of precipitation amount (left axis, cycles) and autumn standardized ratios PROPct/PROPtot for the 14 circulation types (500hPa) and the 22 rainfall stations (right axis, triangle)

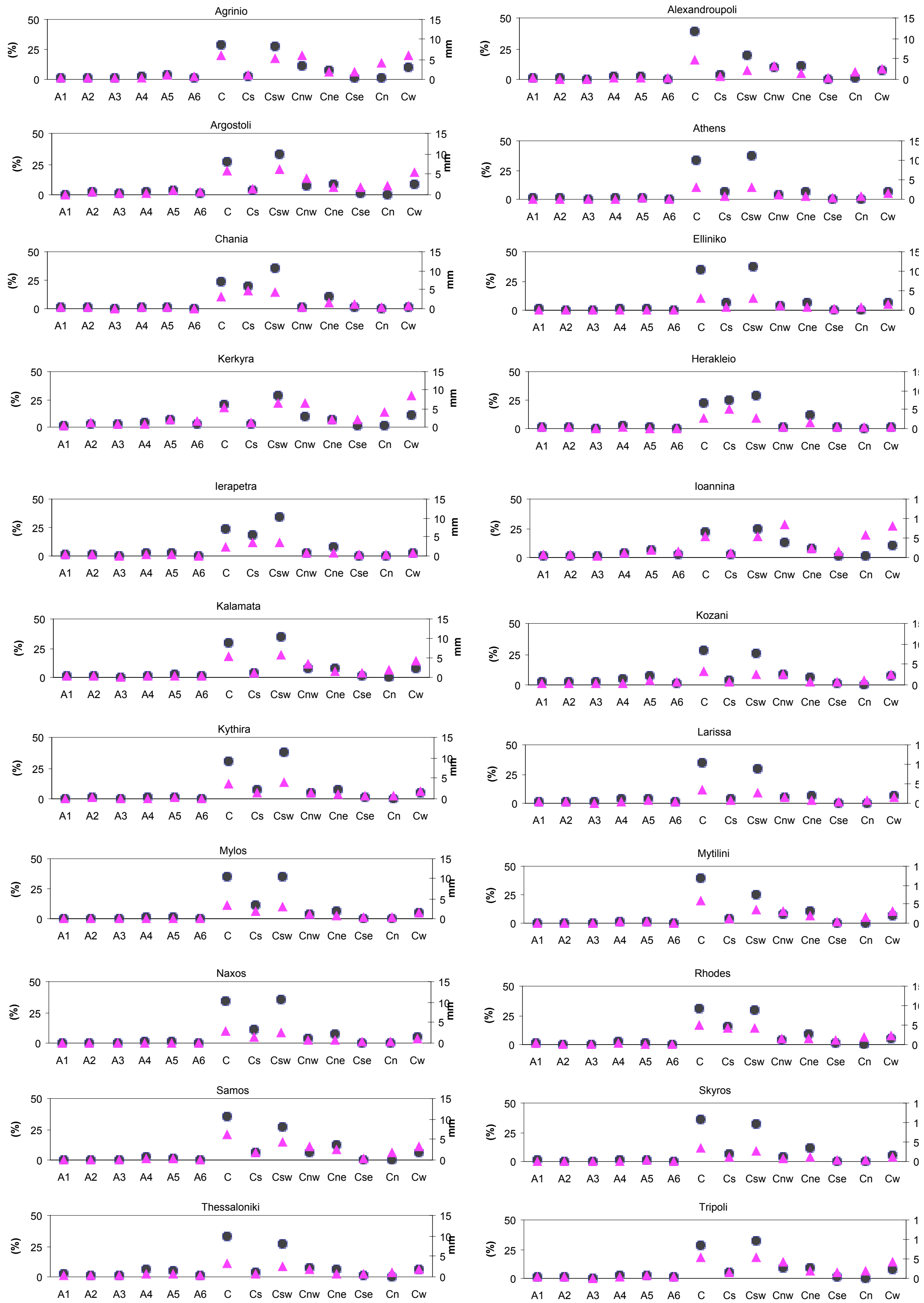

Figure 5e. Annual percentage (%) of precipitation amount (left axis, cycles) and annual standardized ratios PROPct/PROPtot for the 14 circulation types (500hPa) and the 22 rainfall stations (right axis, triangle)

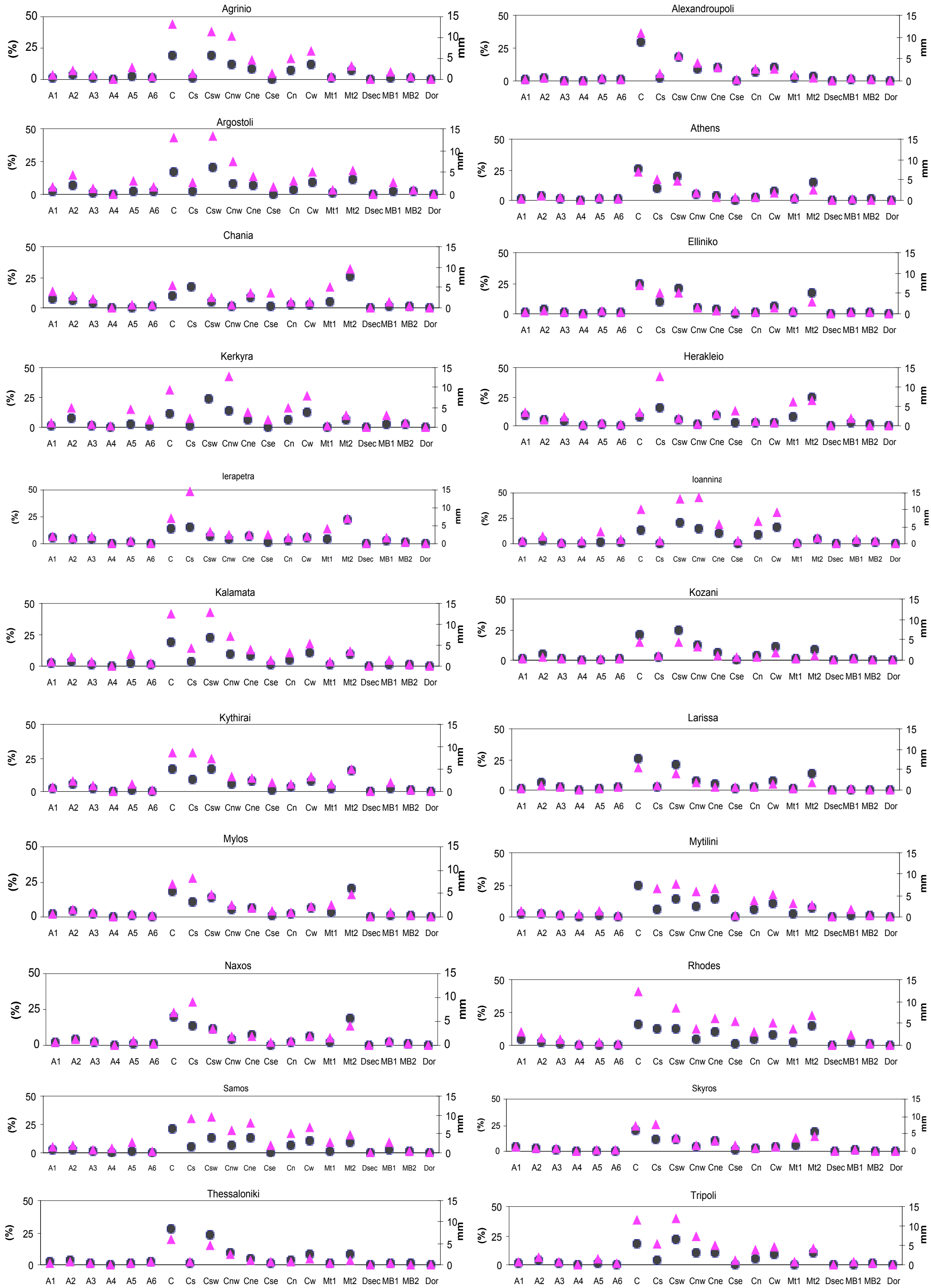

Figure 6a. Winter percentage (%) of precipitation amount (left axis, cycles) and winter standardized ratios PROPct/PROPtot for the 20 circulation types (SLP) and the 22 rainfall stations (right axis, triangle)

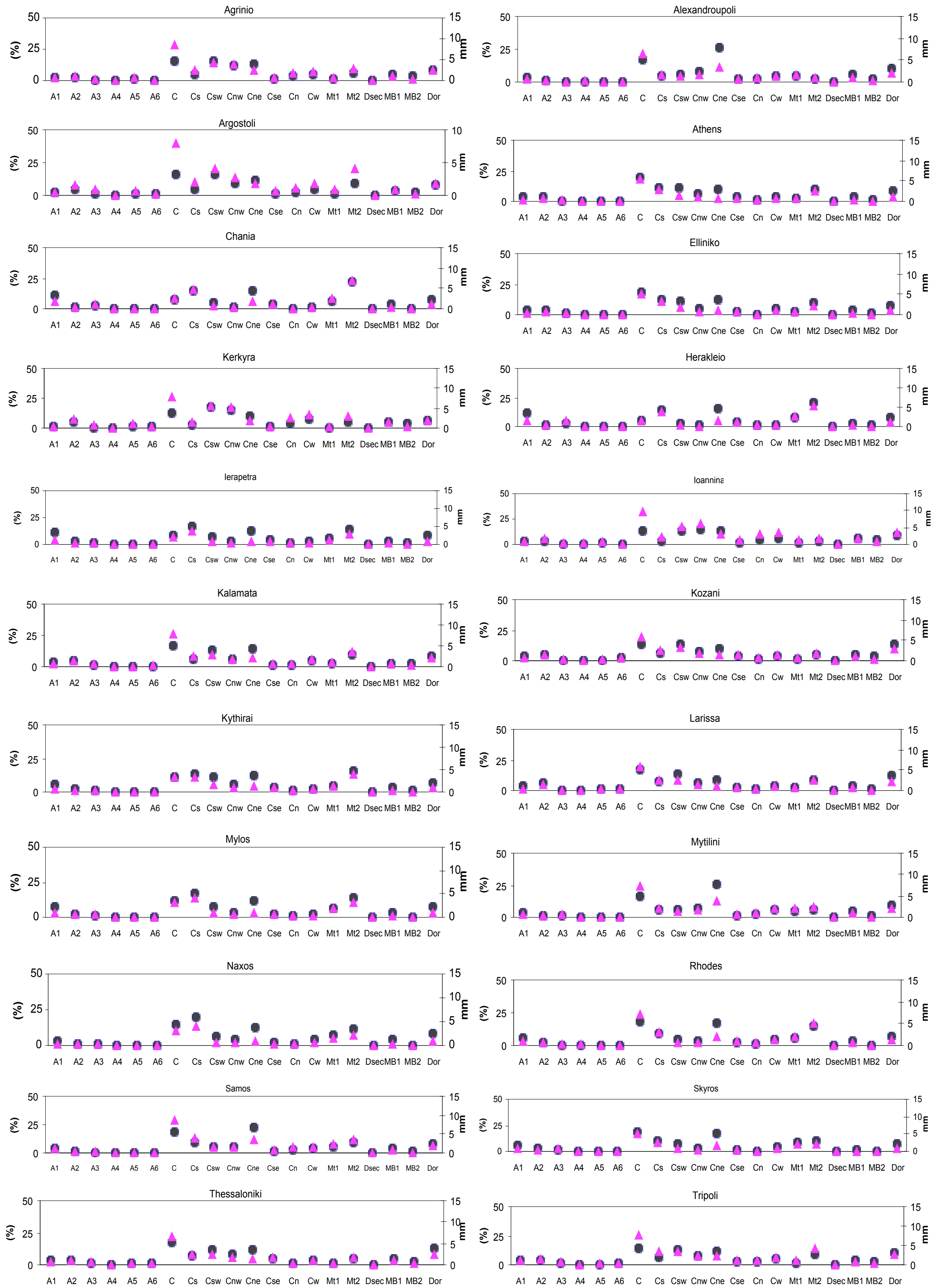

Figure 6b.Spring percentage (%) of precipitation amount (left axis, cycles) and spring standardized ratios PROPct/PROPtot for the 20 circulation types (SLP) and the 22 rainfall stations (right axis, triangle)

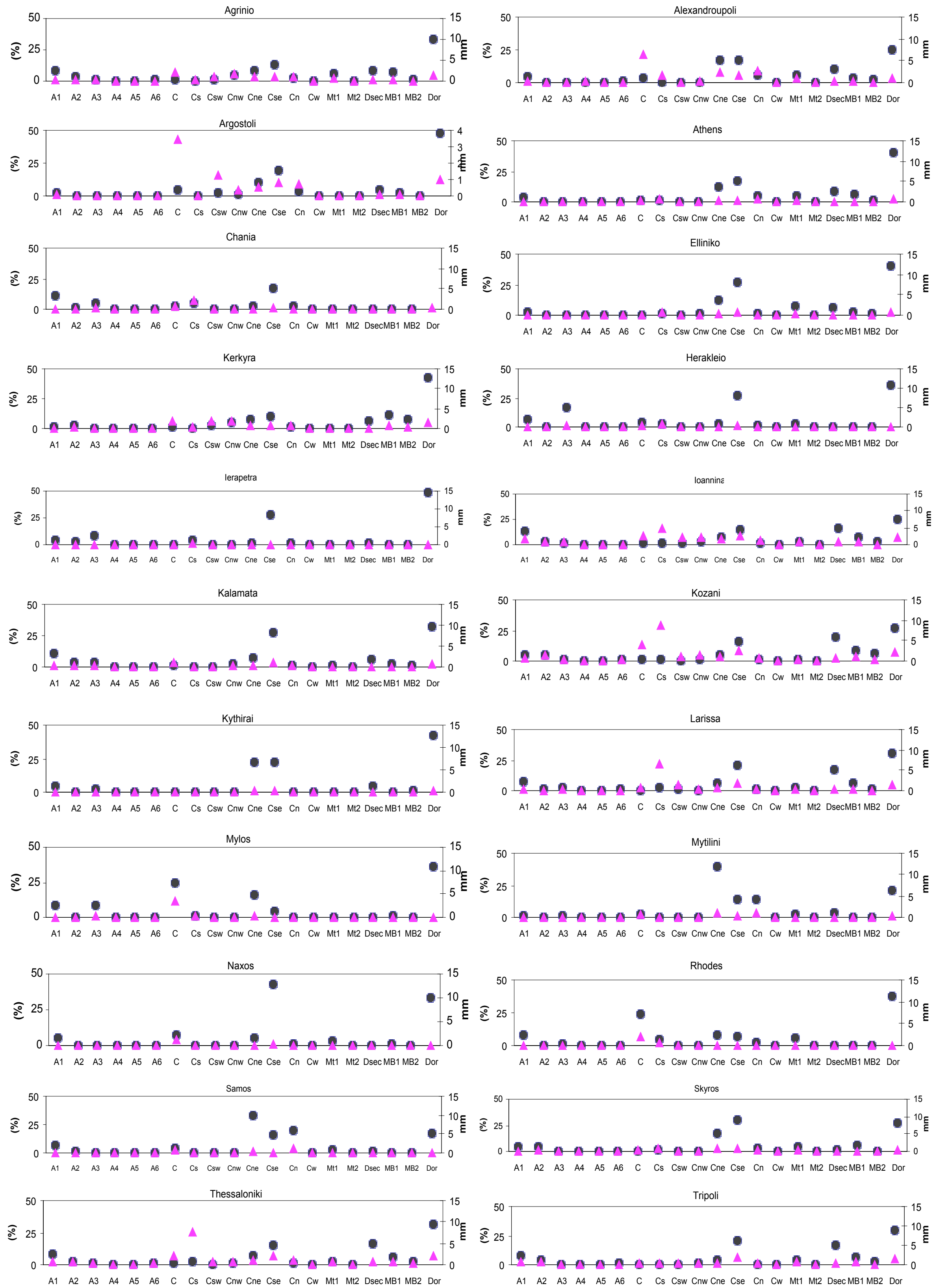

Figure 6c. Summer percentage (%) of precipitation amount (left axis, cycles) and summer standardized ratios PROPct/PROPtot for the 20 circulation types (SLP) and the 22 rainfall stations (right axis, triangle)

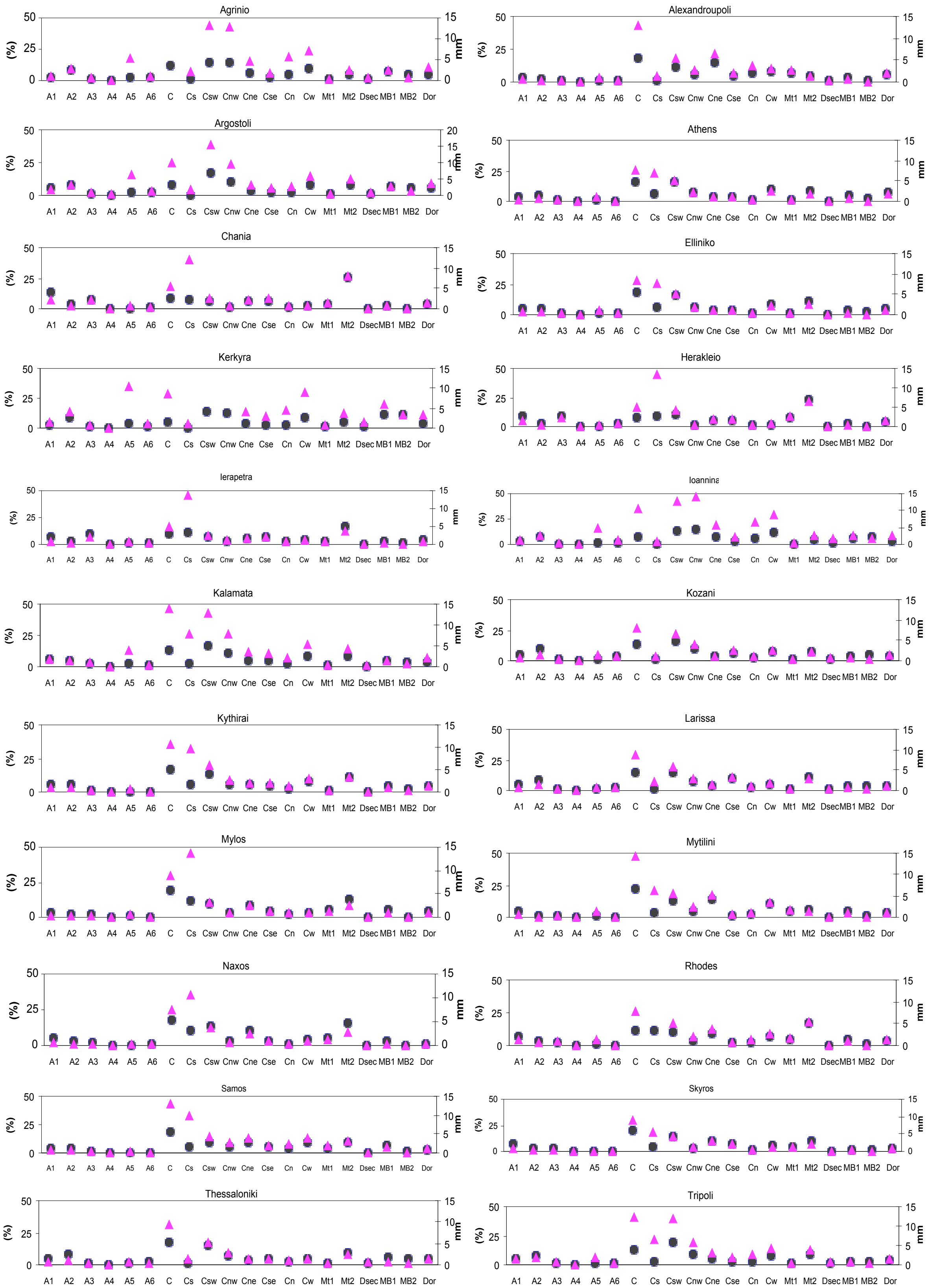

Figure 6d. Autumn percentage (%) of precipitation amount (left axis, cycles) and autumn standardized ratios PROPct/PROPtot for the 20 circulation types (SLP) and the 22 rainfall stations (right axis, triangle)

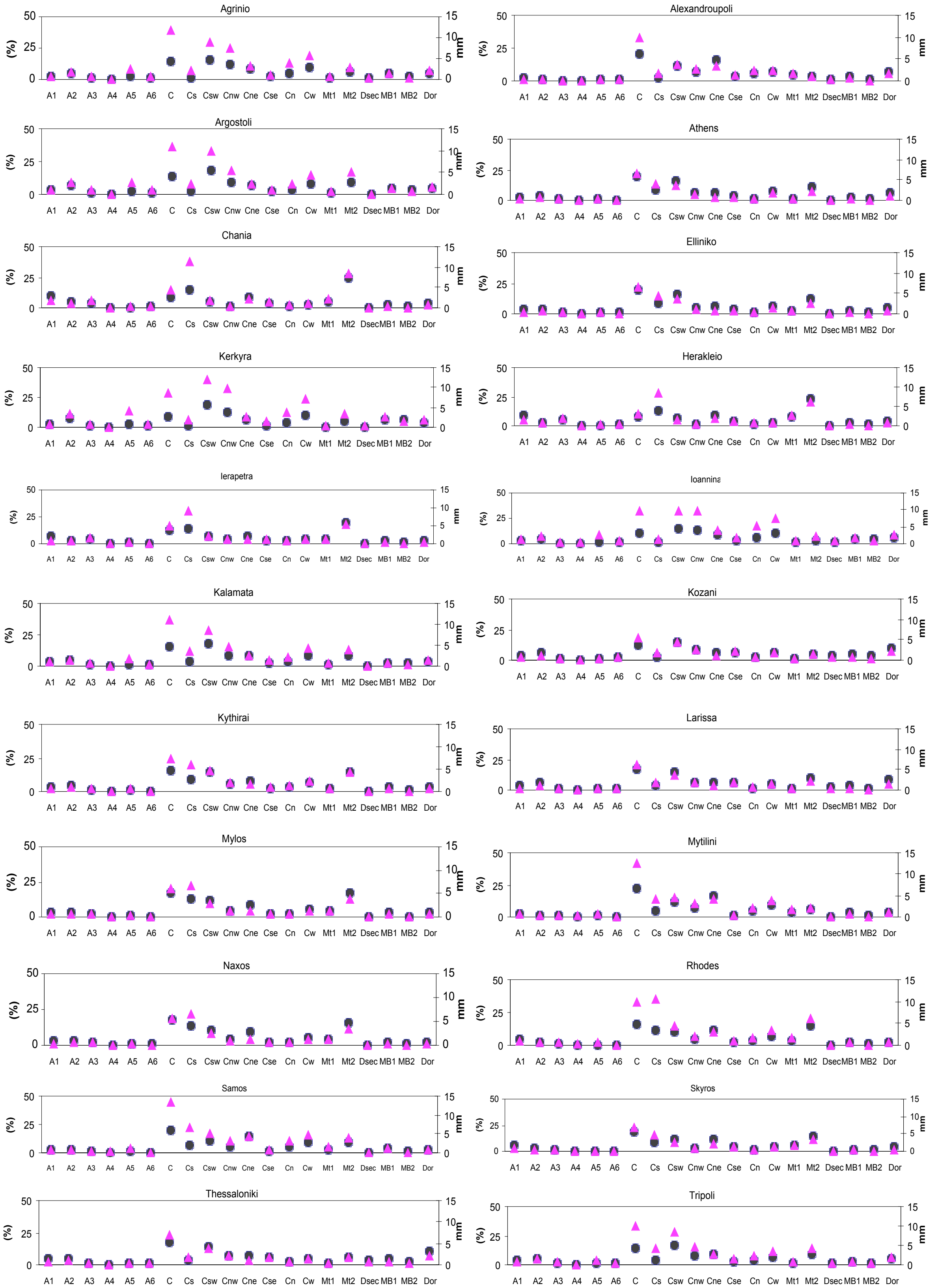

Figure 6e. Annual percentage (%) of precipitation amount (left axis, cycles) and annual standardized ratios PROPct/PROPtot for the 20 circulation types (SLP) and the 22 rainfall stations (right axis, triangle)

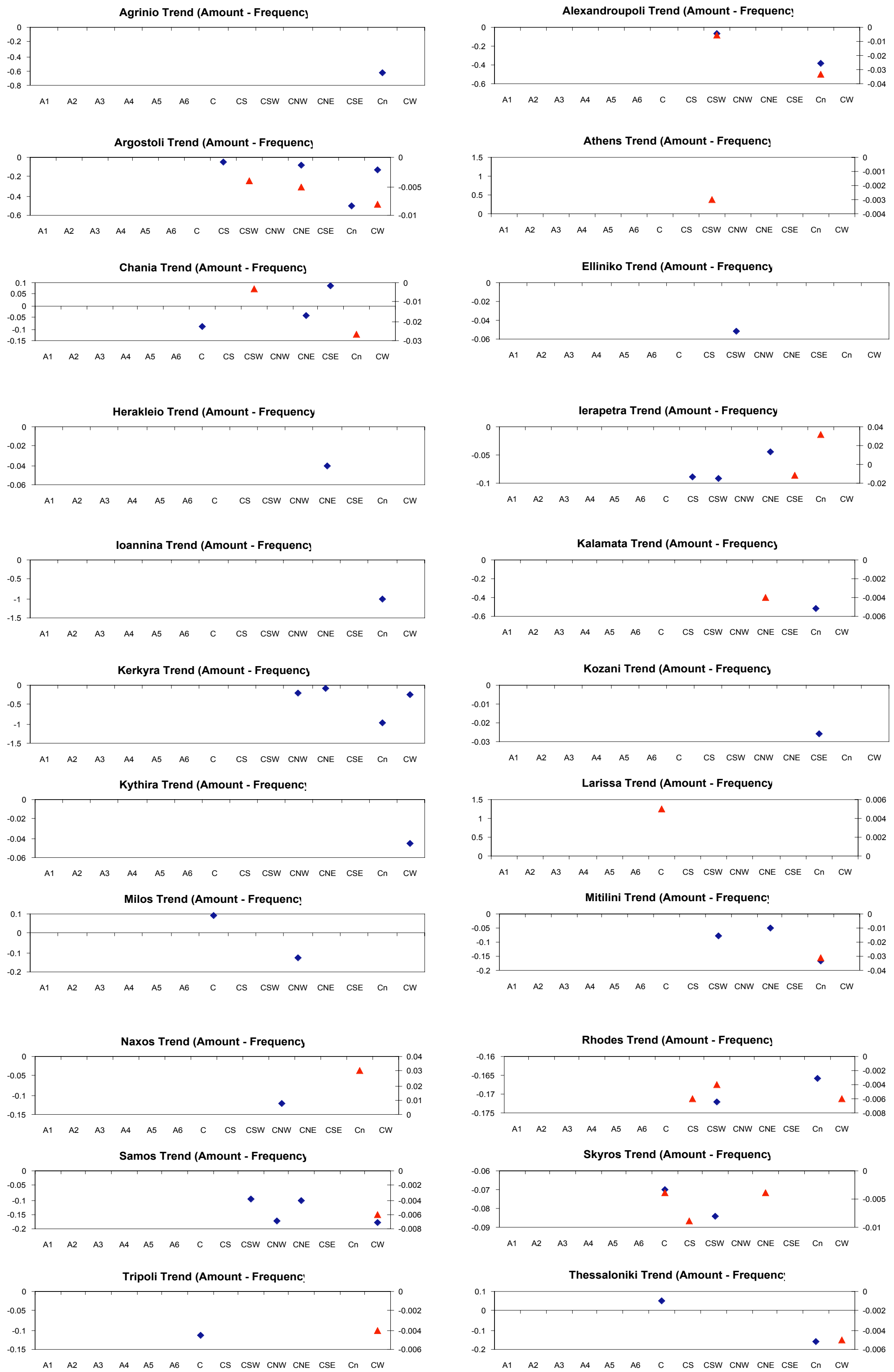

Figure 7a. Trends of the prec. frequencies (red triagles - right axis) and of the prec. amounts (blue rectangles-left axis) by circulation type at 500 hPa in the case of winter. Only the stat. signif. ones at a level 0.05 are marked

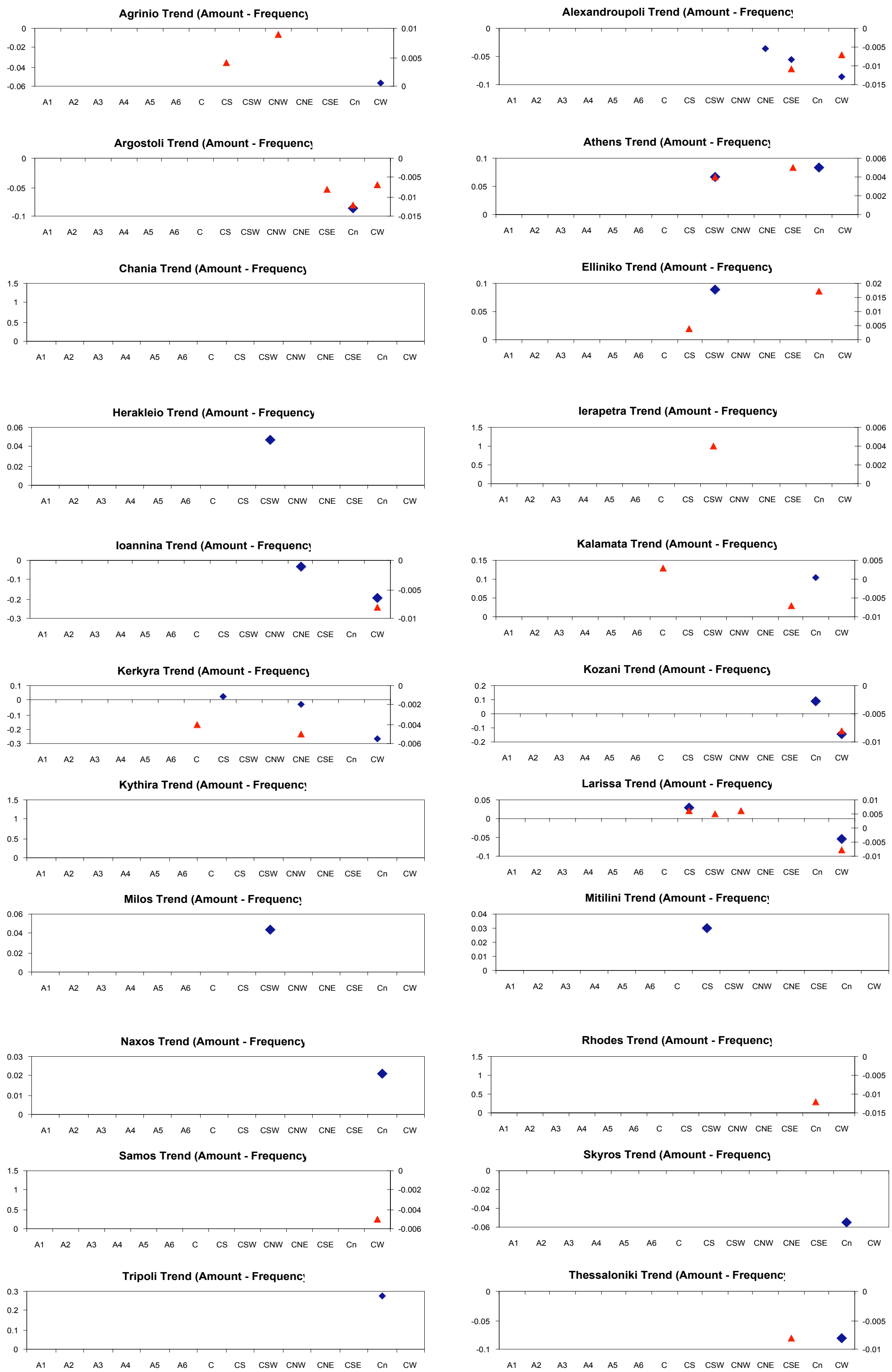

Figure 7b. Trends of the prec. frequencies (red triagles - right axis) and of the prec. amounts (blue rectangles-left axis) by circulation type at 500 hPa in the case of spring. Only the stat. signif. ones at a level 0.05 are marked

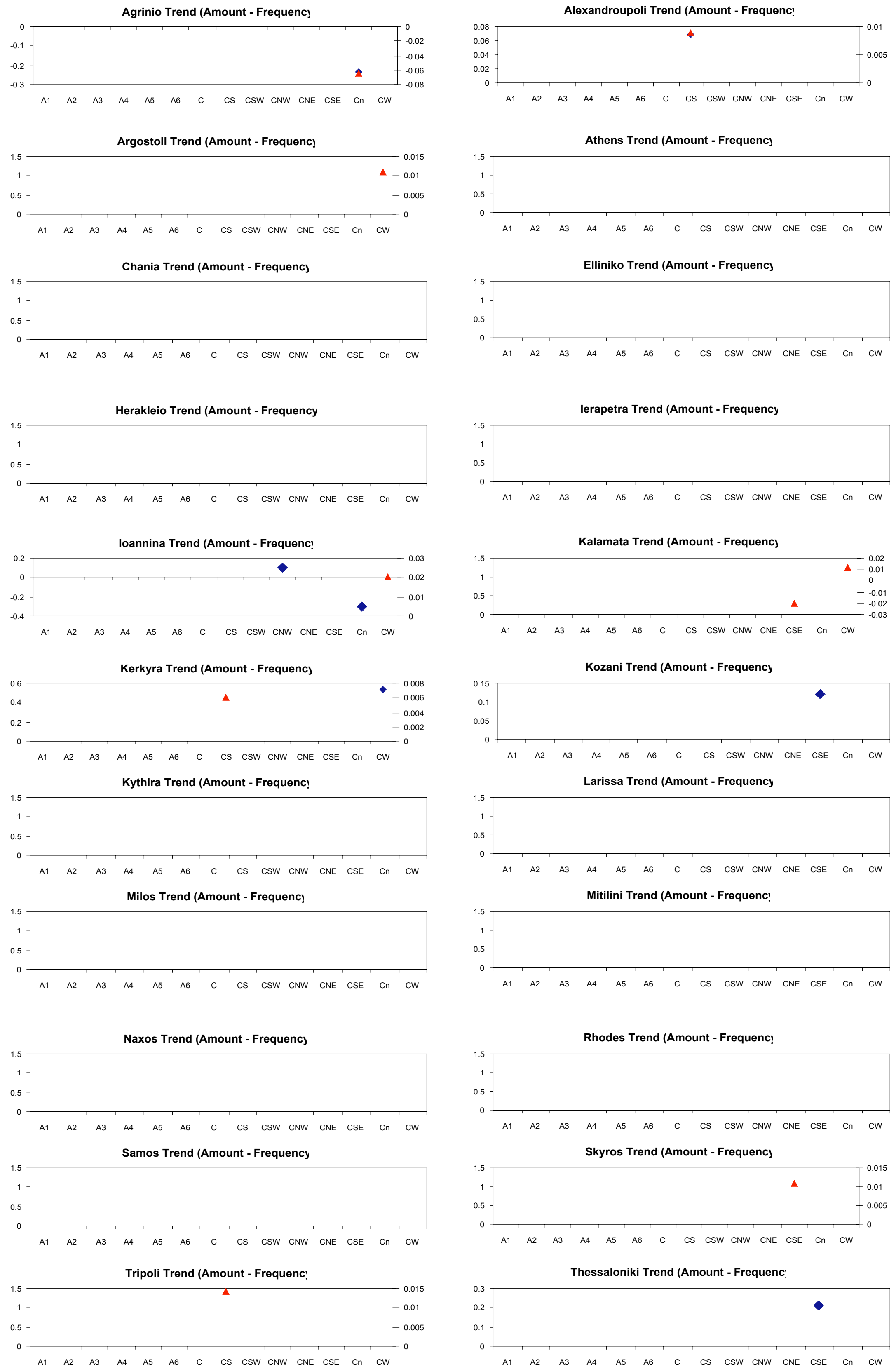

Figure 7c. Trends of the prec. frequencies (red triagles - right axis) and of the prec. amounts (blue rectangles-left axis) by circulation type at 500 hPa in the case of summer. Only the stat. signif. ones at a level 0.05 are marked

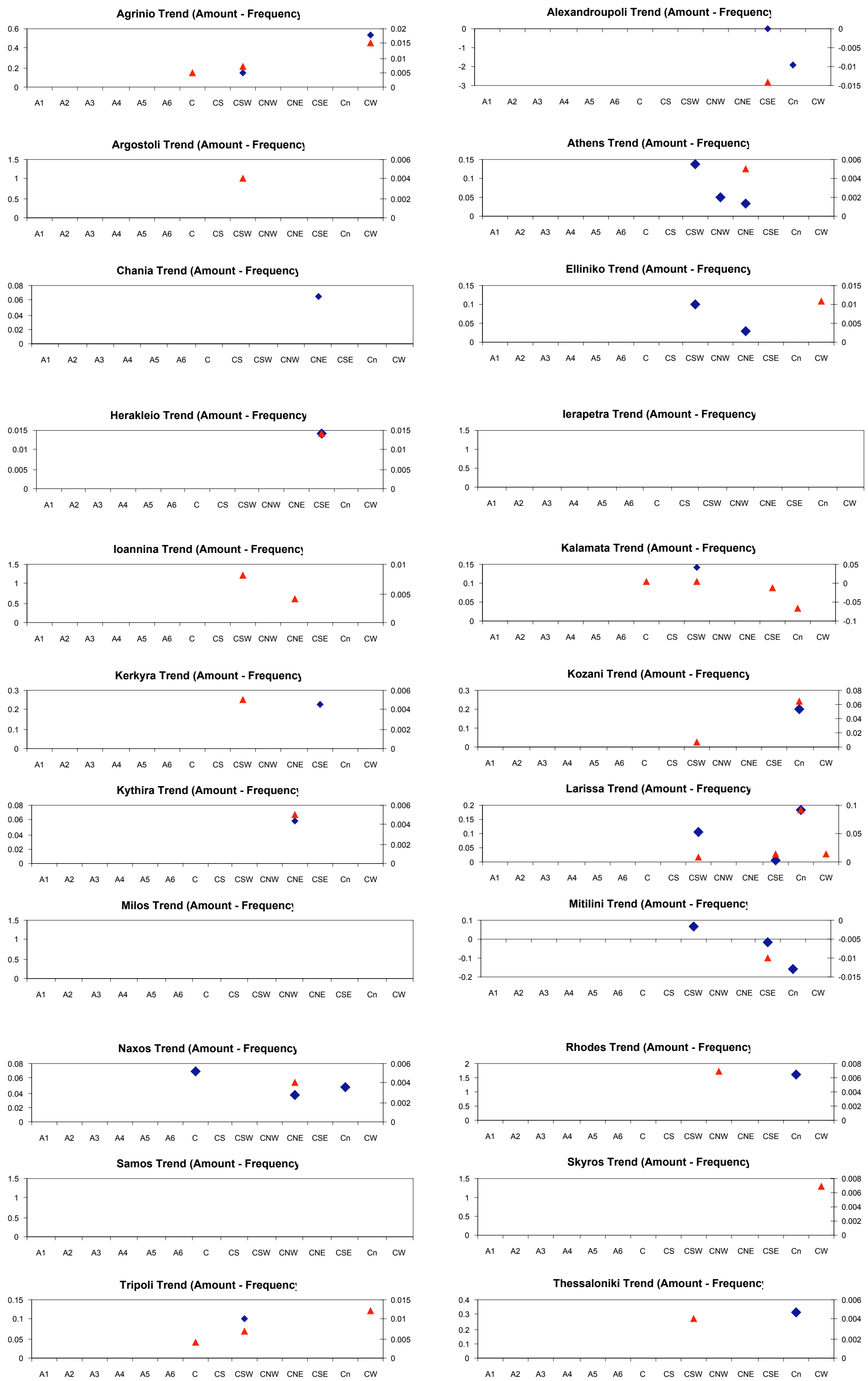

Figure 7d. Trends of the prec. frequencies (red triagles - right axis) and of the prec. amounts (blue rectangles-left axis) by circulation type at 500 hPa in the case of autumn. Only the stat. signif. ones at a level 0.05 are marked

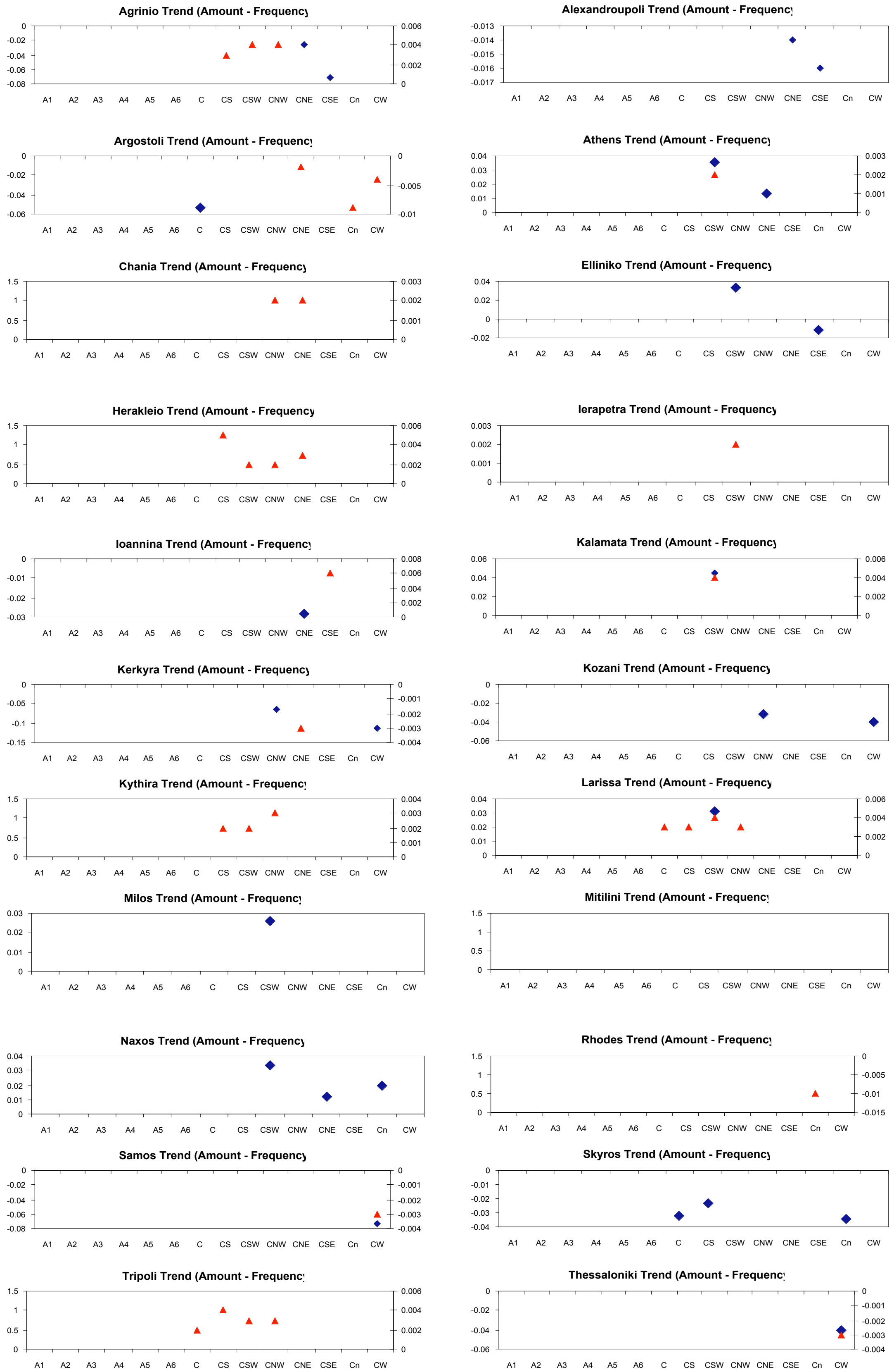

Figure 7e. Trends of the prec. frequencies (red triagles - right axis) and of the prec. amounts (blue rectangles-left axis) by circulation type at 500 hPa in the case of year. Only the stat. signif. ones at a level 0.05 are marked

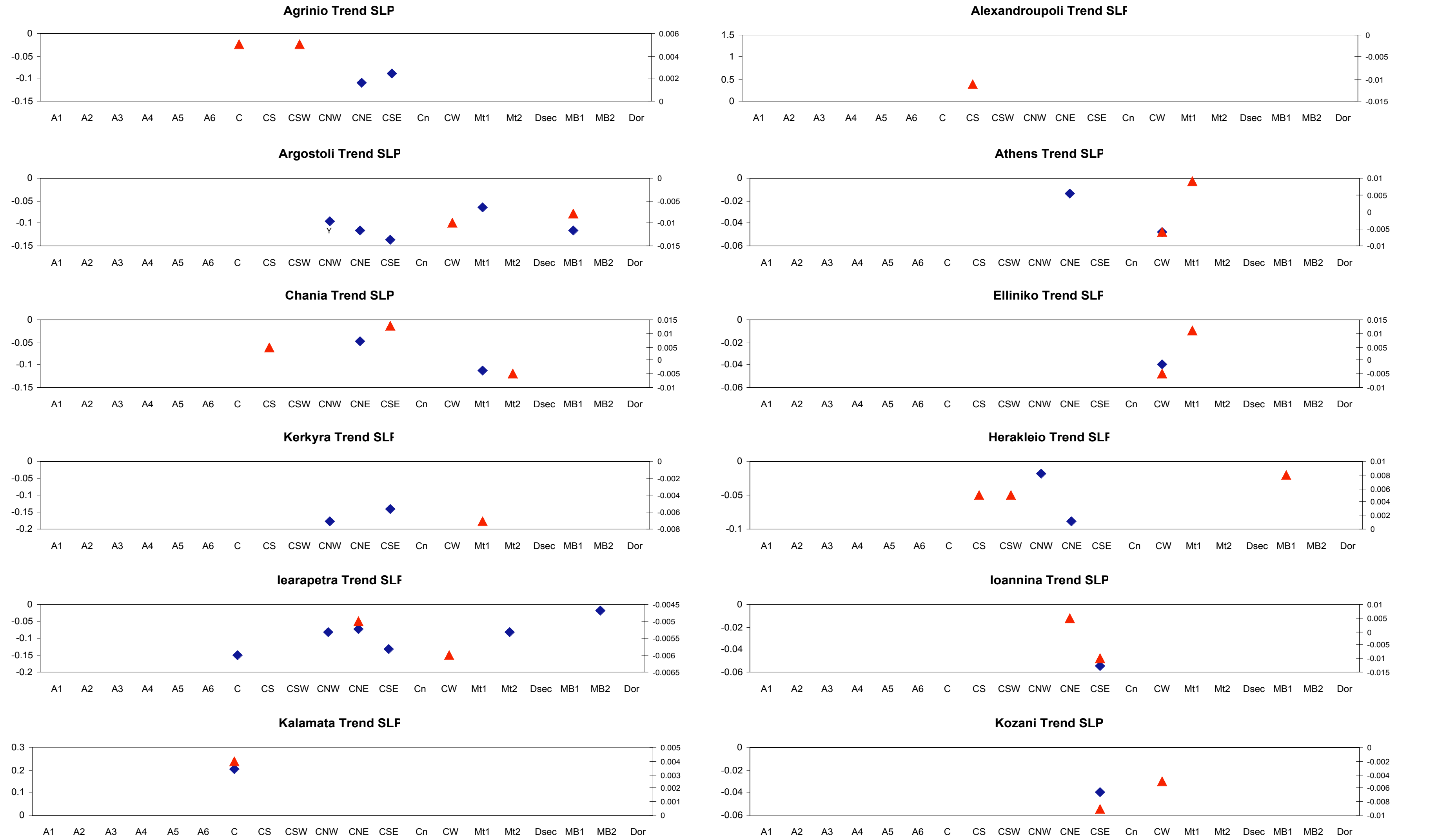

Figure 8a. Trends of the precipitation frequencies (red triagles-right axis) and of the precipitation amounts (blue rectangles-left axis) by circulation type (SLP) in the case of winter. Only the stat. signif. ones at a level 0.05 are marked

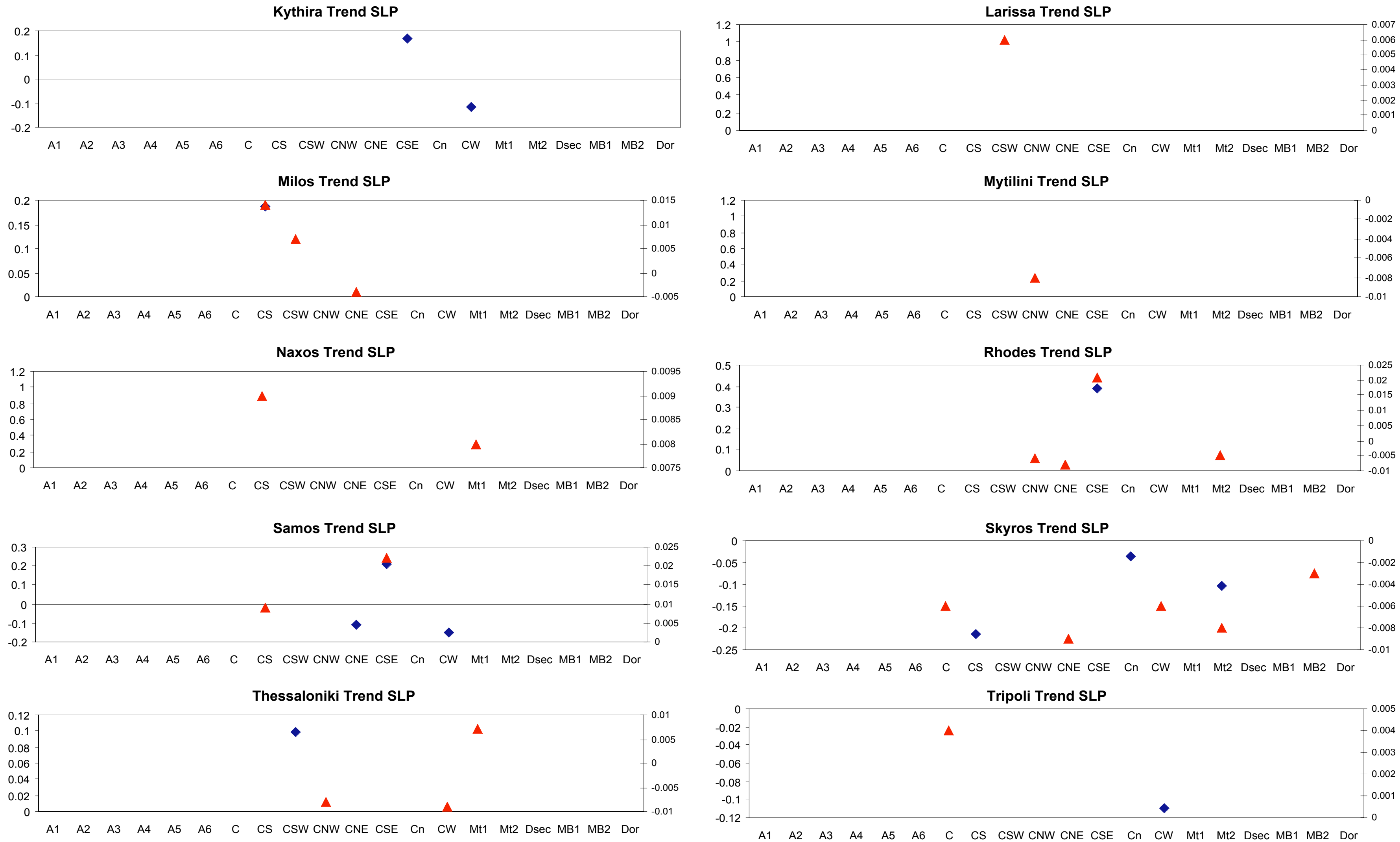

Figure 8a. Trends of the precipitation frequencies (red triagles-right axis) and of the precipitation amounts (blue rectangles-left axis) by circulation type (SLP) in the case of winter. Only the stat. signif. ones at a level 0.05 are marked

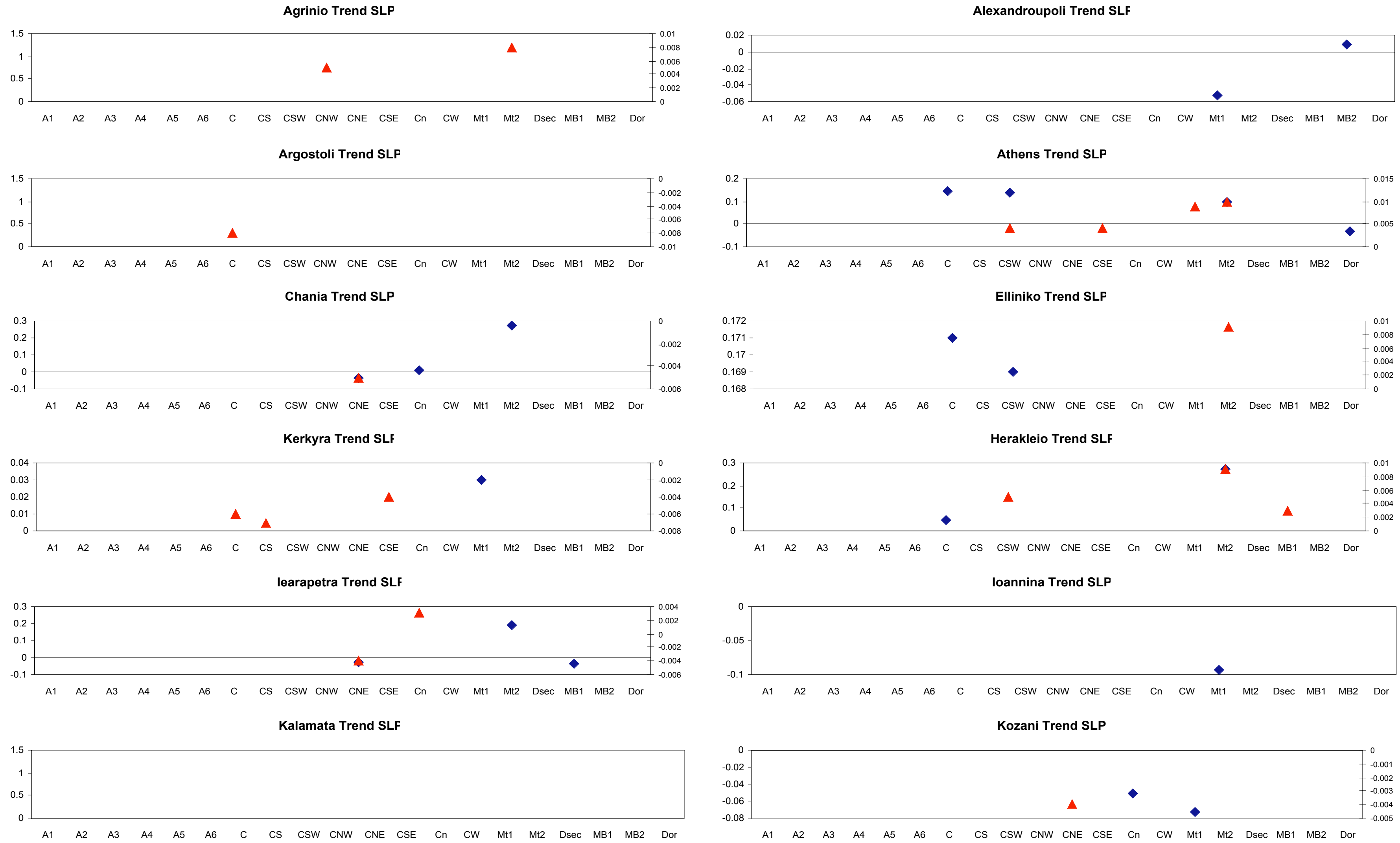

Figure 8b. Trends of the precipitation frequencies (red triagles-right axis) and of the precipitation amounts (blue rectangles-left axis) by circulation type (SLP) in the case of spring. Only the stat. signif. ones are marked at a level of significance 0.05

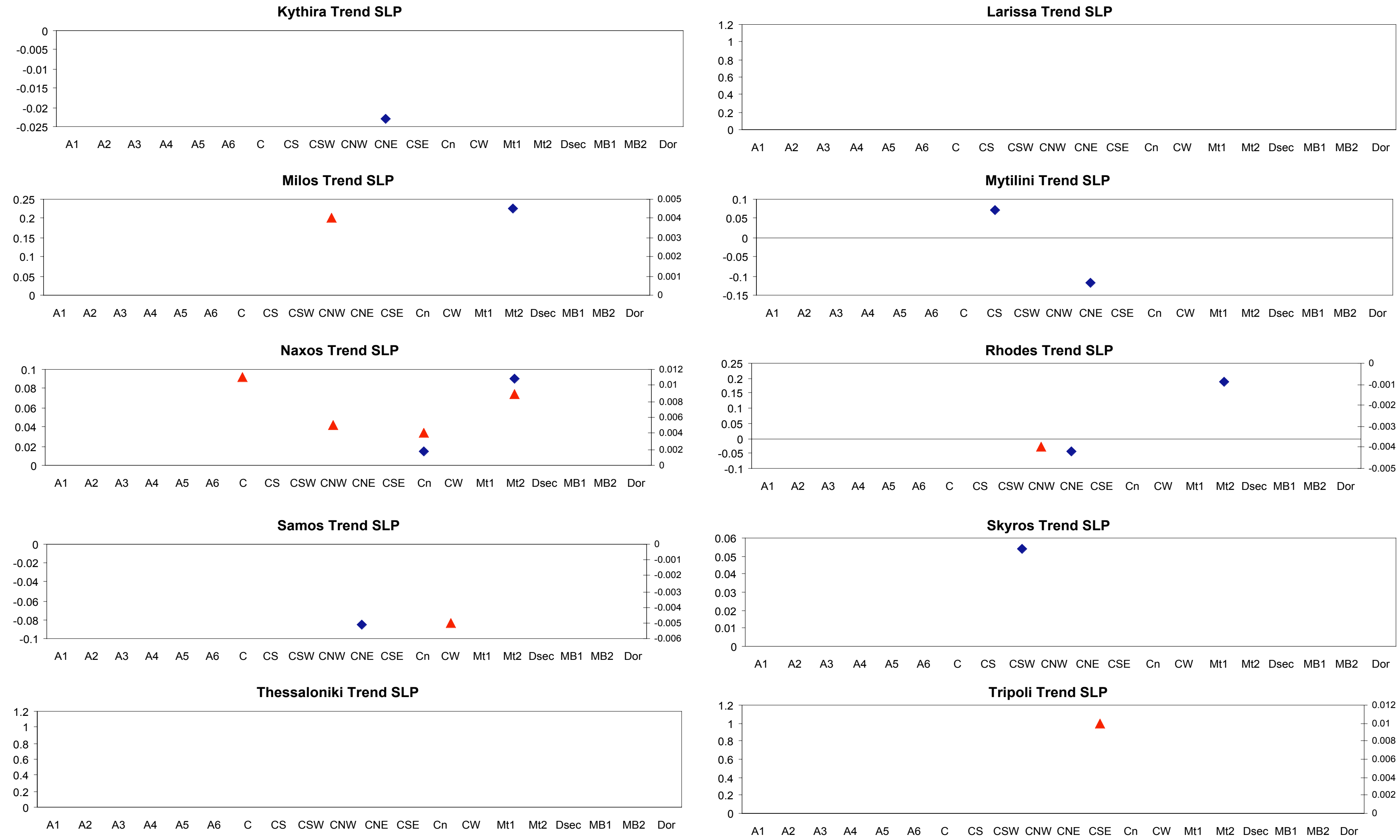

Figure 8b. Trends of the precipitation frequencies (red triagles-right axis) and of the precipitation amounts (blue rectangles-left axis) by circulation type (SLP) in the case of spring. Only the stat. signif. ones are marked at a level of significance 0.05

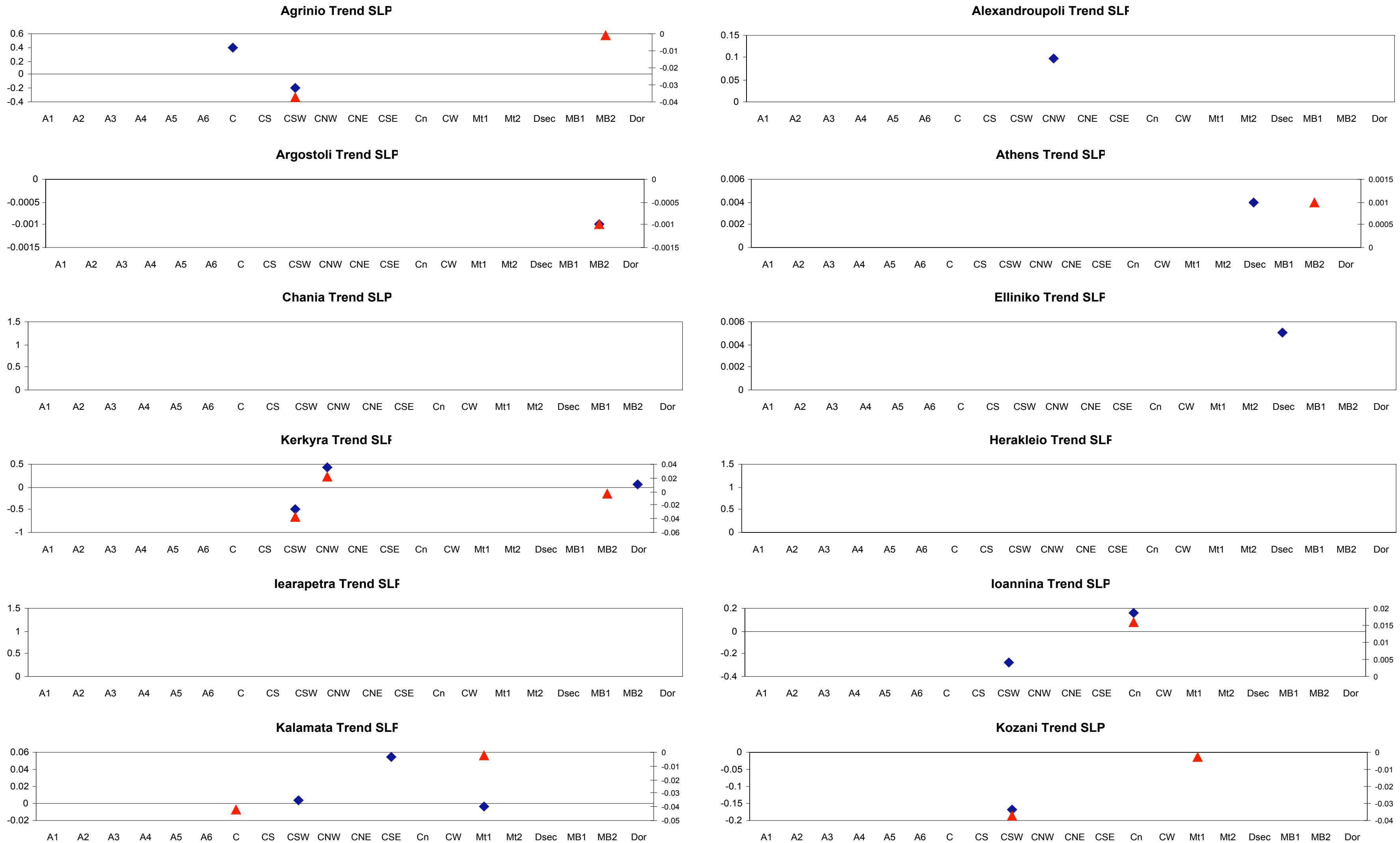

Figure 8c. Trends of the precipitation frequencies (red triagles-right axis) and of the precipitation amounts (blue rectangles-left axis) by circulation type (SLP) in the case of summer. Only the stat. signif. ones at a level 0.05 are marked

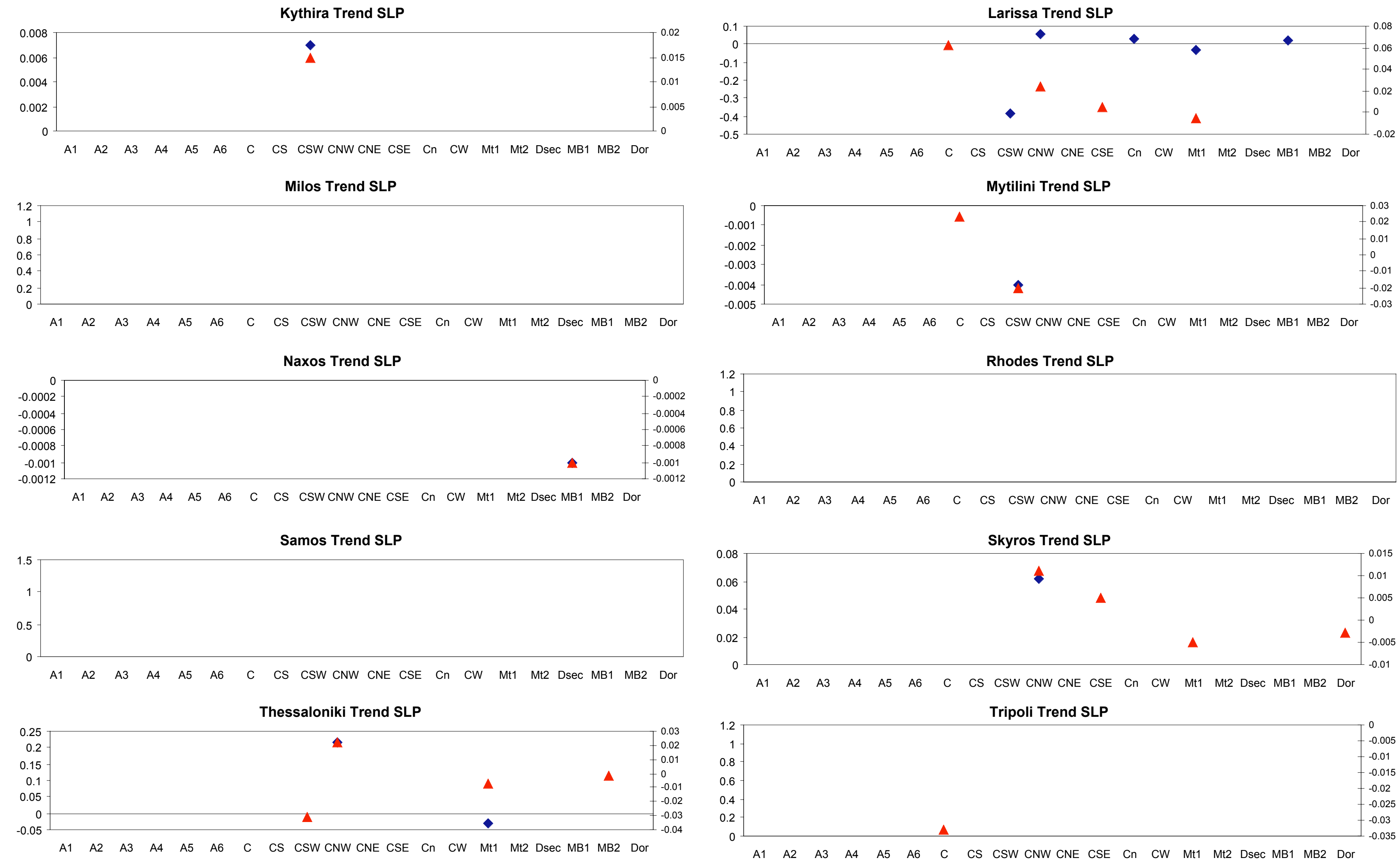

Figure 8c. Trends of the precipitation frequencies (red triagles-right axis) and of the precipitation amounts (blue rectangles-left axis) by circulation type (SLP) in the case of summer. Only the stat. signif. ones at a level 0.05 are marked

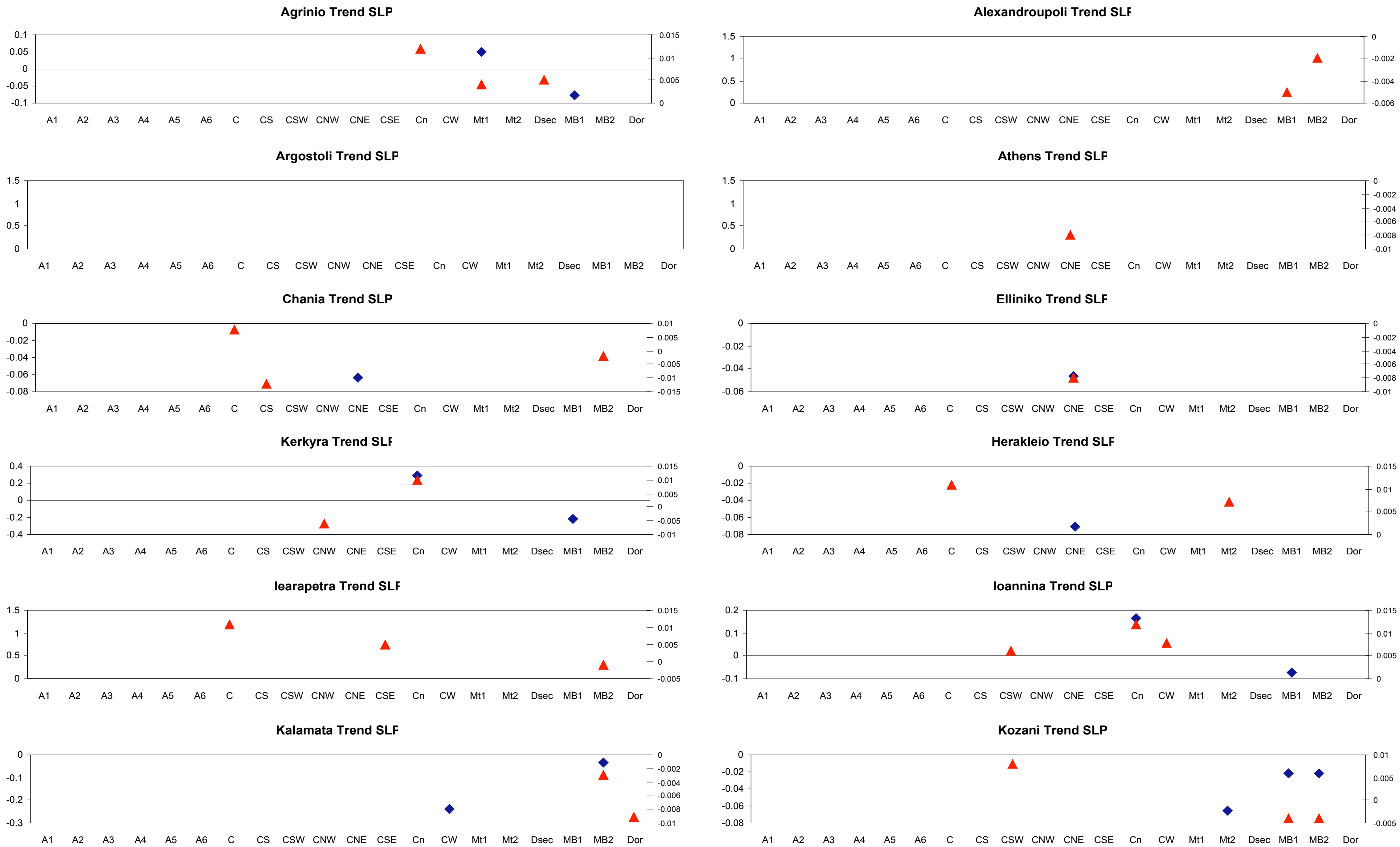

Figure 8d. Trends of the precipitation frequencies (red triagles-right axis) and of the precipitation amounts (blue rectangles-left axis) by circulation type (SLP) in the case of autumn. Only the stat. signif. ones at a level 0.05 are marked

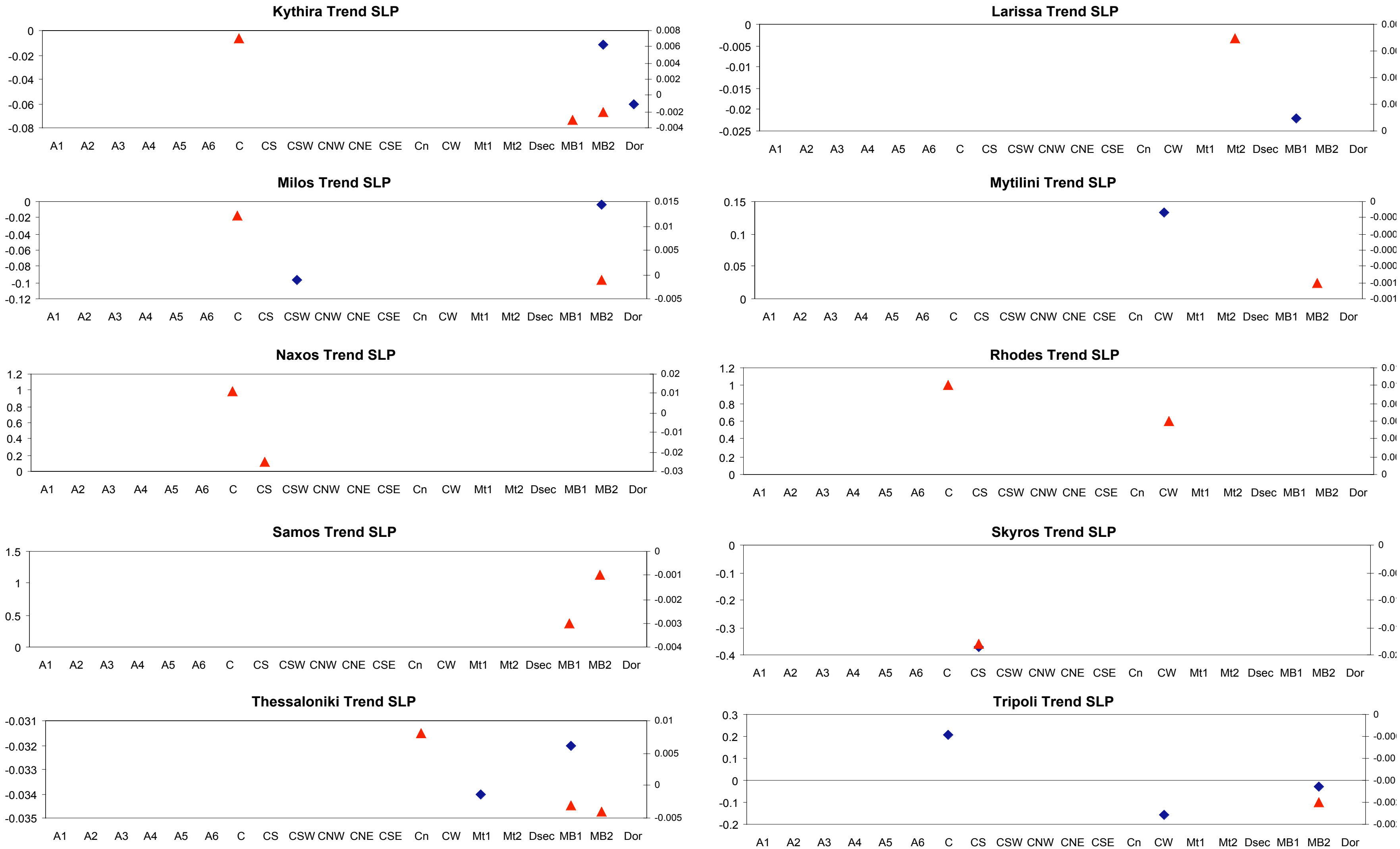

Figure 8d. Trends of the precipitation frequencies (red triagles-right axis) and of the precipitation amounts (blue rectangles-left axis) by circulation type (SLP) in the case of autumn. Only the stat. signif. ones at a level 0.05 are marked

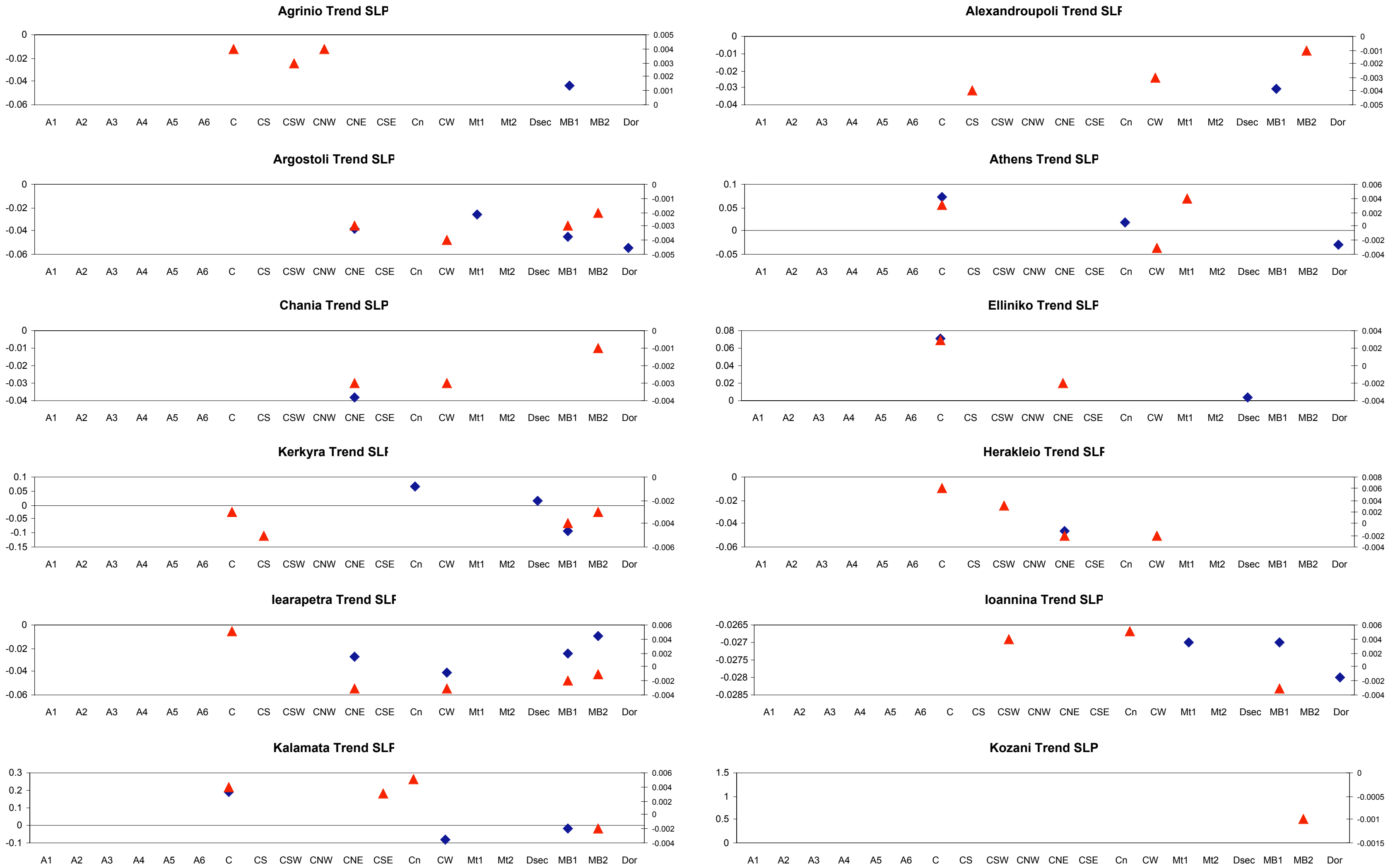

Figure 8e. Trends of the precipitation frequencies (red triagles-right axis) and of the precipitation amounts (blue rectangles-left axis) by circulation type (SLP) in the case of year. Only the stat. signif. ones at a level 0.05 are marked

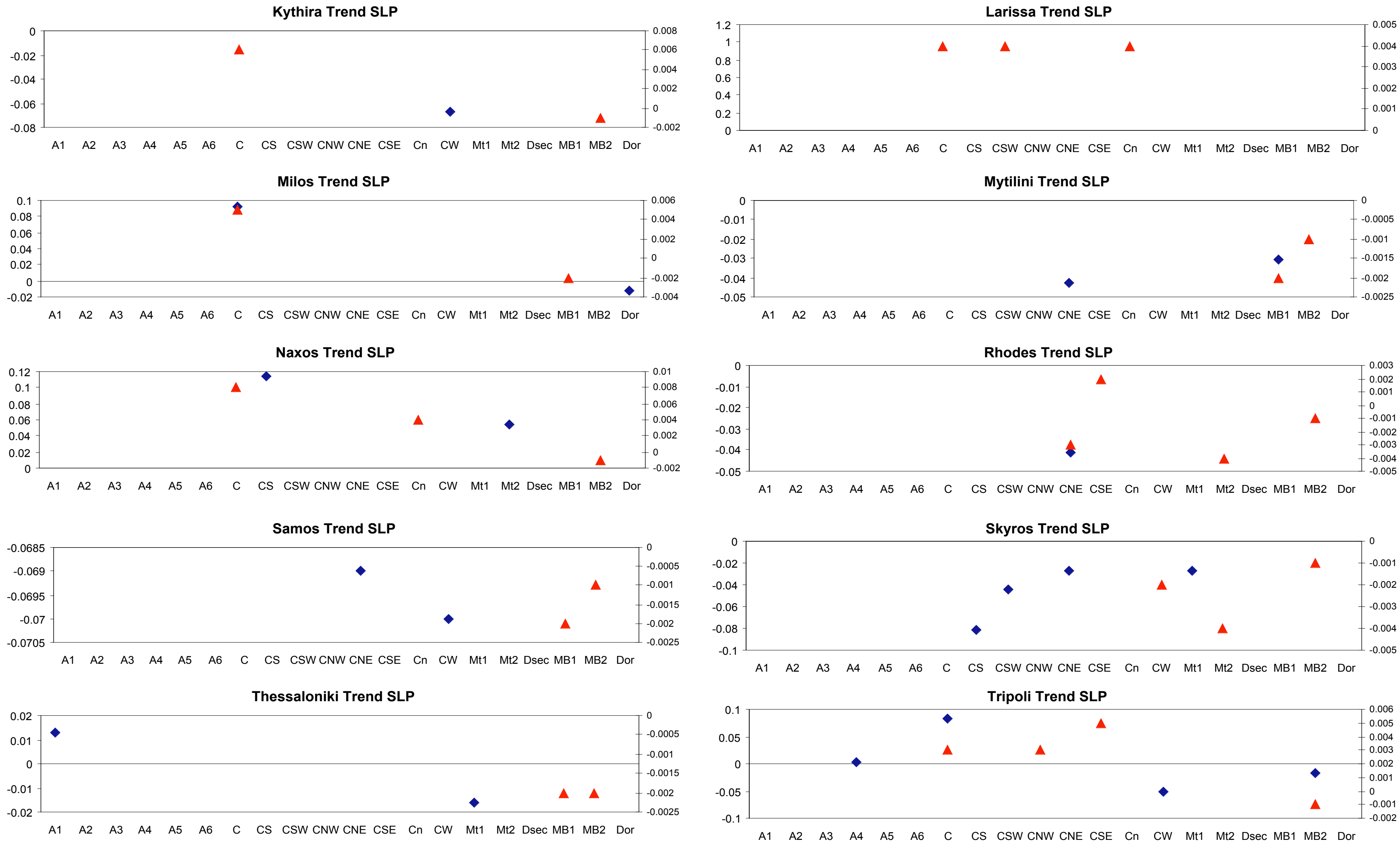

Figure 8e. Trends of the precipitation frequencies (red triagles-right axis) and of the precipitation amounts (blue rectangles-left axis) by circulation type (SLP) in the case of year. Only the stat. signif. ones at a level 0.05 are marked

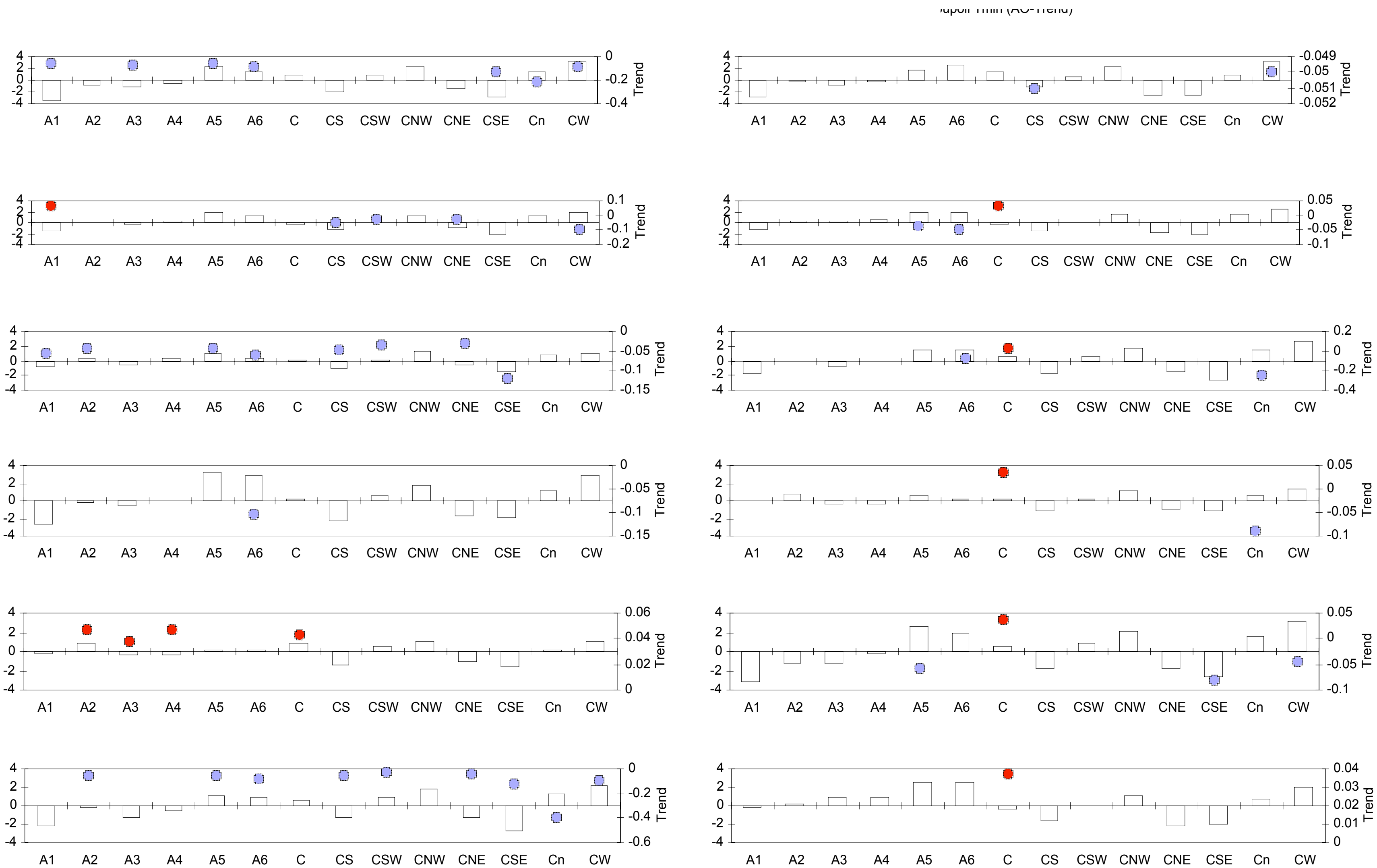

Figure 9a. Anomalies (__-bars) and trend of minimum Temperature (positive trends with red circles and negative trends with blue circles) by circulation type in the case of Winter at 500hPa (1958-2000). Only the stat. signif. ones at a level 0.05 are marked

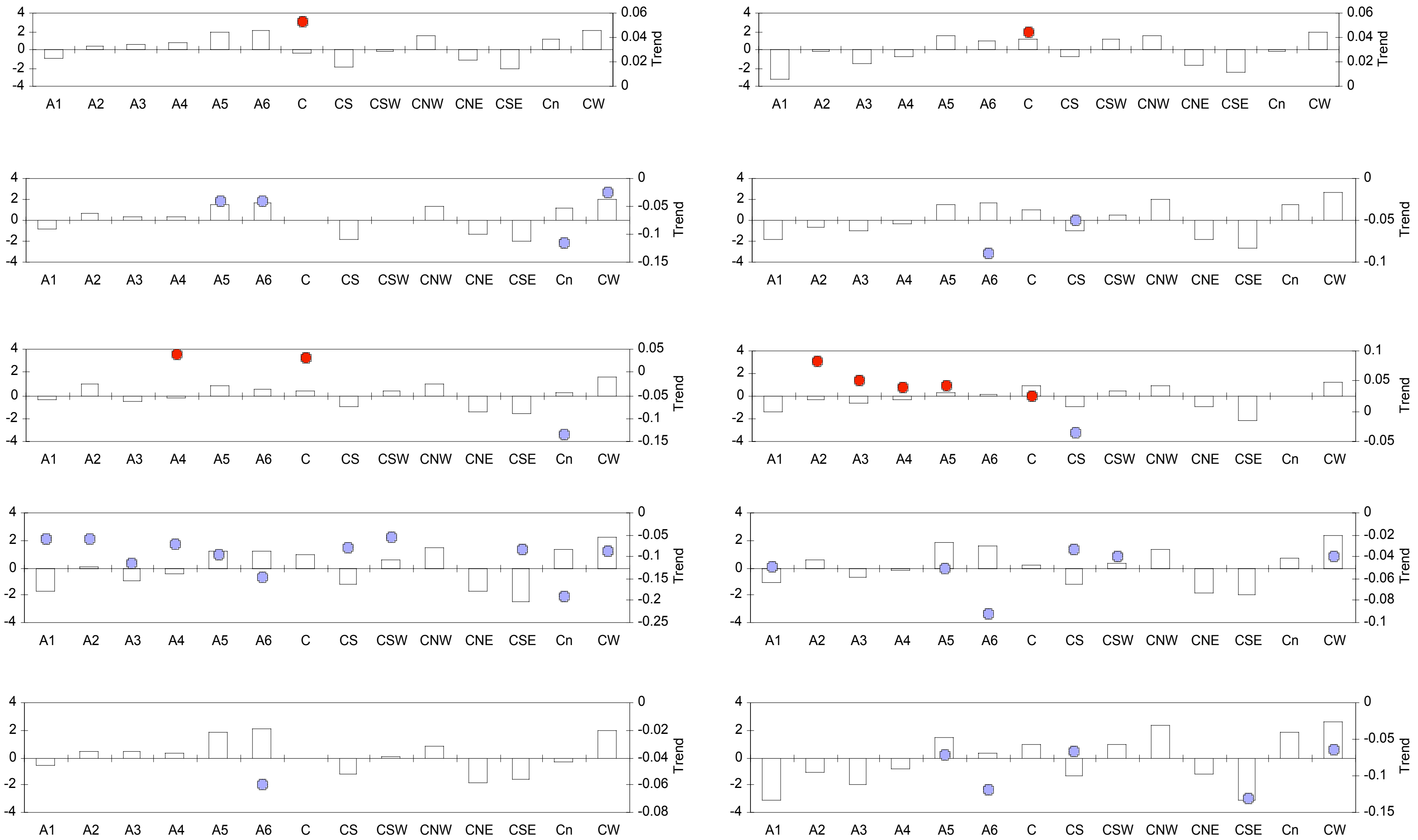

Figure 9a. Anomalies (__-bars) and trend of minimum Temperature (positive trends with red circles and negative trends with blue circles) by circulation type in the case of Winter at 500hPa (1958-2000). Only the stat. signif. ones at a level 0.05 are marked

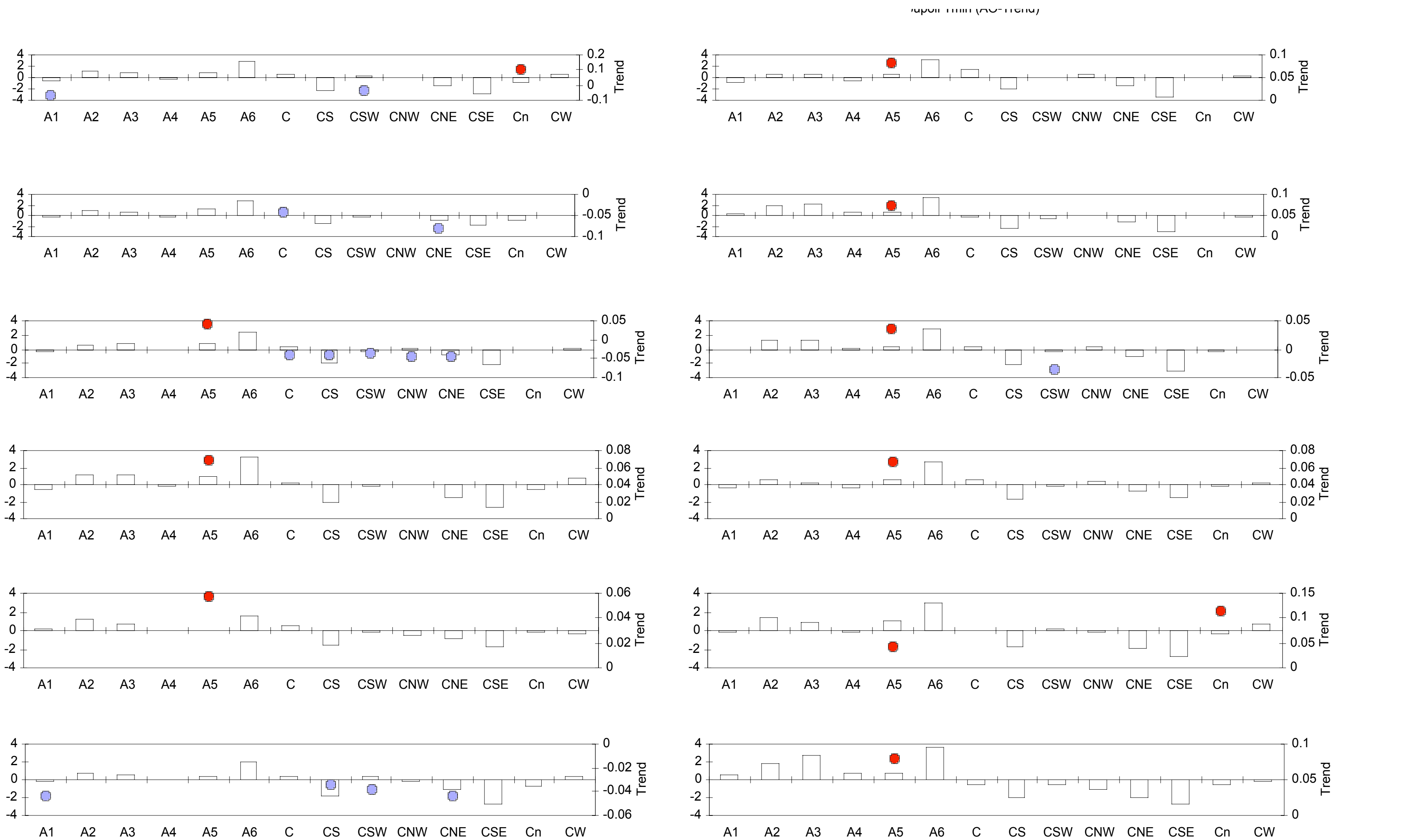

Figure 9b. Anomalies (__-bars) and trend of minimum Temperature (positive trends with red circles and negative trends with blue circles) by circulation type in the case of Spring at 500hPa (1958-2000). Only the stat. signif. ones at a level 0.05 are marked

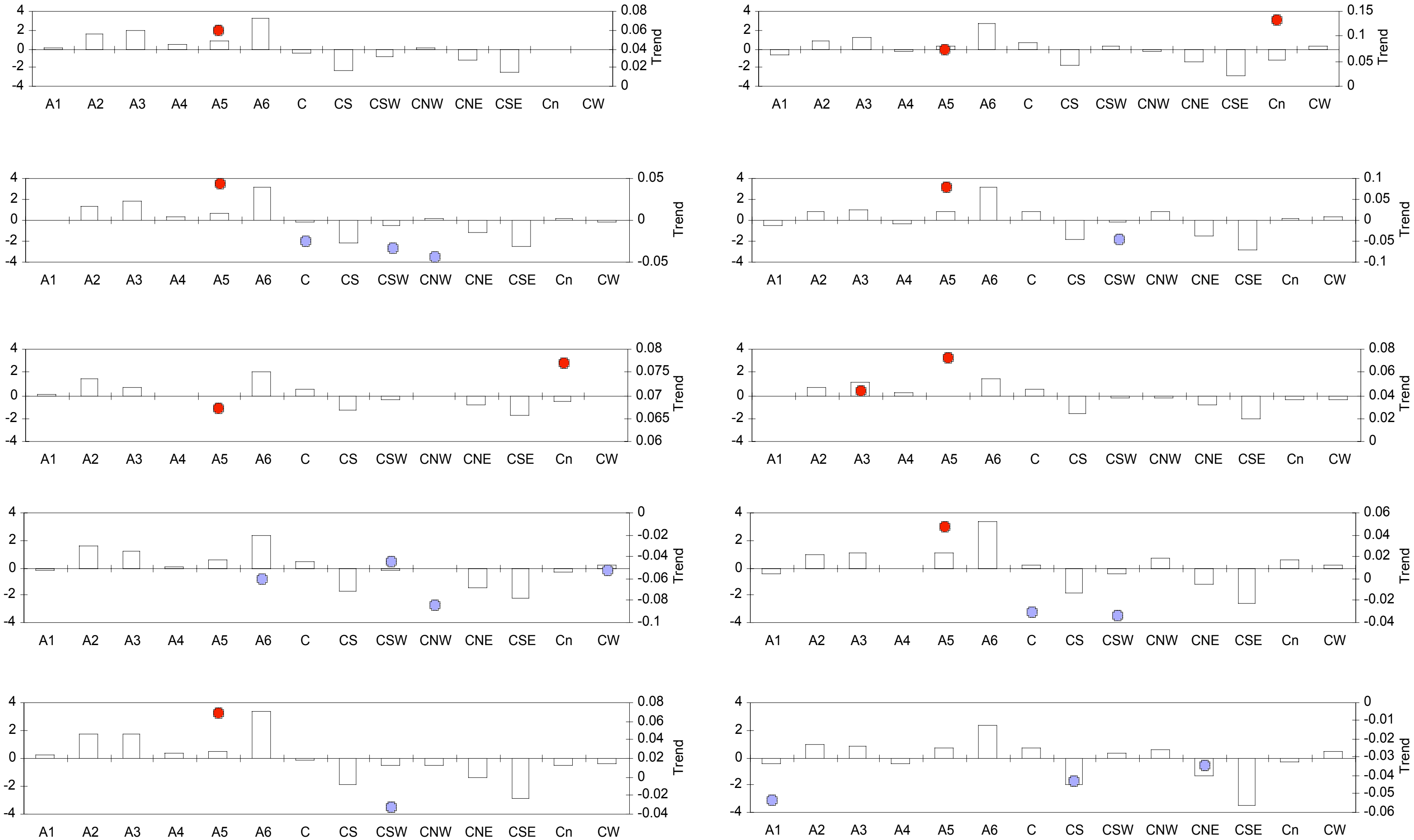

Figure 9b. Anomalies (__-bars) and trend of minimum Temperature (positive trends with red circles and negative trends with blue circles) by circulation type in the case of Spring at 500hPa (1958-2000). Only the stat. signif. ones at a level 0.05 are marked

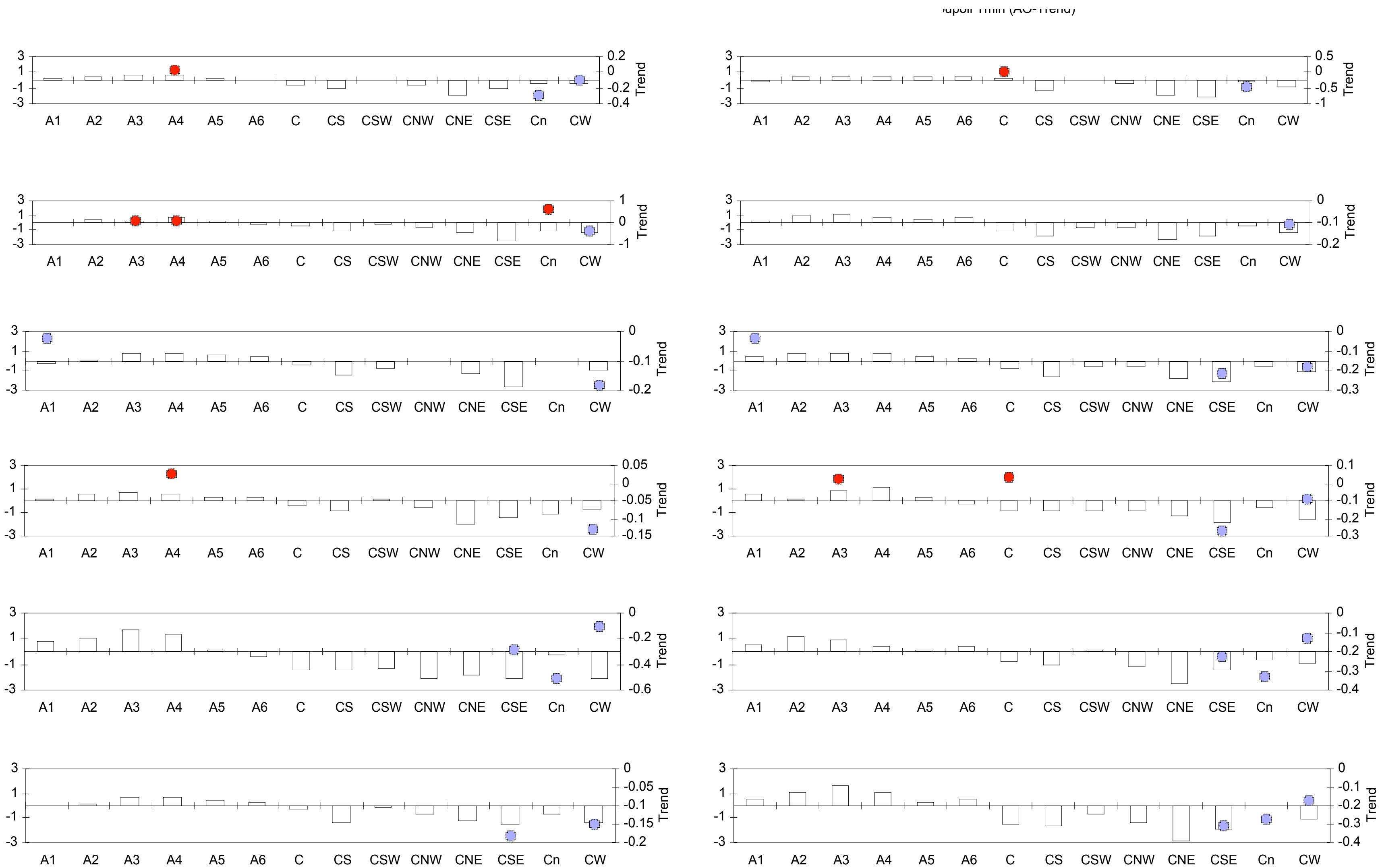

Figure 9c. Anomalies (__-bars) and trend of minimum Temperature (positive trends with red circles and negative trends with blue circles) by circulation type in the case of Summer at 500hPa (1958-2000). Only the stat. signif. ones at a level 0.05 are marked

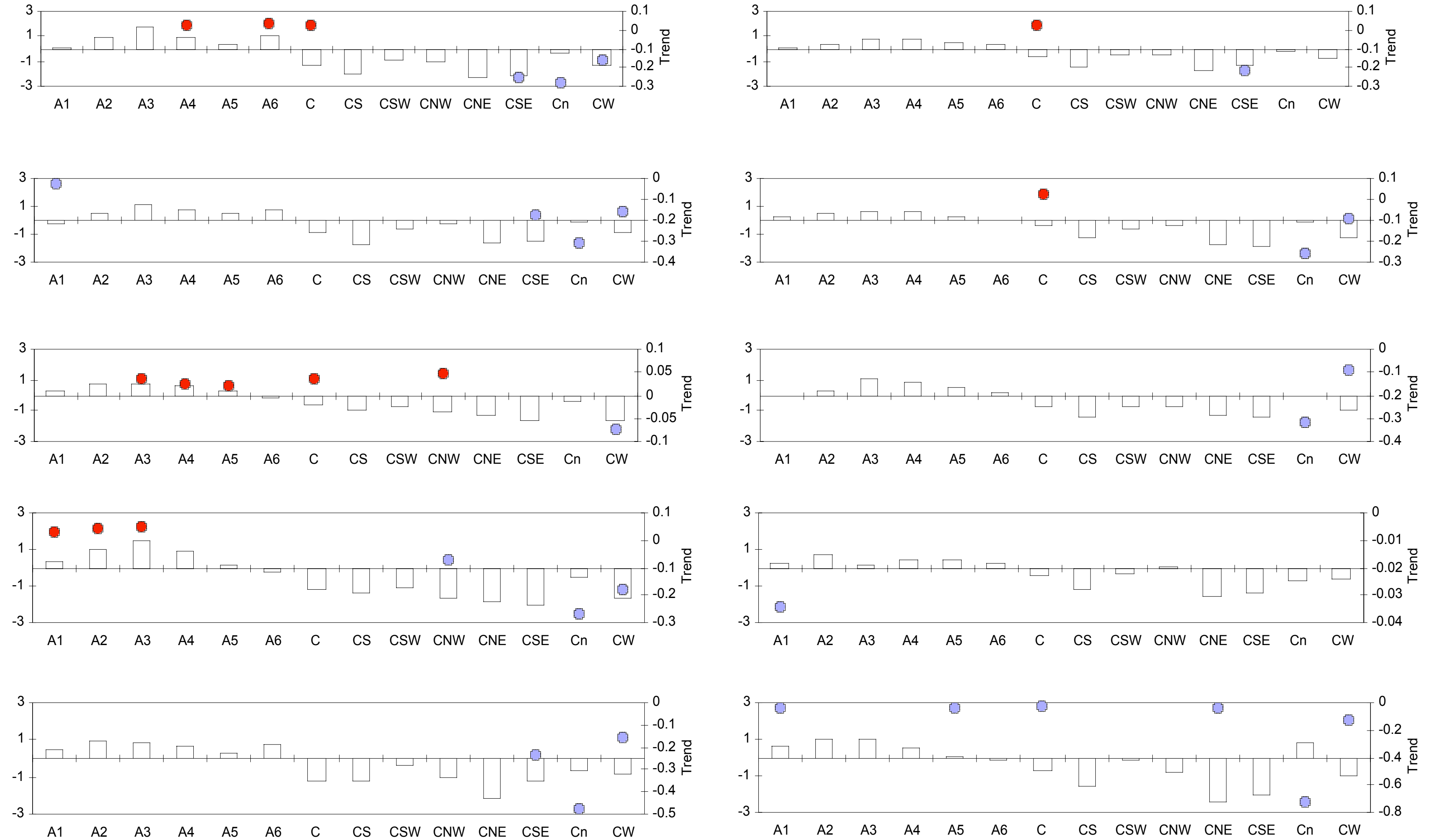

Figure 9c. Anomalies (__-bars) and trend of minimum Temperature (positive trends with red circles and negative trends with blue circles) by circulation type in the case of Summer at 500hPa (1958-2000). Only the stat. signif. ones at a level 0.05 are marked

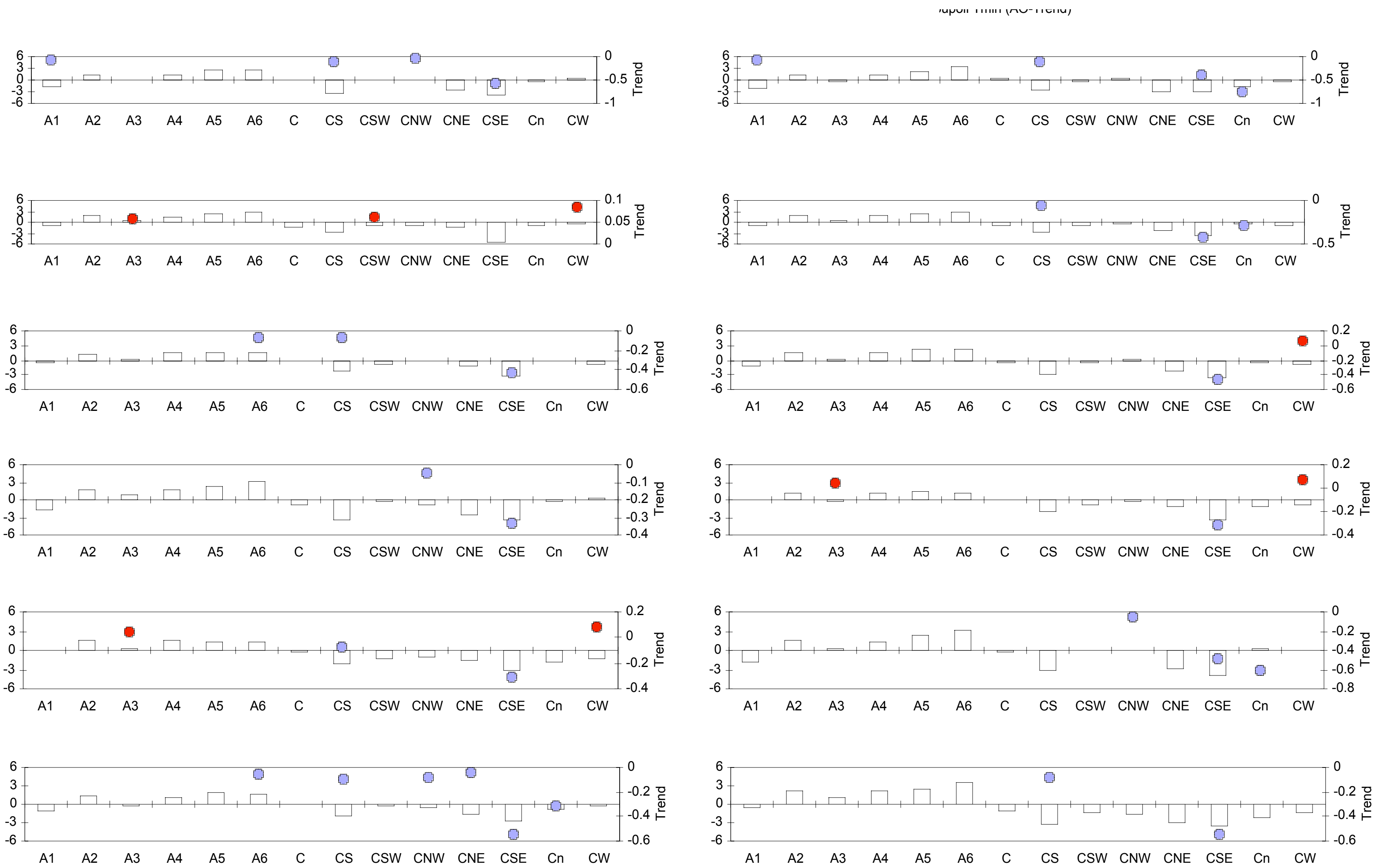

Figure 9d. Anomalies (__-bars) and trend of minimum Temperature (positive trends with red circles and negative trends with blue circles) by circulation type in the case of Autumn at 500hPa (1958-2000). Only the stat. signif. ones at a level 0.05 are marked

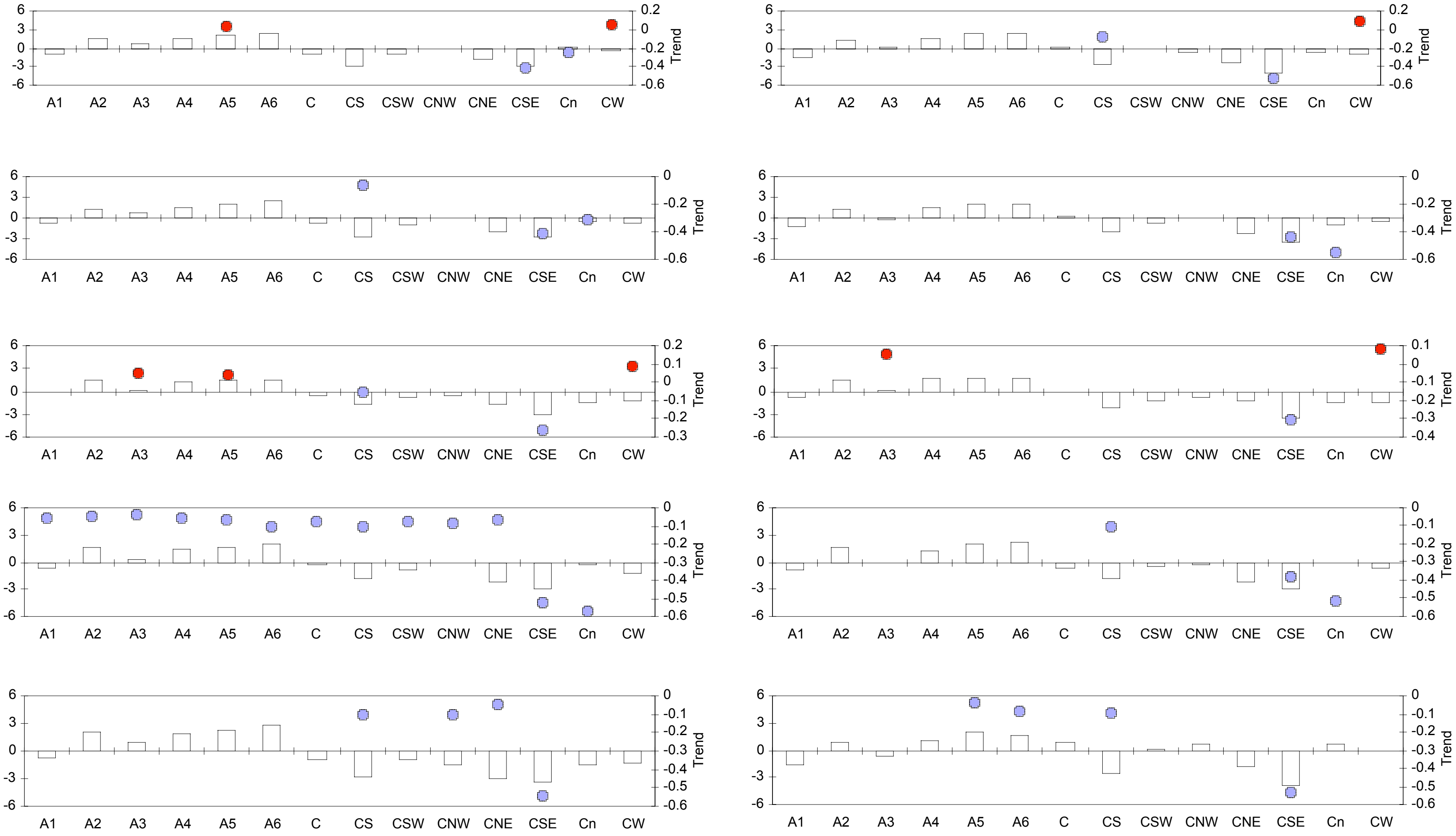

Figure 9d. Anomalies (__-bars) and trend of minimum Temperature (positive trends with red circles and negative trends with blue circles) by circulation type in the case of Autumn at 500hPa (1958-2000). Only the stat. signif. ones at a level 0.05 are marked

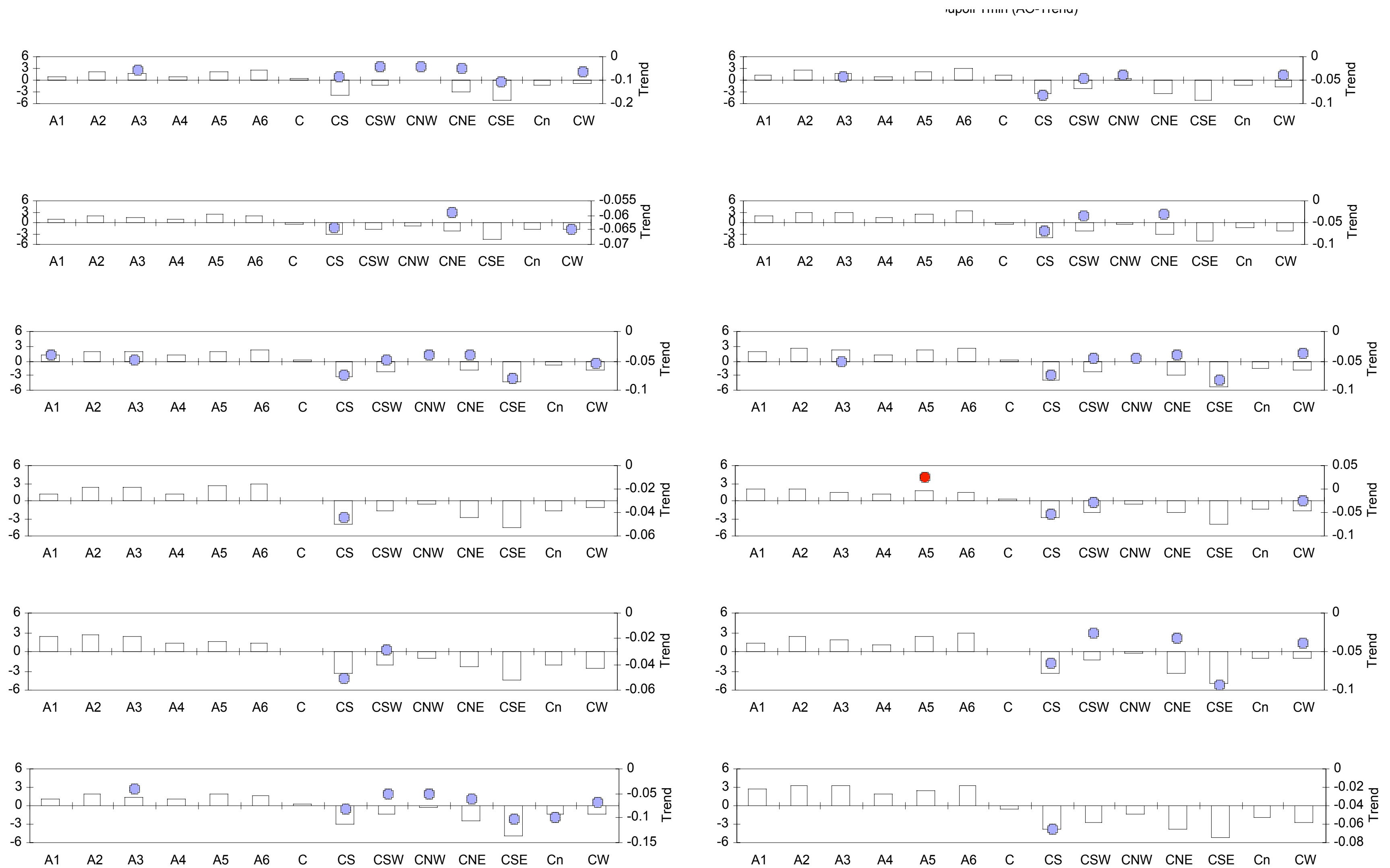

Figure 9e. Anomalies (__-bars) and trend of minimum Temperature (positive trends with red circles and negative trends with blue circles) by circulation type in the case of Year at 500hPa (1958-2000). Only the stat. signif. ones at a level 0.05 are marked

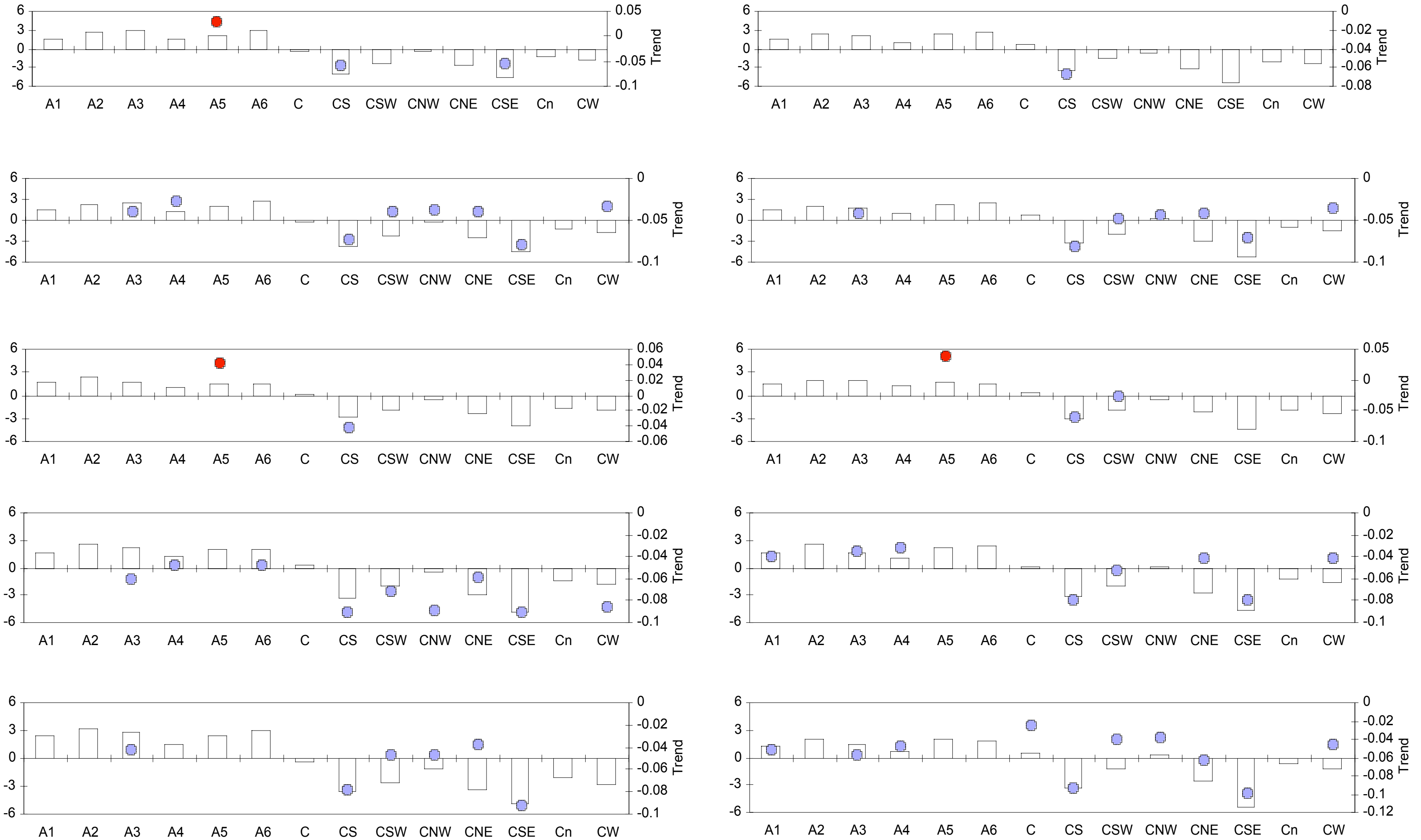

Figure 9e. Anomalies (__-bars) and trend of minimum Temperature (positive trends with red circles and negative trends with blue circles) by circulation type in the case of Year at 500hPa (1958-2000). Only the stat. signif. ones at a level 0.05 are marked

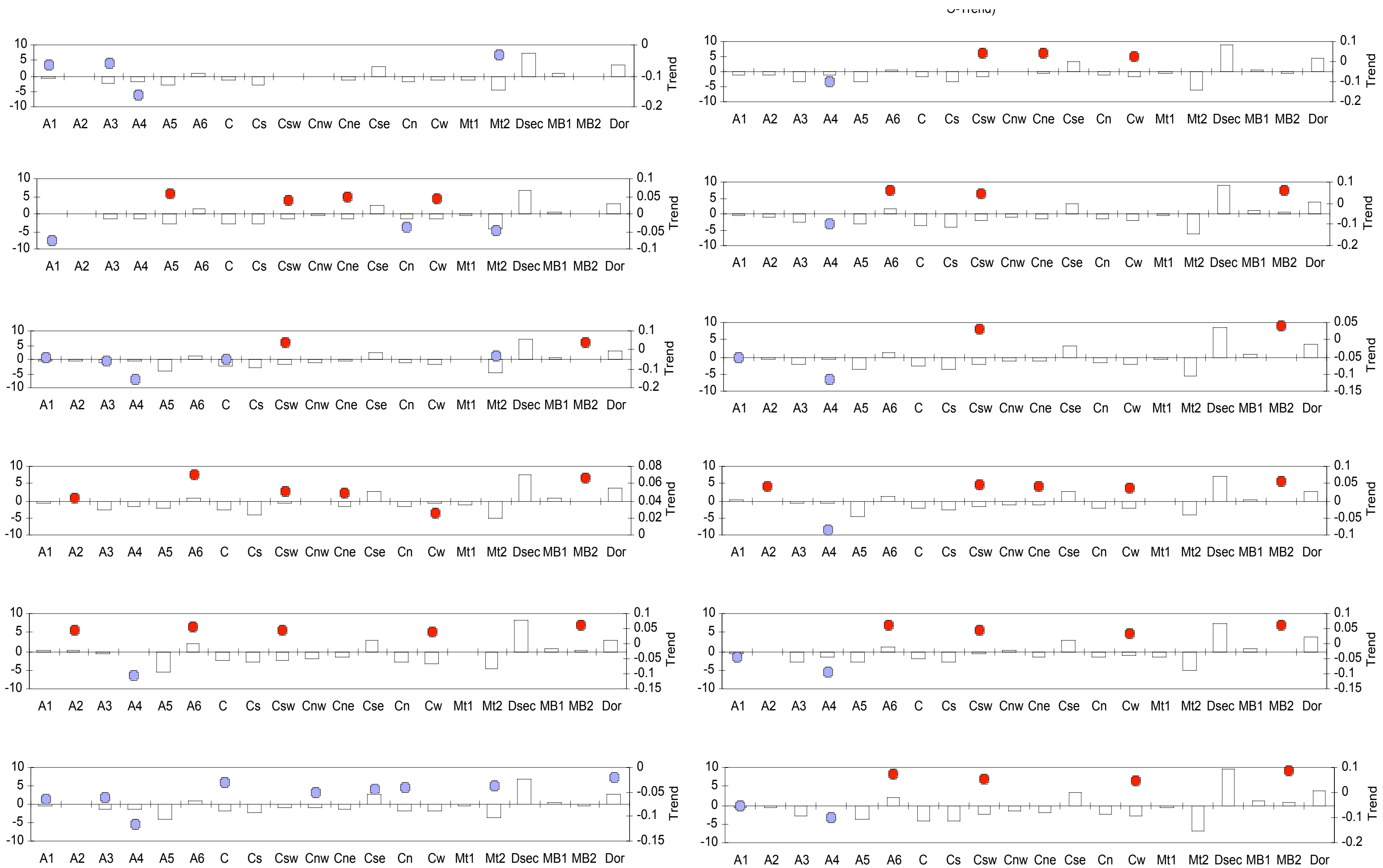

Figure 10a. Anomalies (__-bars) and trend of minimum Temperature (positive trends with red circles and negative trends with blue circles) by circulation type in the case of Winter at SLP (1958-2000). Only the stat. signif. ones at a level 0.05 are marked

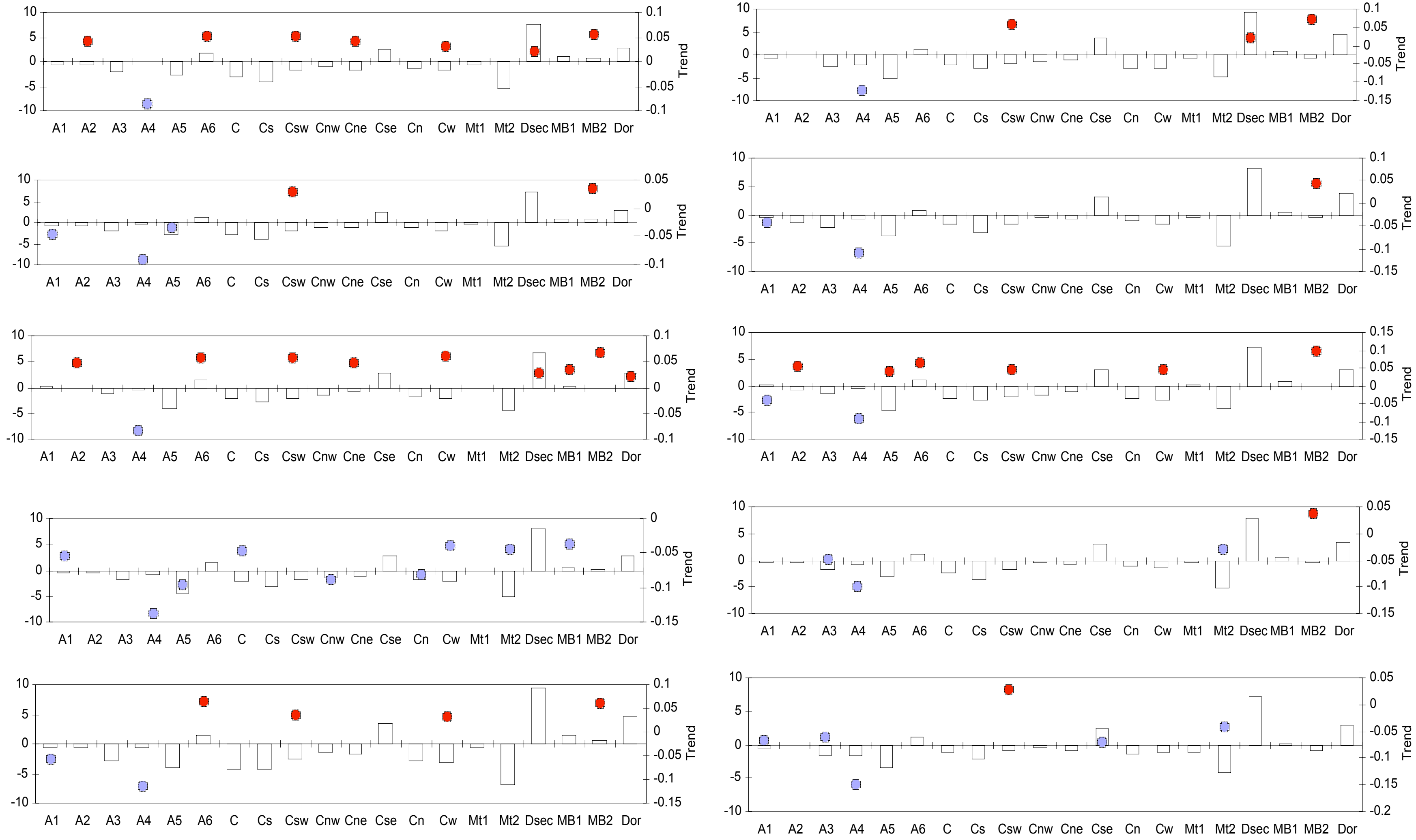

Figure 10a. Anomalies (__-bars) and trend of minimum Temperature (positive trends with red circles and negative trends with blue circles) by circulation type in the case of Winter at SLP (1958-2000). Only the stat. signif. ones at a level 0.05 are marked

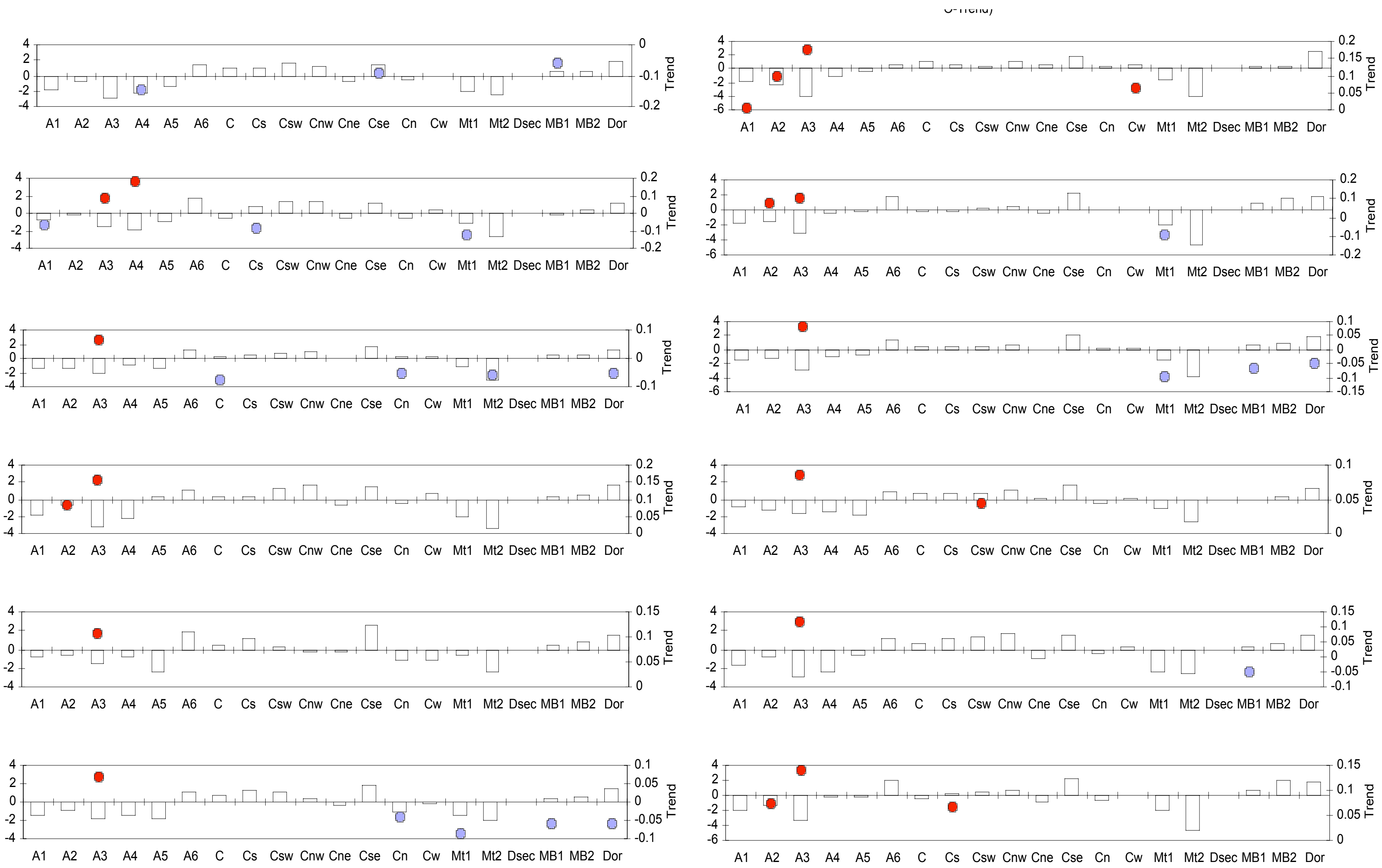

Figure 10b. Anomalies (__-bars) and trend of minimum Temperature (positive trends with red circles and negative trends with blue circles) by circulation type in the case of Spring at SLP (1958-2000). Only the stat. signif. ones at a level 0.05 are marked

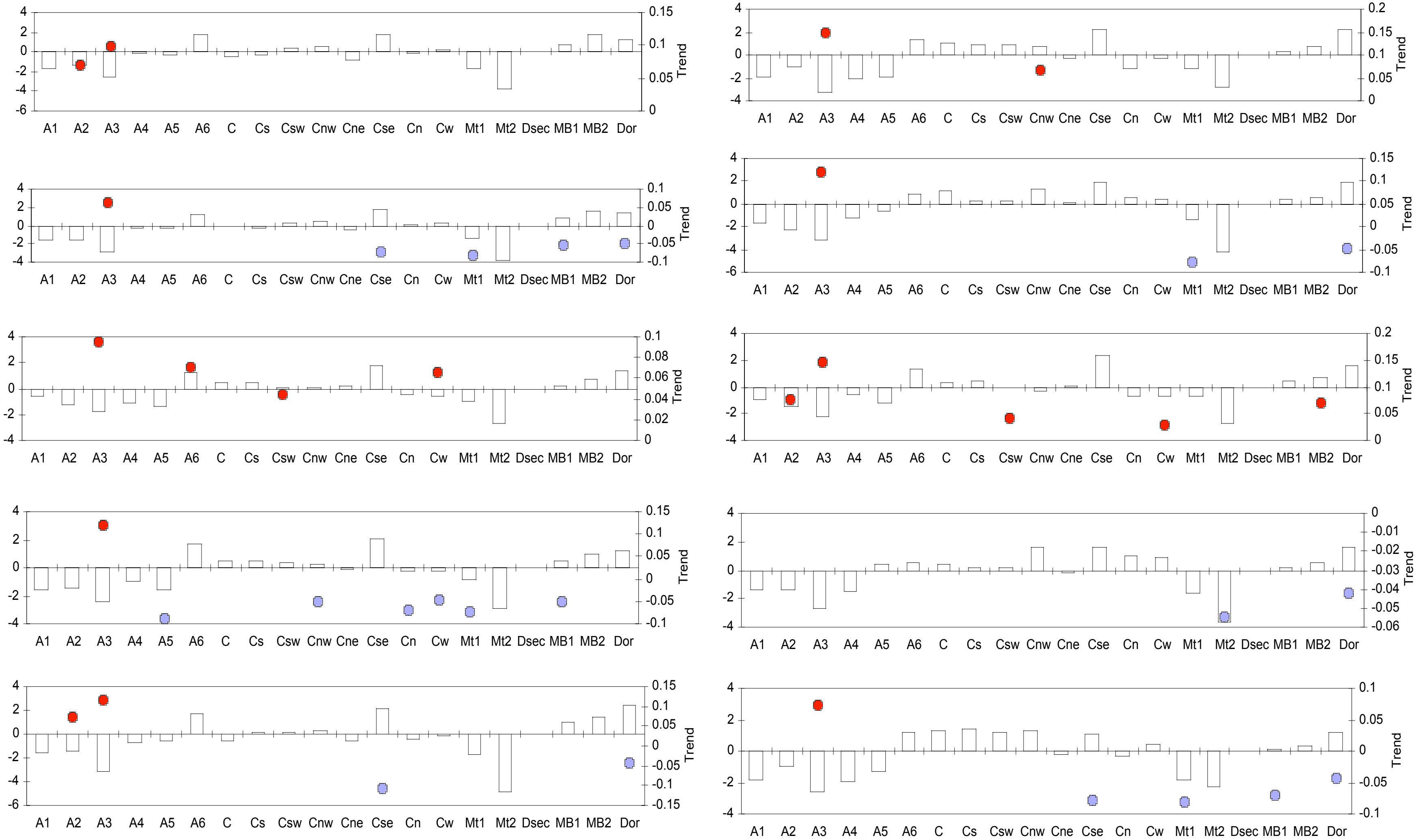

Figure 10b. Anomalies (__-bars) and trend of minimum Temperature (positive trends with red circles and negative trends with blue circles) by circulation type in the case of Spring at SLP (1958-2000). Only the stat. signif. ones at a level 0.05 are marked

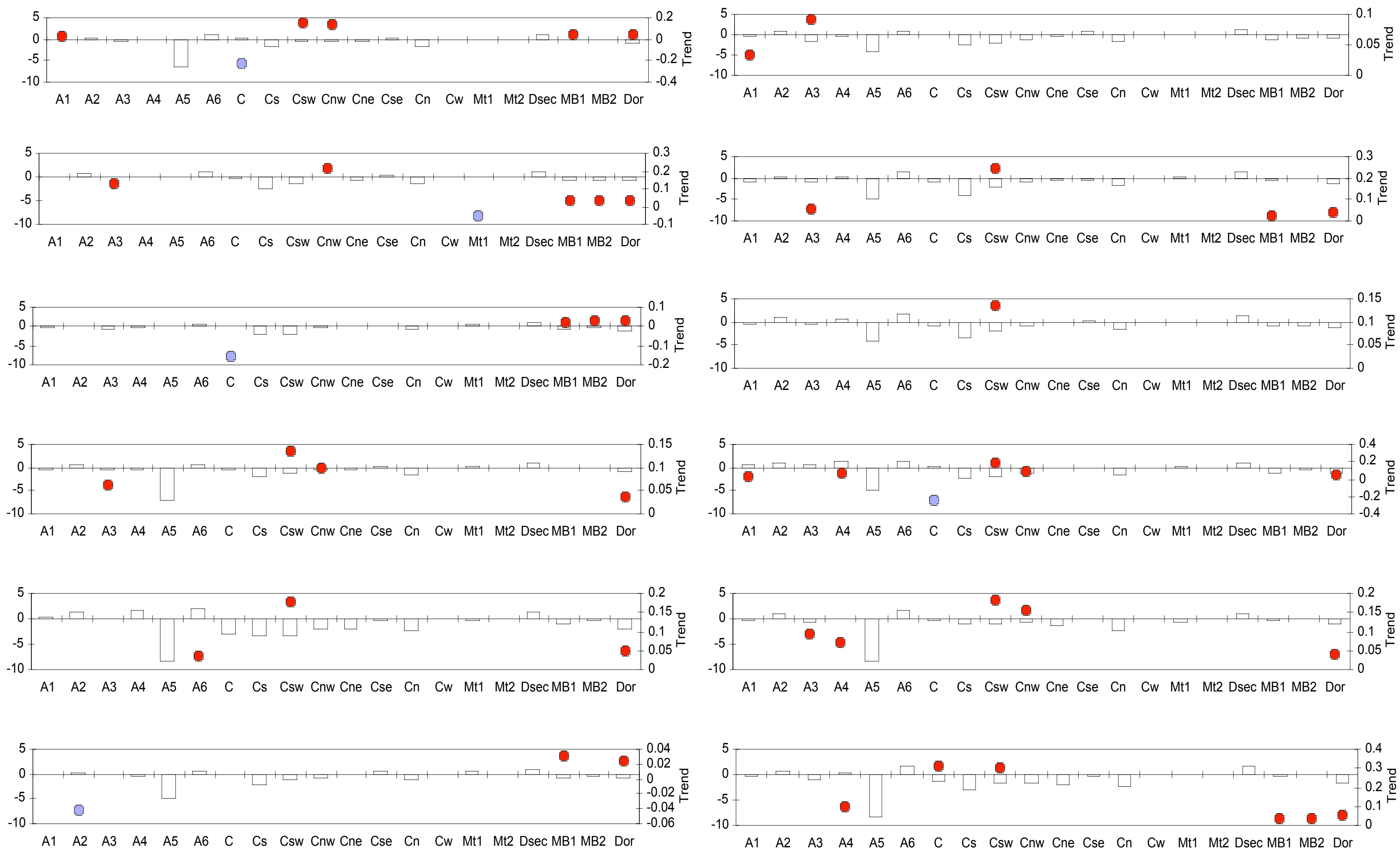

Figure 10c. Anomalies (__-bars) and trend of minimum Temperature (positive trends with red circles and negative trends with blue circles) by circulation type in the case of Summer at SLP (1958-2000). Only the stat. signif. ones at a level 0.05 are marked

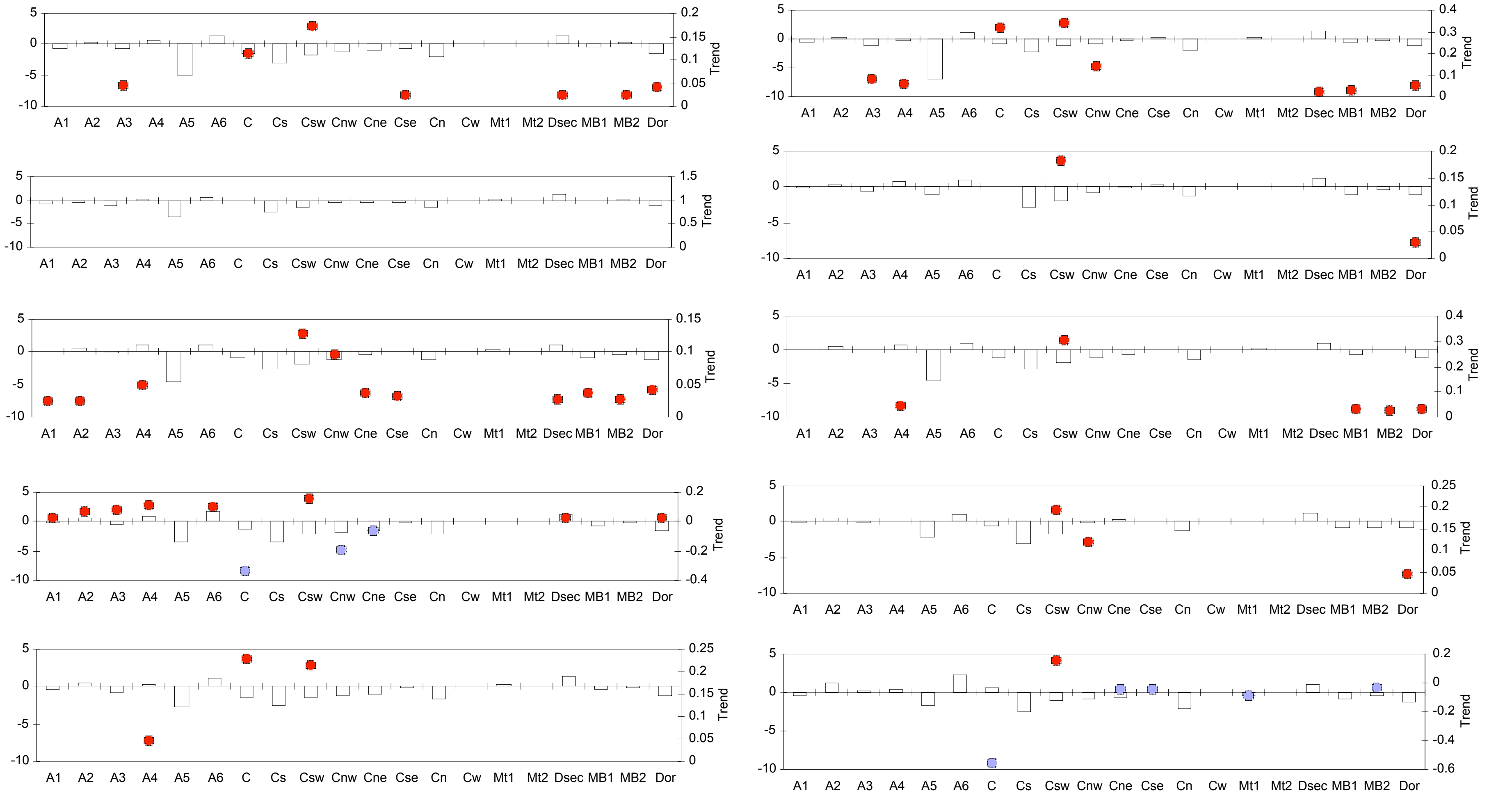

Figure 10c. Anomalies (__-bars) and trend of minimum Temperature (positive trends with red circles and negative trends with blue circles) by circulation type in the case of Summer at SLP (1958-2000). Only the stat. signif. ones at a level 0.05 are marked

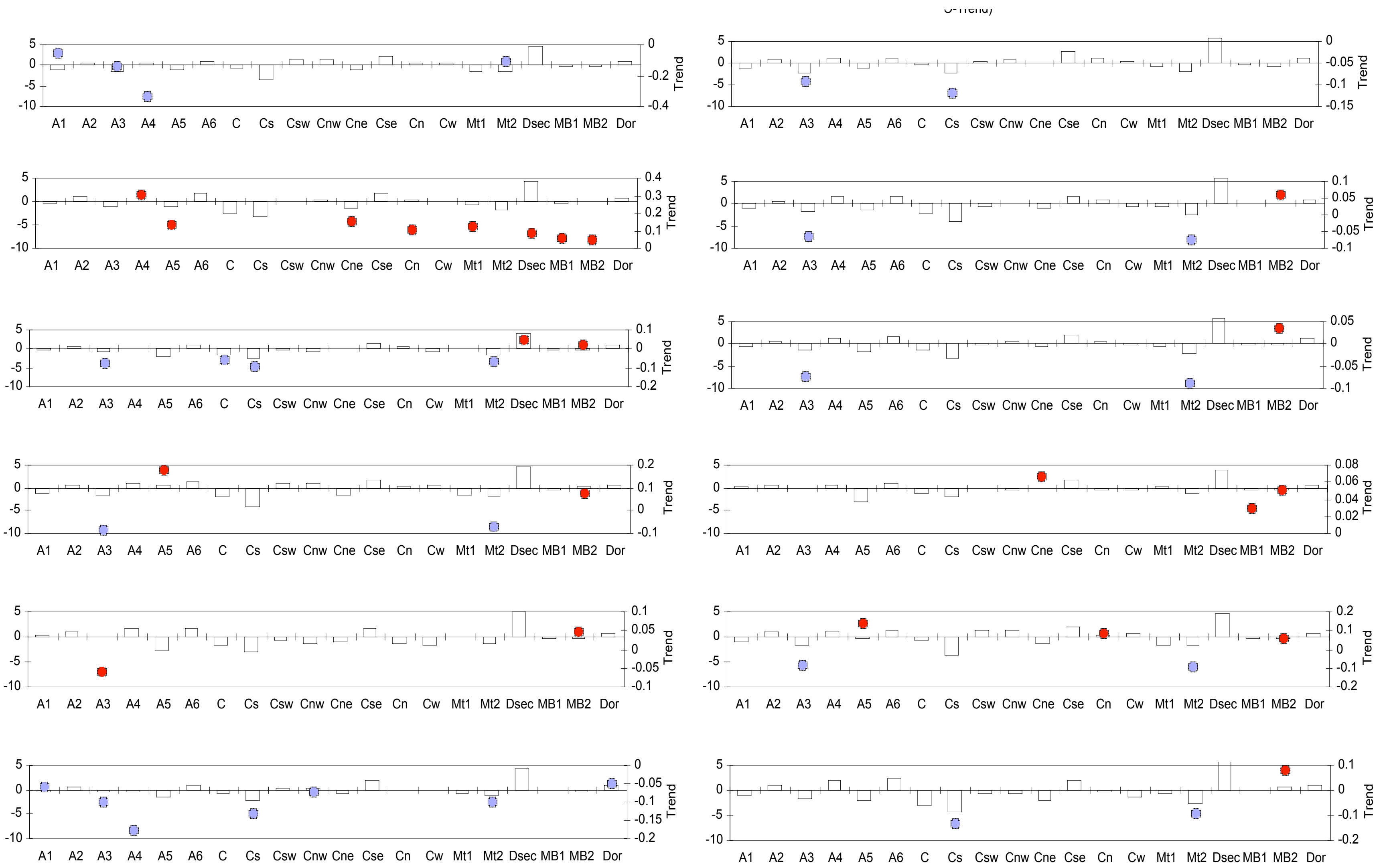

Figure 10d. Anomalies (__-bars) and trend of minimum Temperature (positive trends with red circles and negative trends with blue circles) by circulation type in the case of Autumn at SLP (1958-2000). Only the stat. signif. ones at a level 0.05 are marked

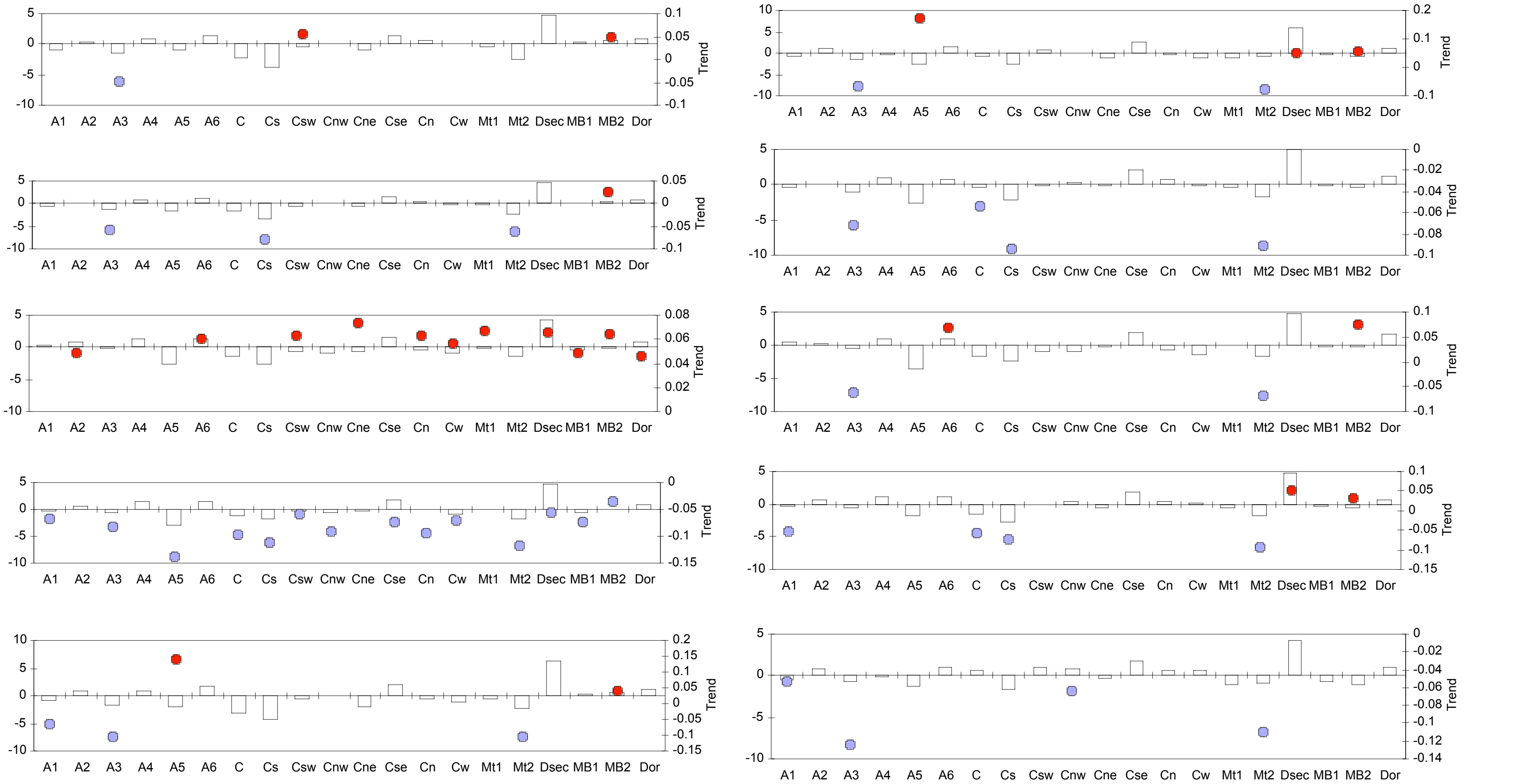

Figure 10d. Anomalies (__-bars) and trend of minimum Temperature (positive trends with red circles and negative trends with blue circles) by circulation type in the case of Autumn at SLP (1958-2000). Only the stat. signif. ones at a level 0.05 are marked

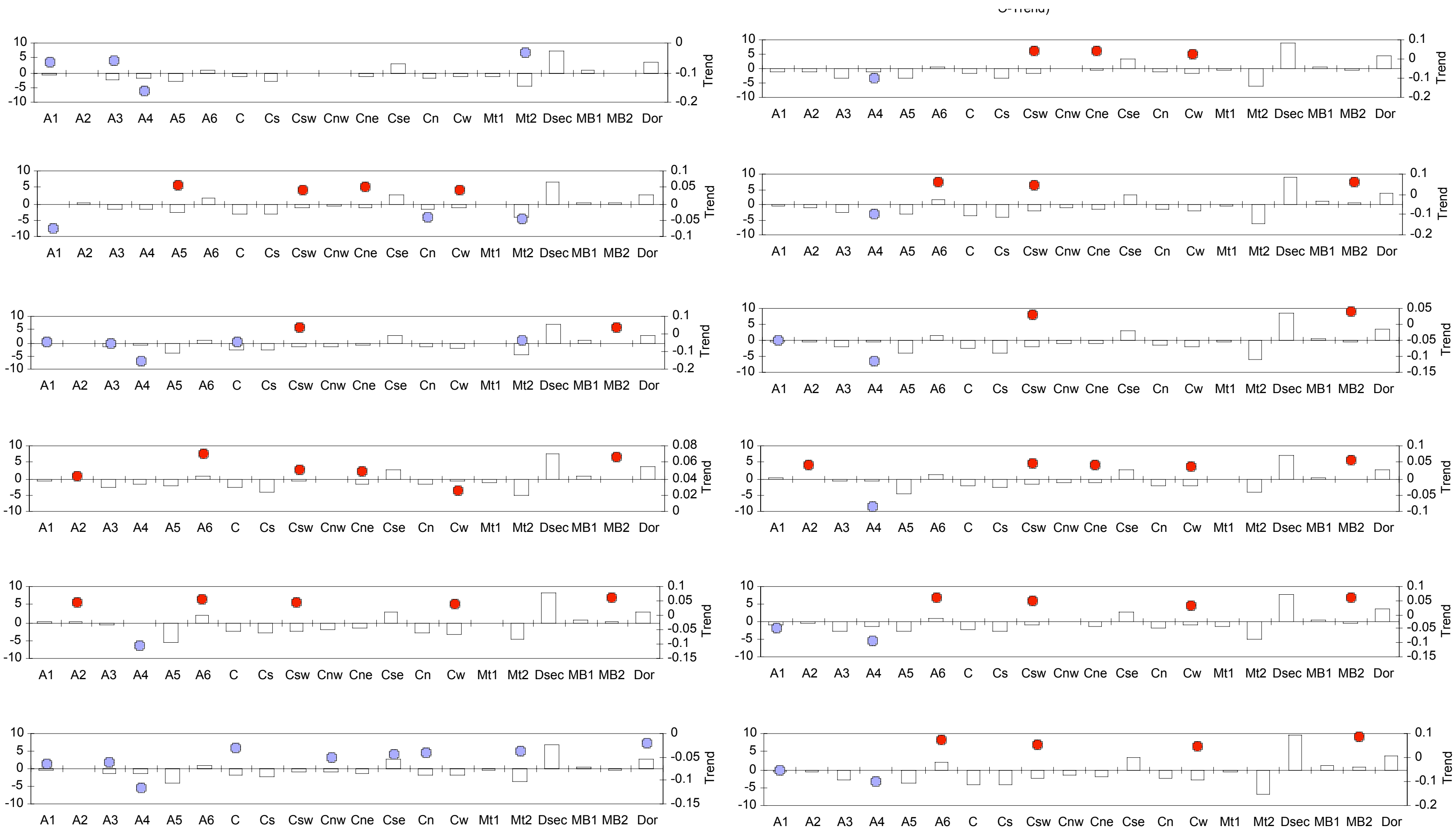

Figure 10e. Anomalies (__-bars) and trend of minimum Temperature (positive trends with red circles and negative trends with blue circles) by circulation type in the case of Year at SLP (1958-2000). Only the stat. signif. ones at a level 0.05 are marked

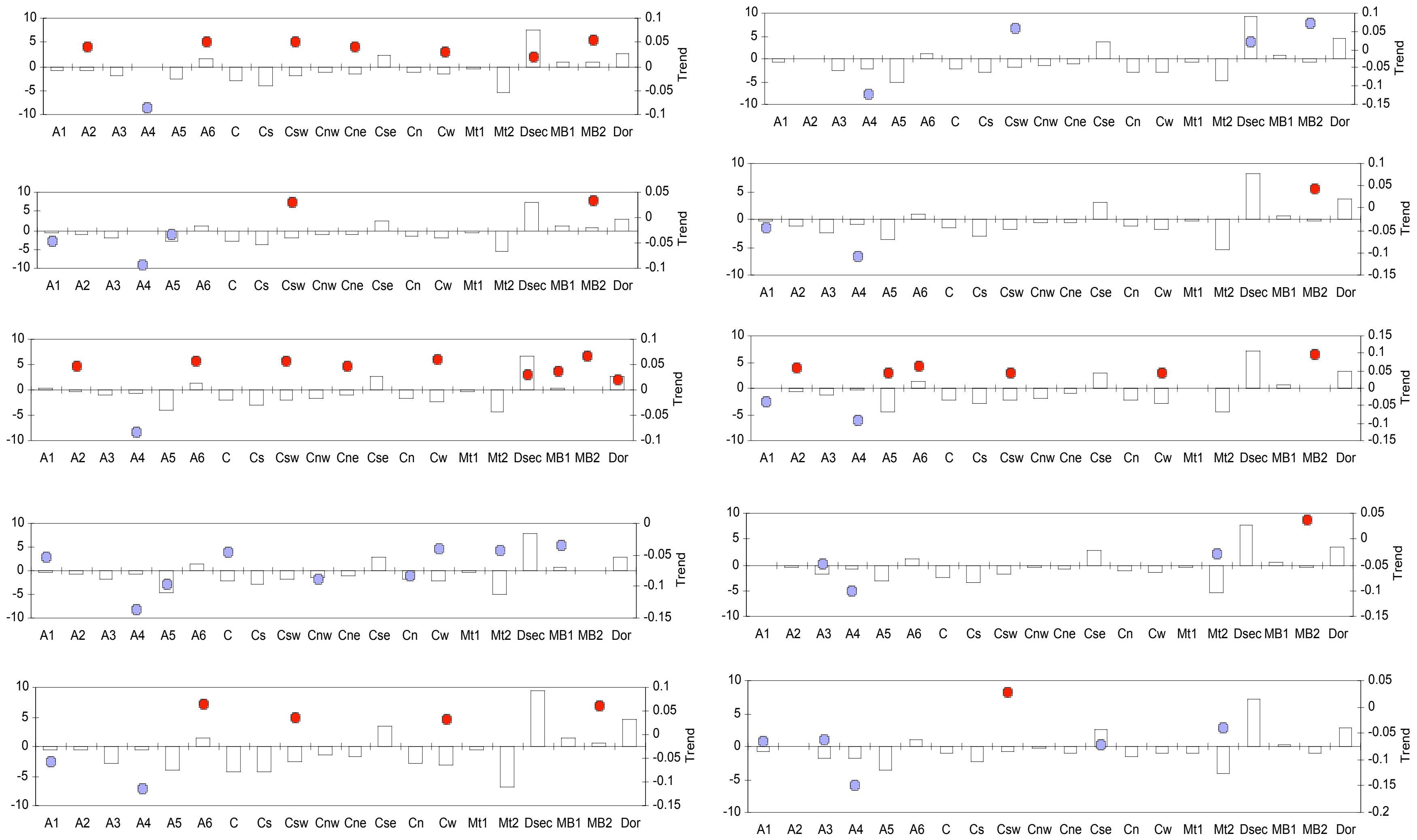

Figure 10e. Anomalies (__-bars) and trend of minimum Temperature (positive trends with red circles and negative trends with blue circles) by circulation type in the case of Year at SLP (1958-2000). Only the stat. signif. ones at a level 0.05 are marked

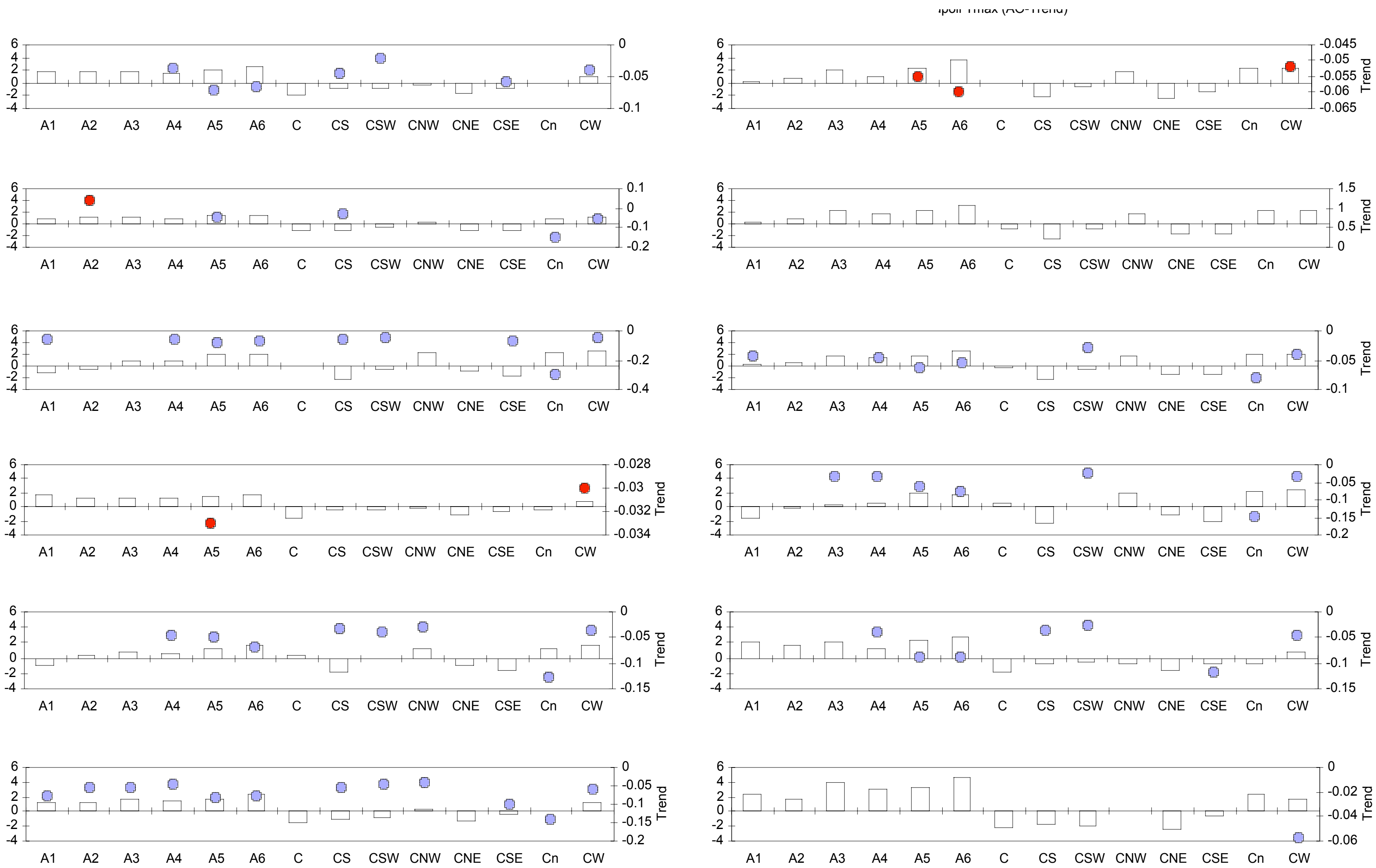

Figure 11a. Anomalies (__ -bars) and trends (red circles positive - blue circles negative) of maximum Temperature by circulation type in the case of Winter at 500hPa (1958-2000). Only the stat. signif. ones at a level 0.05 are marked

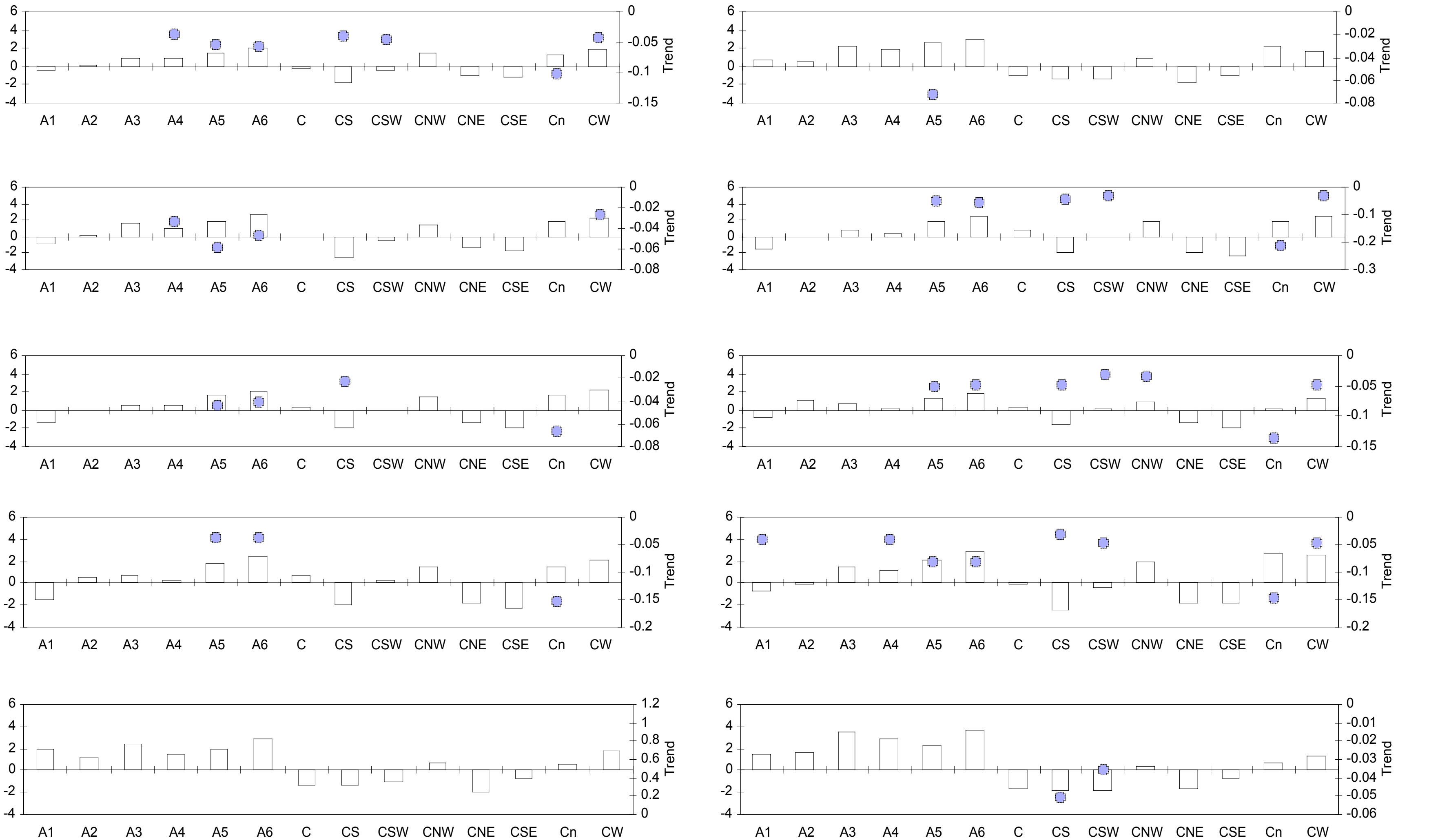

Figure 11a. Anomalies (__ -bars) and trends (red circles positive - blue circles negative) of maximum Temperature by circulation type in the case of Winter at 500hPa (1958-2000). Only the stat. signif. ones at a level 0.05 are marked

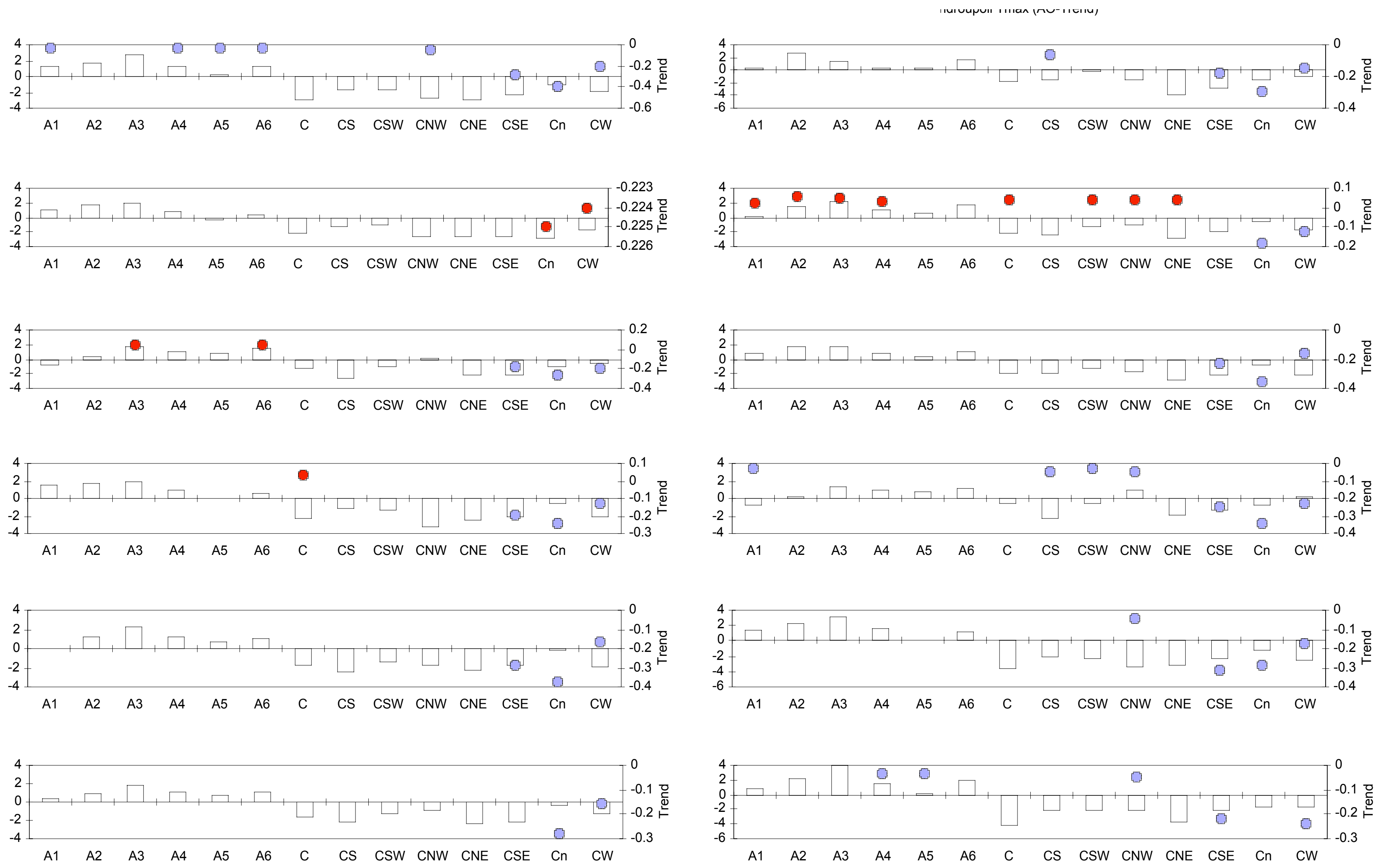

Figure 11b. Anomalies (__ -bars) and trends (red circles positive - blue circles negative) of maximum Temperature by circulation type in the case of Srping at 500hPa (1958-2000). Only the stat. signif. ones at a level 0.05 are marked

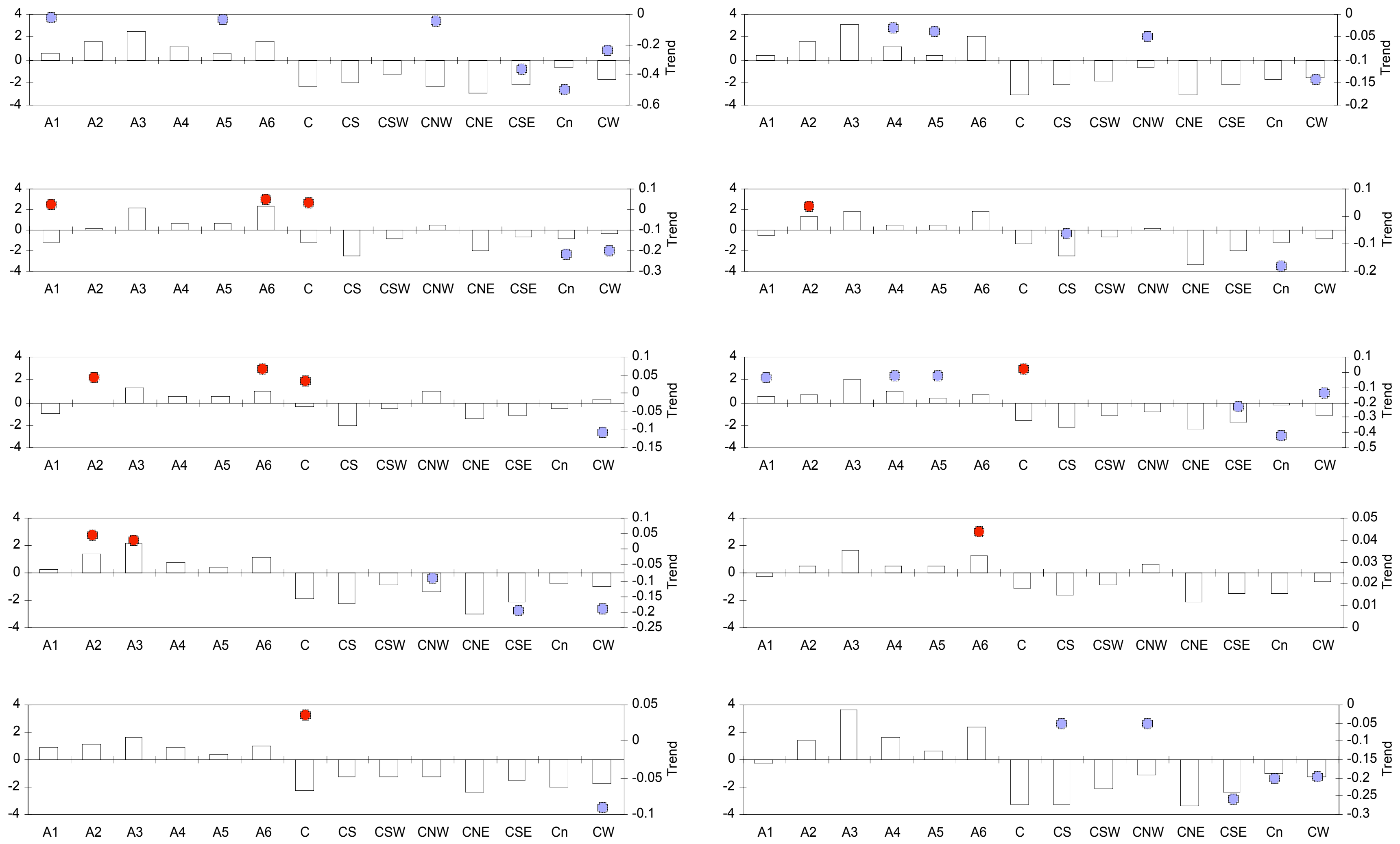

Figure 11b. Anomalies (__ -bars) and trends (red circles positive - blue circles negative) of maximum Temperature by circulation type in the case of Srping at 500hPa (1958-2000). Only the stat. signif. ones at a level 0.05 are marked

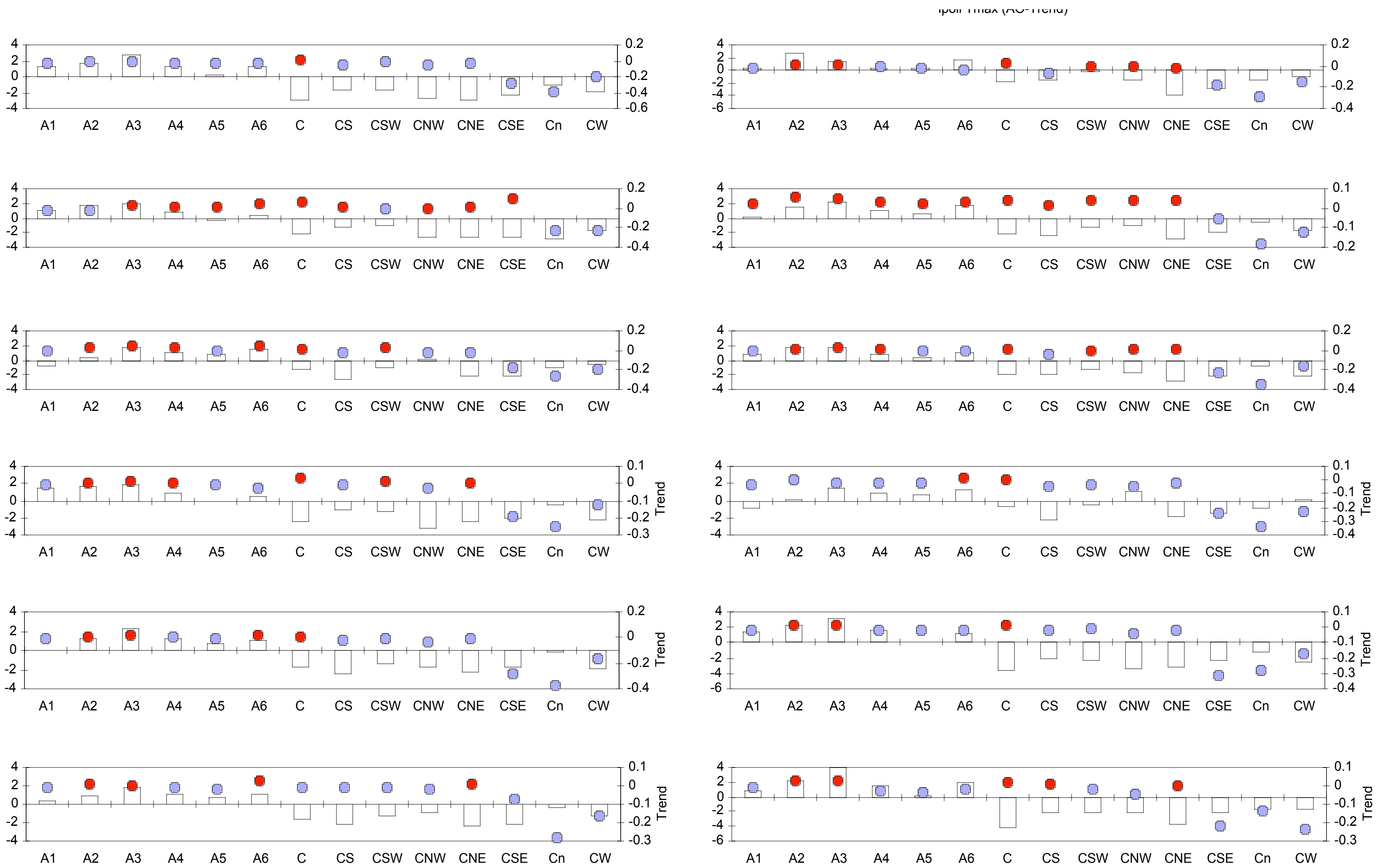

Figure 11c. Anomalies (__ -bars) and trends (red circles positive - blue circles negative) of maximum Temperature by circulation type in the case of Summer at 500hPa (1958-2000). Only the stat. signif. ones at a level 0.05 are marked

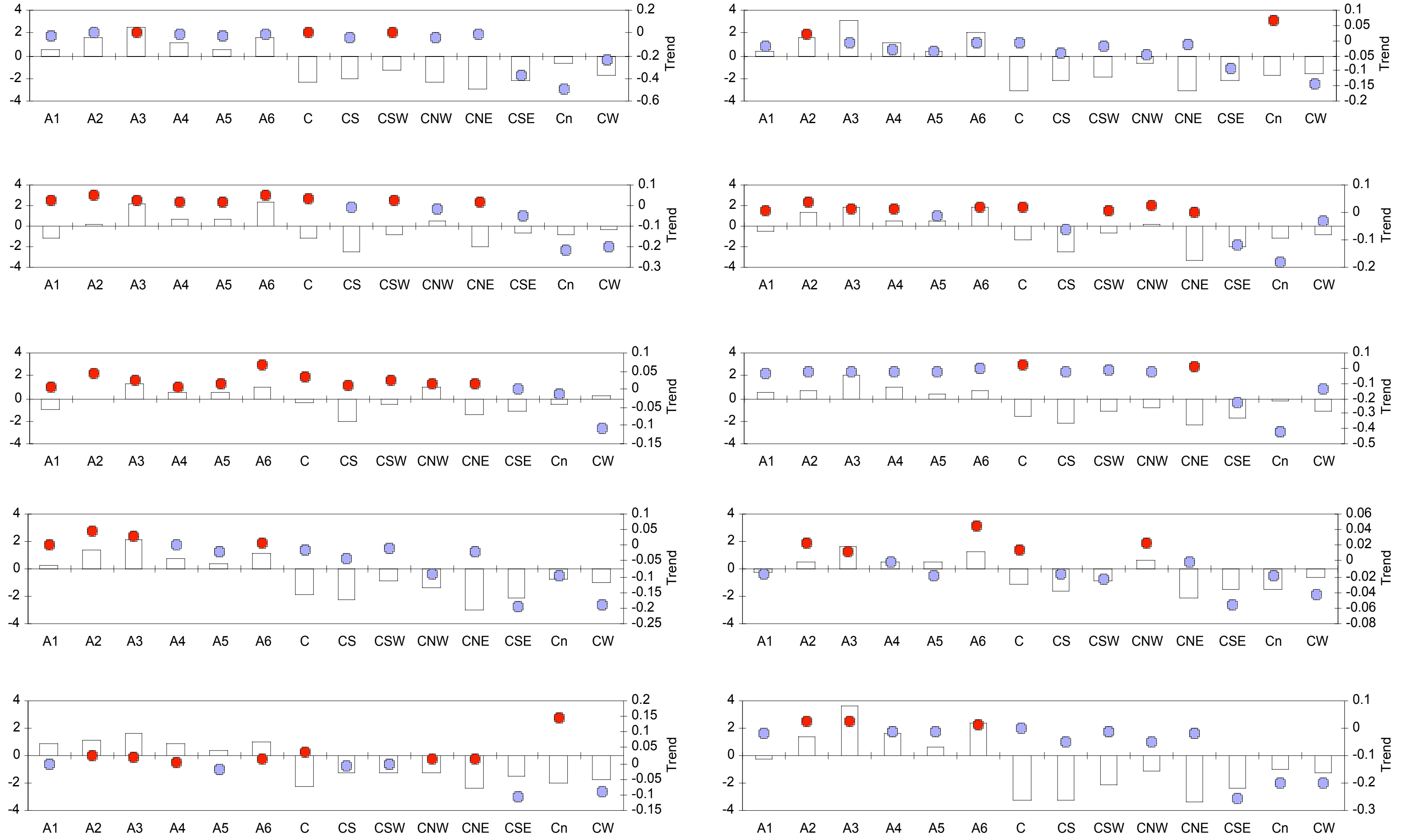

Figure 11c. Anomalies (__ -bars) and trends (red circles positive - blue circles negative) of maximum Temperature by circulation type in the case of Summer at 500hPa (1958-2000). Only the stat. signif. ones at a level 0.05 are marked

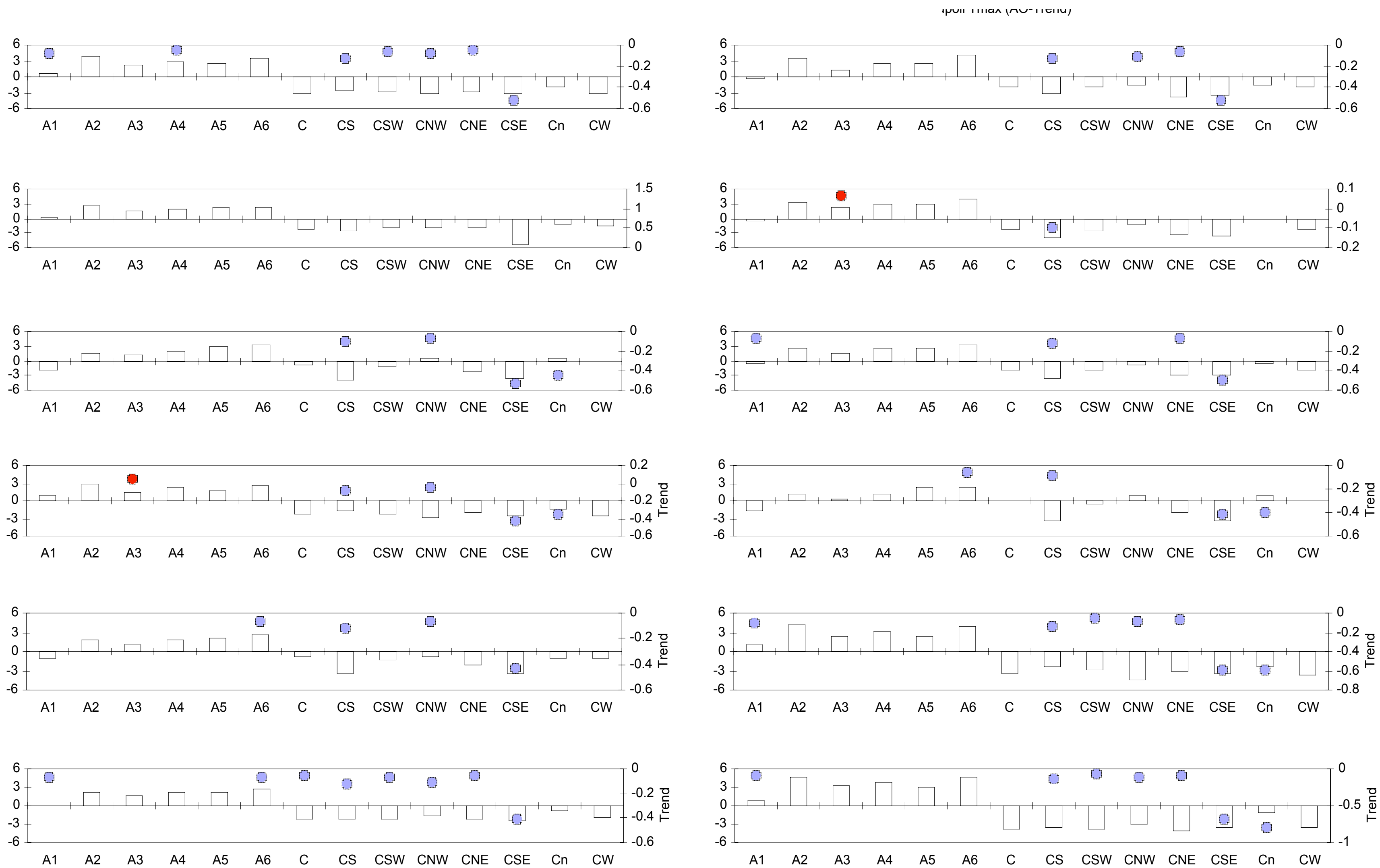

Figure 11d. Anomalies (__ -bars) and trends (red circles positive - blue circles negative) of maximum Temperature by circulation type in the case of Autumn at 500hPa (1958-2000). Only the stat. signif. ones at a level 0.05 are marked

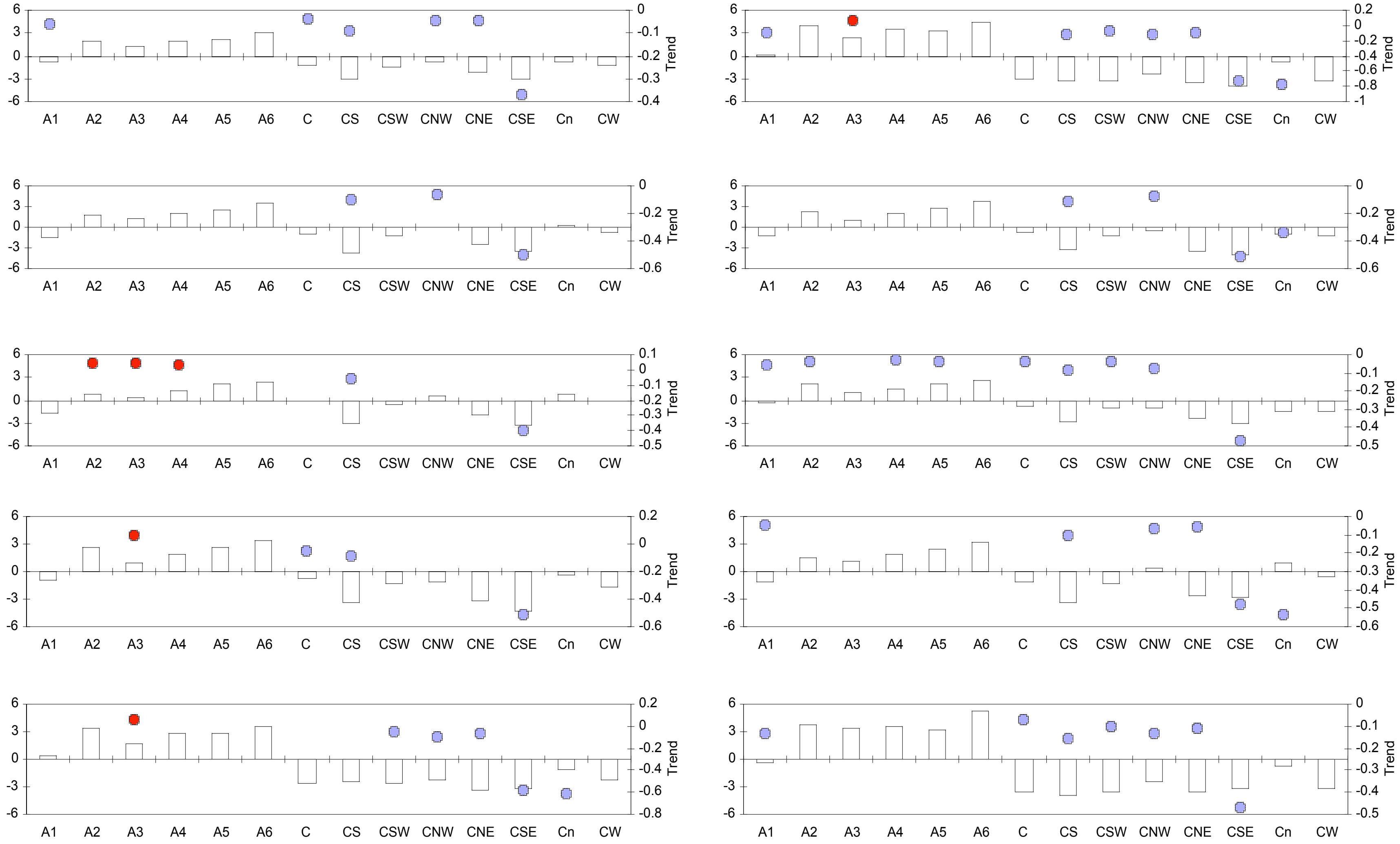

Figure 11d. Anomalies (__ -bars) and trends (red circles positive - blue circles negative) of maximum Temperature by circulation type in the case of Autumn at 500hPa (1958-2000). Only the stat. signif. ones at a level 0.05 are marked

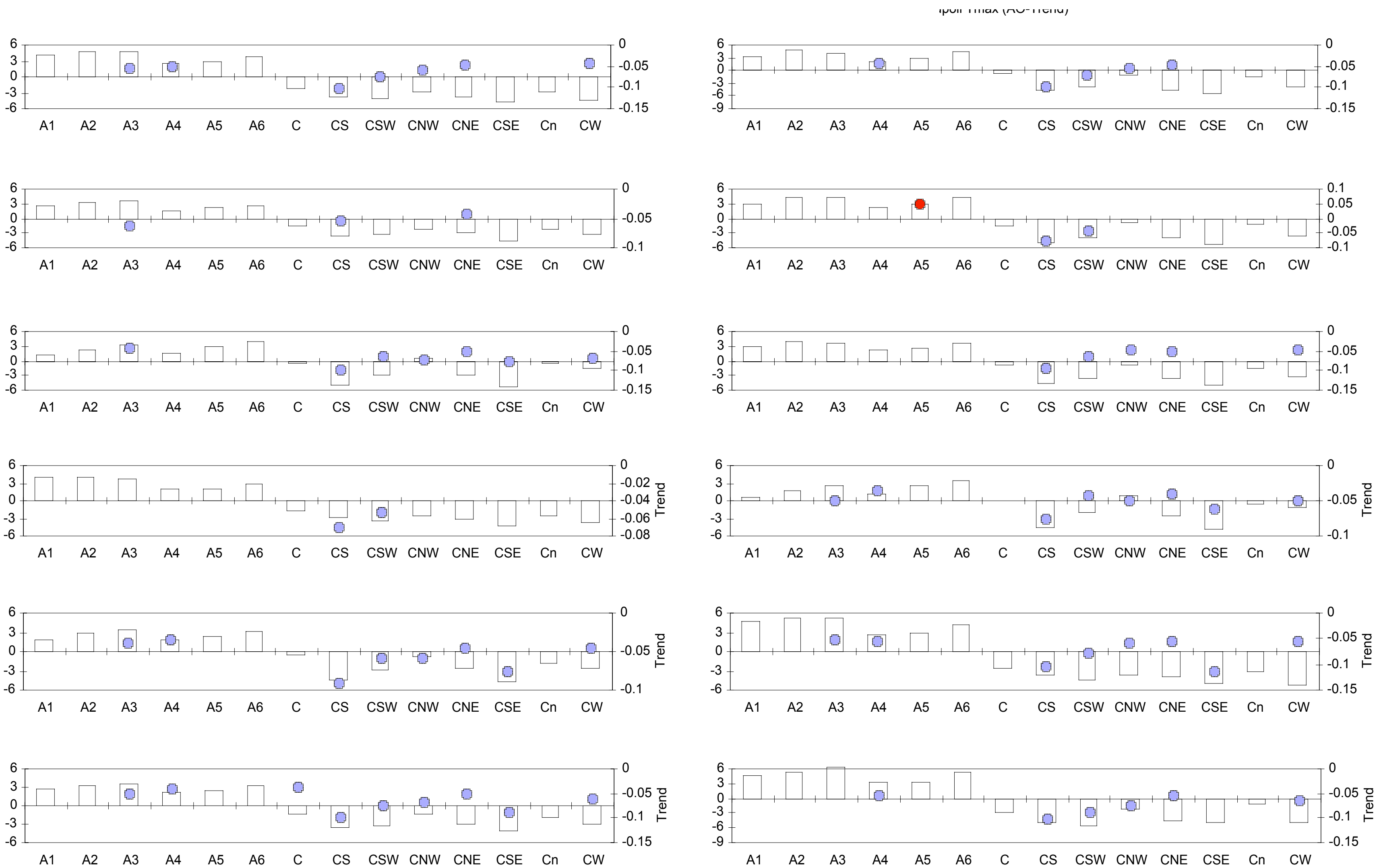

Figure 11e. Anomalies (__ -bars) and trends (red circles positive - blue circles negative) of maximum Temperature by circulation type in the case of Year at 500hPa (1958-2000). Only the stat. signif. ones at a level 0.05 are marked

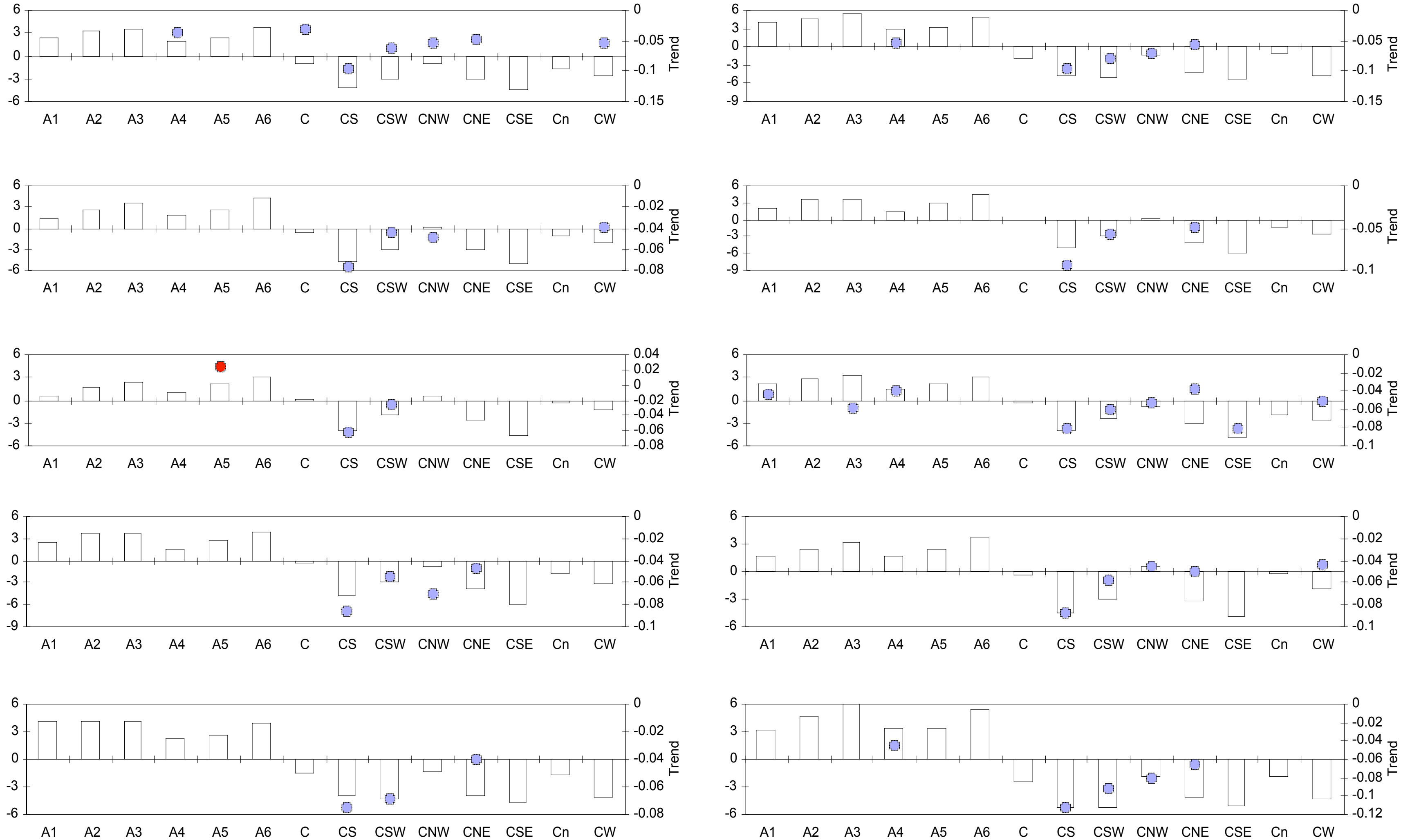

Figure 11e. Anomalies (__ -bars) and trends (red circles positive - blue circles negative) of maximum Temperature by circulation type in the case of Year at 500hPa (1958-2000). Only the stat. signif. ones at a level 0.05 are marked

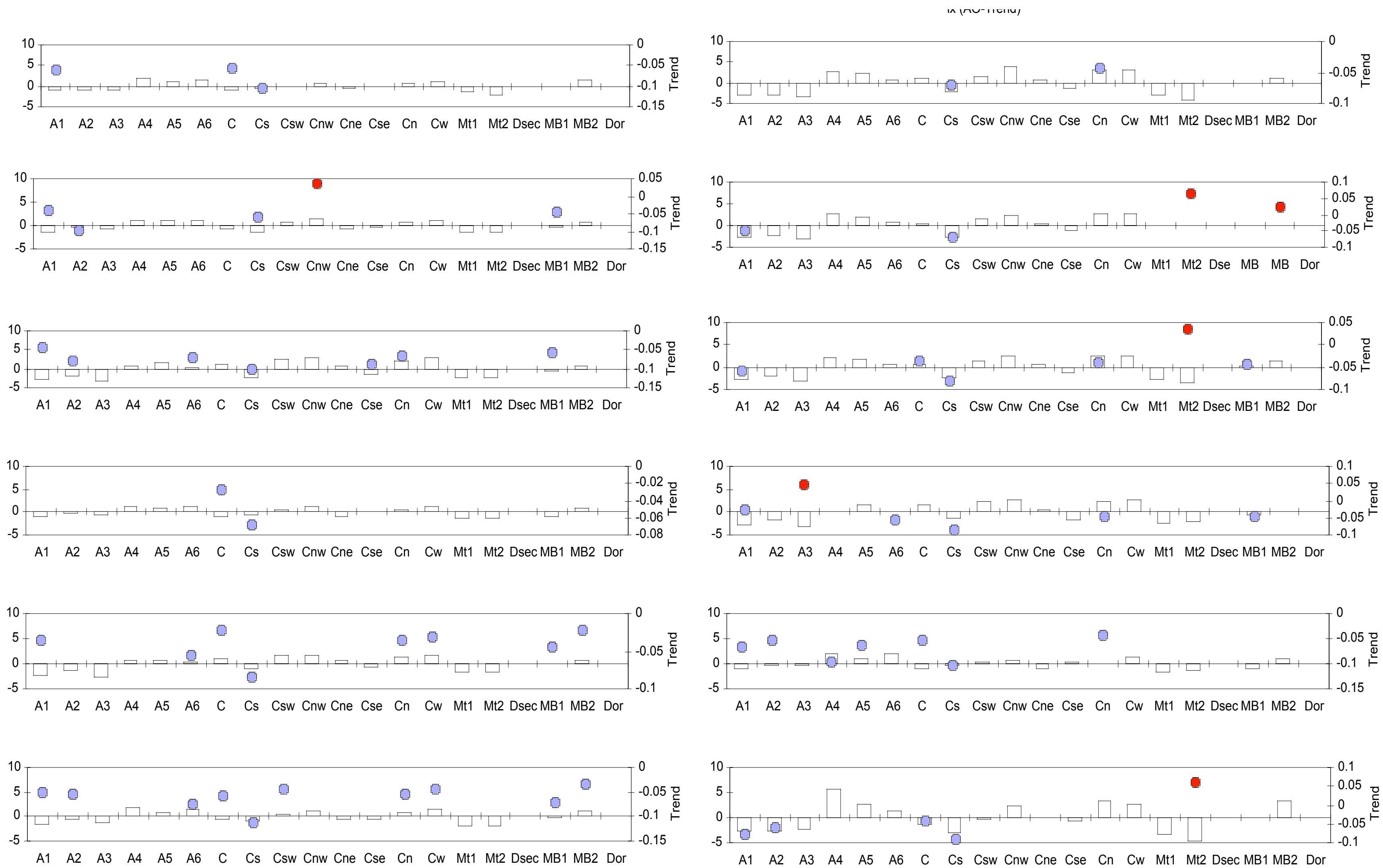

Figure 12a. Anomalies (__-bars) and trend of maximum Temperature (positive trends with red circles and negative trends with blue circles) by circulation type in the case of Winter at SLP (1958-2000). Only the stat. signif. ones at a level 0.05 are marked

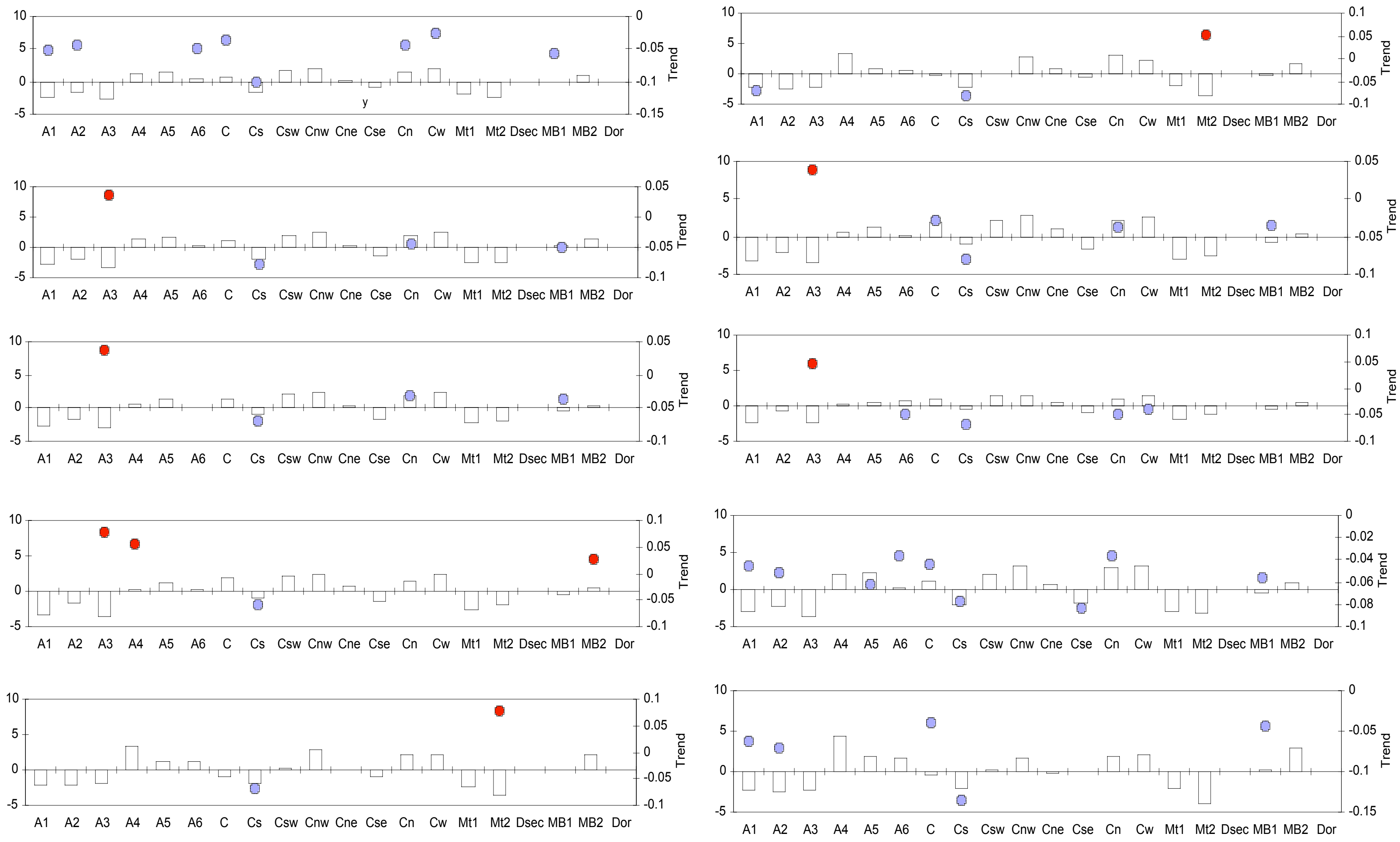

Figure 12a. Anomalies (__-bars) and trend of maximum Temperature (positive trends with red circles and negative trends with blue circles) by circulation type in the case of Winter at SLP (1958-2000). Only the stat. signif. ones at a level 0.05 are marked

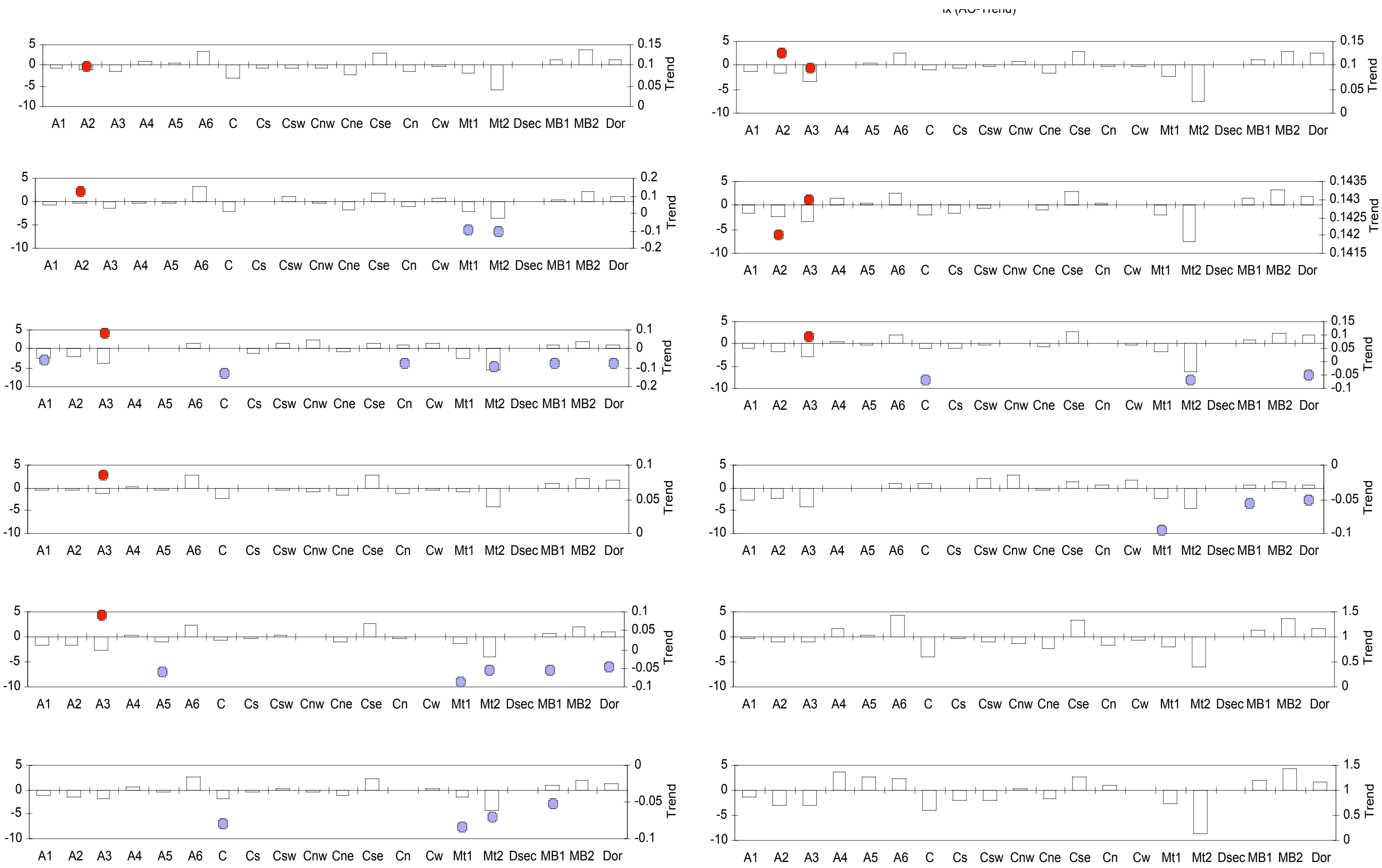

Figure 12b. Anomalies (__-bars) and trend of maximum Temperature (positive trends with red circles and negative trends with blue circles) by circulation type in the case of Spring at SLP (1958-2000). Only the stat. signif. ones at a level 0.05 are marked

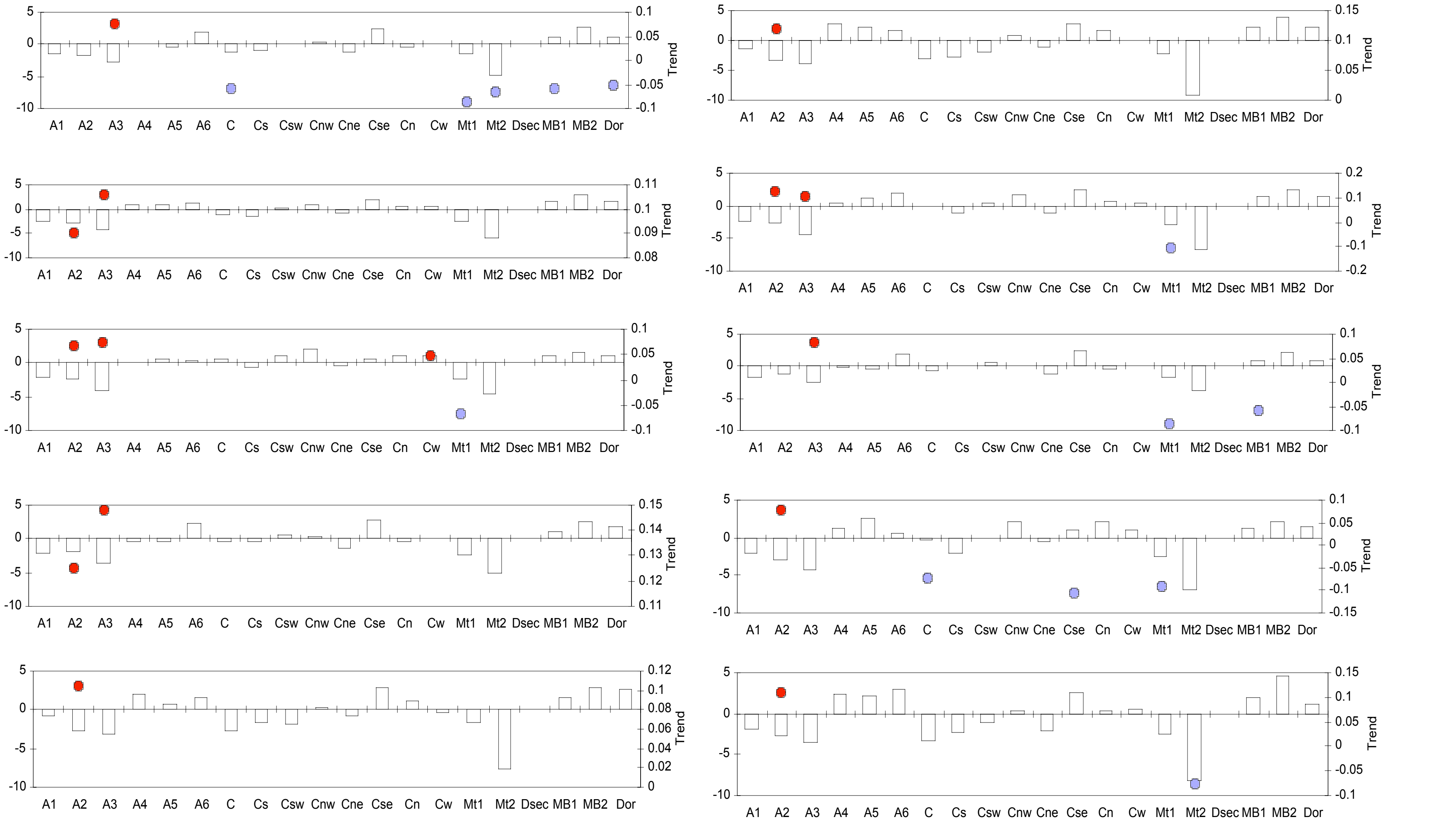

Figure 12b. Anomalies (__-bars) and trend of maximum Temperature (positive trends with red circles and negative trends with blue circles) by circulation type in the case of Spring at SLP (1958-2000). Only the stat. signif. ones at a level 0.05 are marked

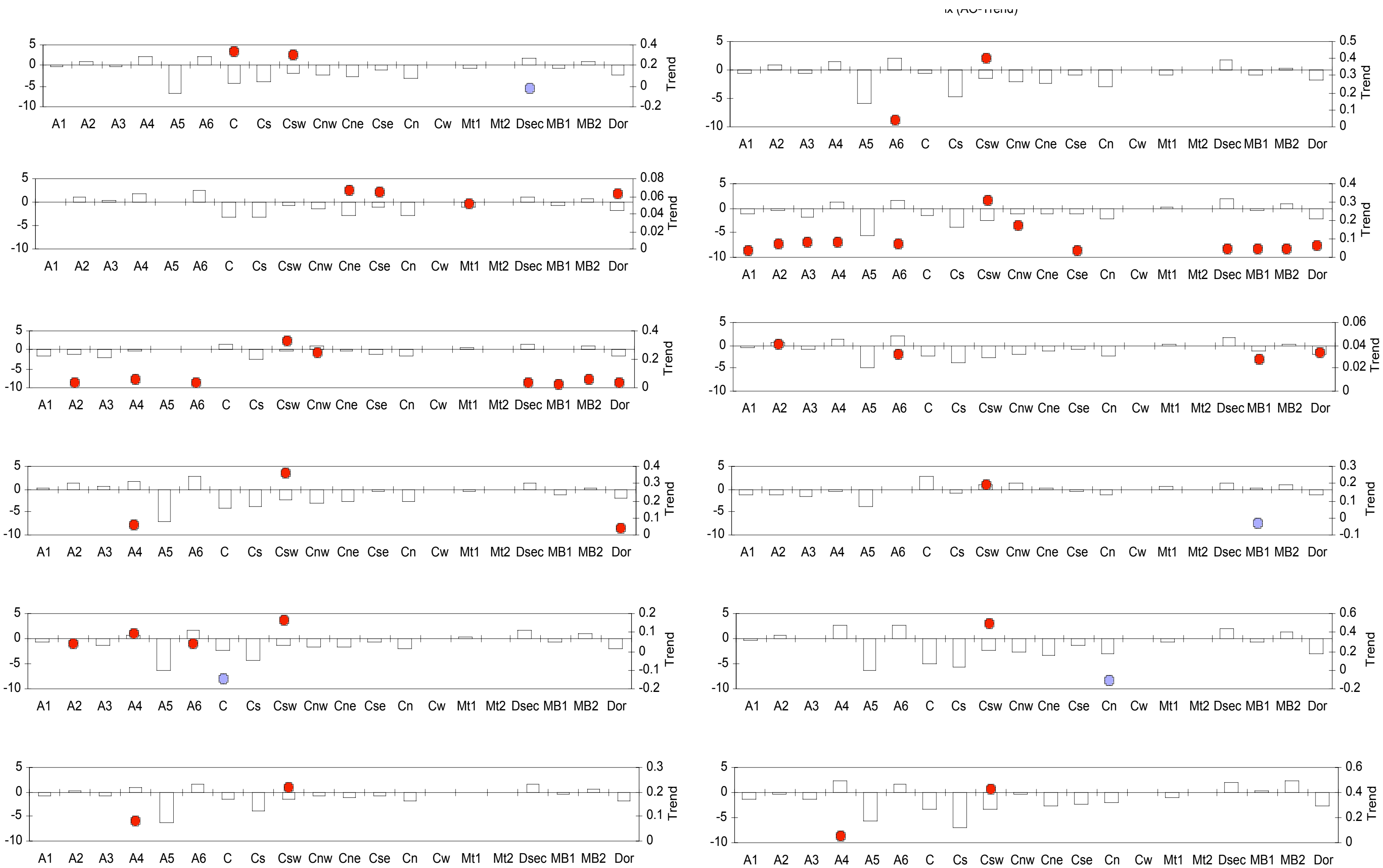

Figure 12c. Anomalies (__-bars) and trend of maximum Temperature (positive trends with red circles and negative trends with blue circles) by circulation type in the case of Summer at SLP (1958-2000). Only the stat. signif. ones at a level 0.05 are marked

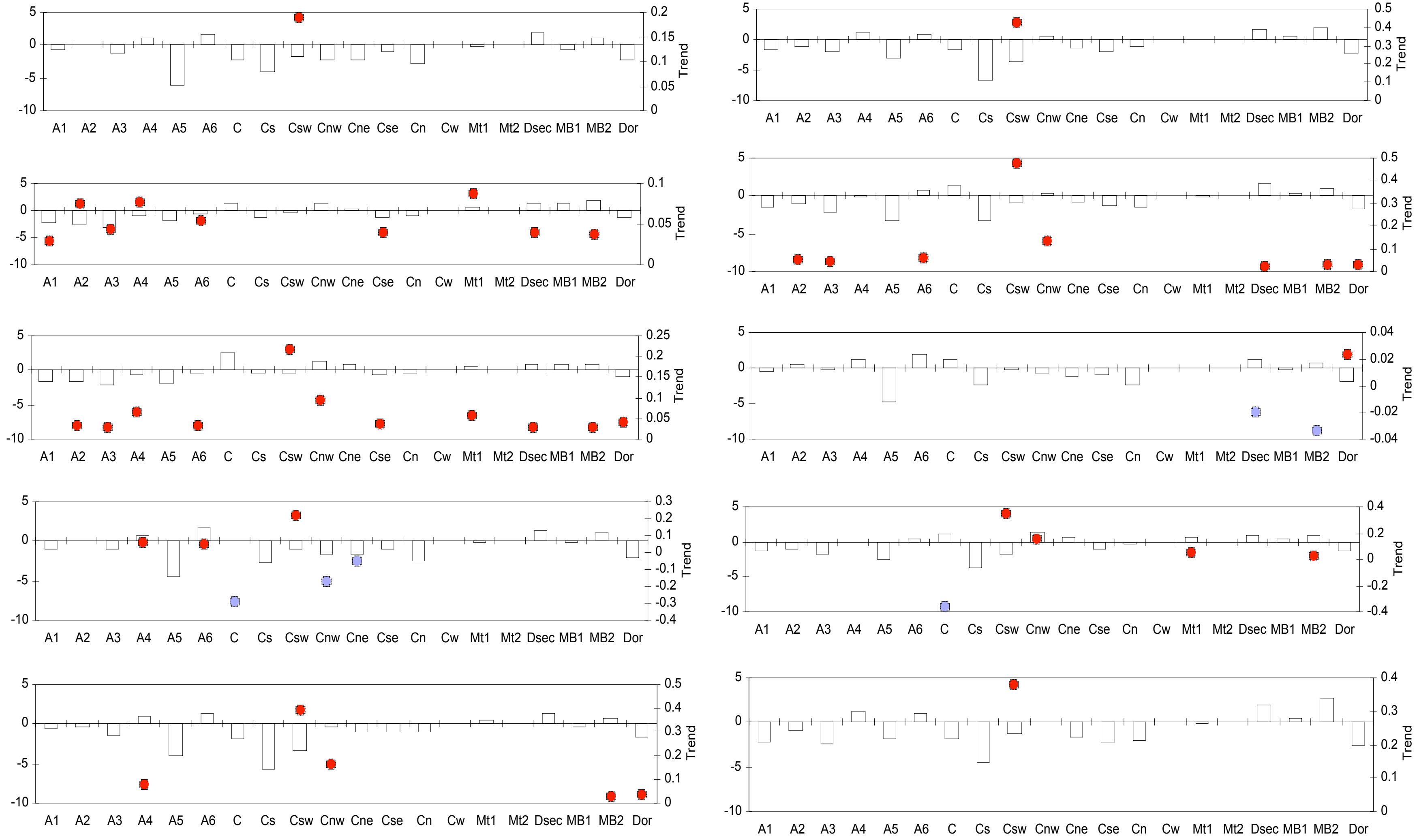

Figure 12c. Anomalies (__-bars) and trend of maximum Temperature (positive trends with red circles and negative trends with blue circles) by circulation type in the case of Summer at SLP (1958-2000). Only the stat. signif. ones at a level 0.05 are marked

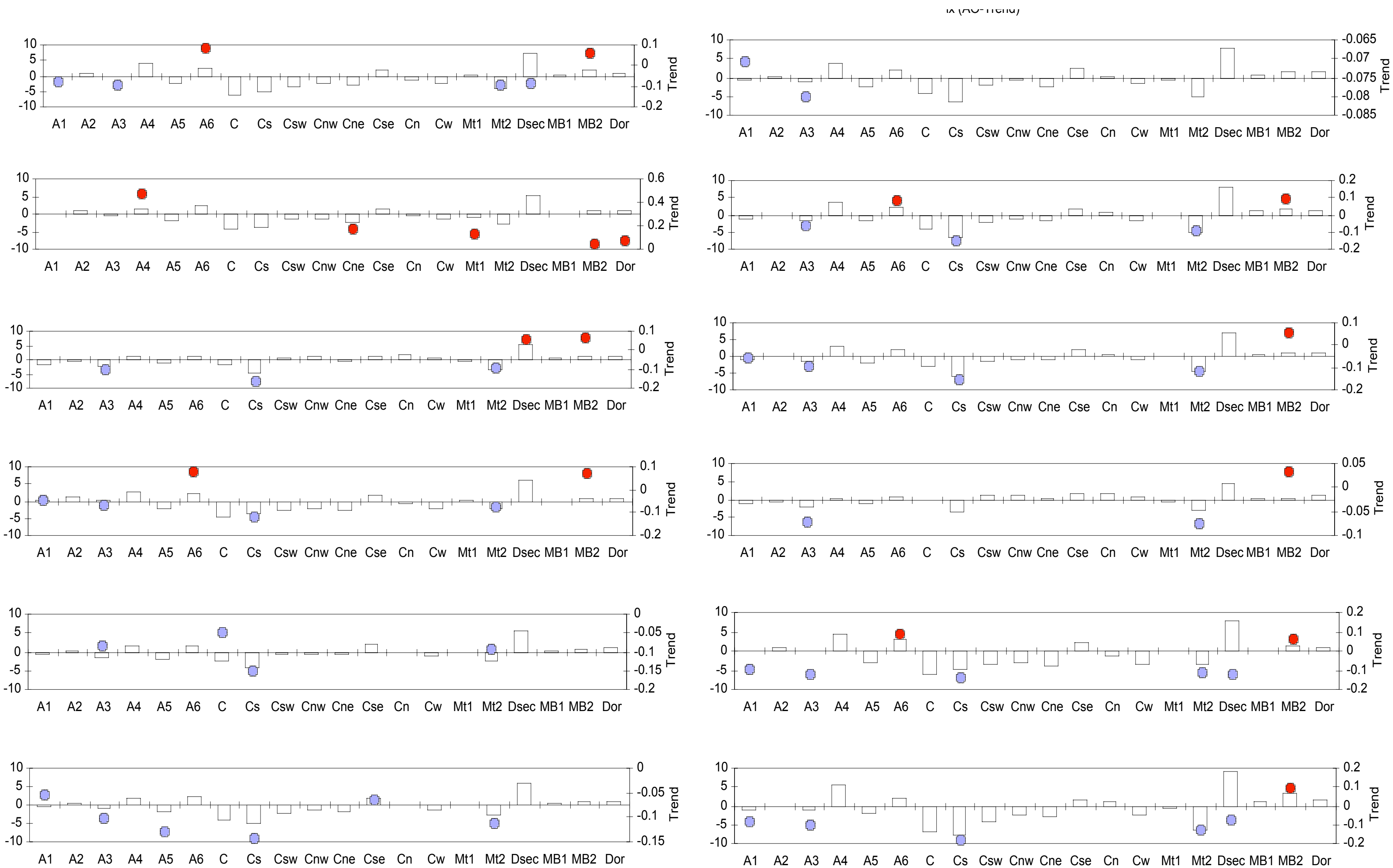

Figure 12d. Anomalies (__-bars) and trend of maximum Temperature (positive trends with red circles and negative trends with blue circles) by circulation type in the case of Autumn at SLP (1958-2000). Only the stat. signif. ones at a level 0.05 are marked

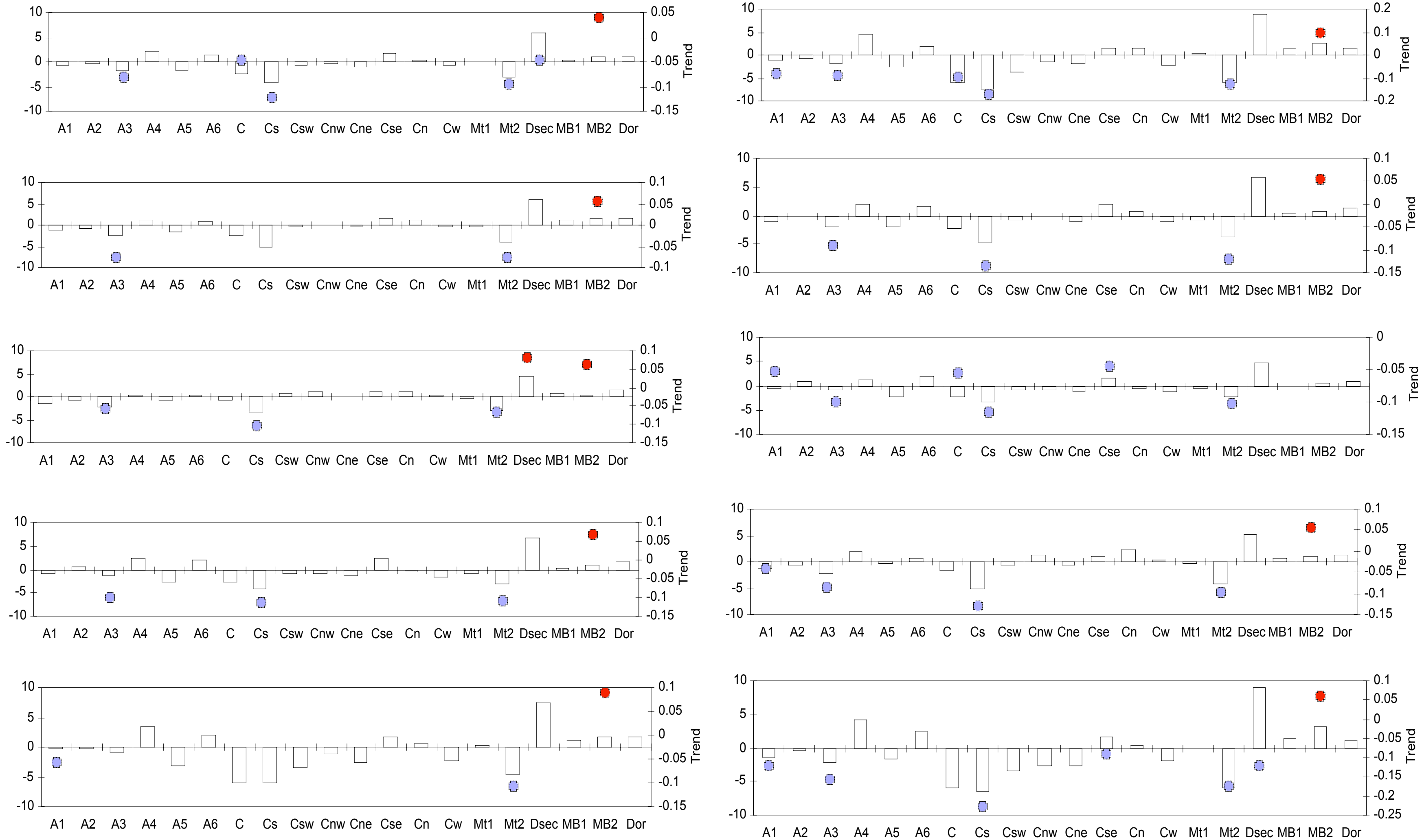

Figure 12d. Anomalies (__-bars) and trend of maximum Temperature (positive trends with red circles and negative trends with blue circles) by circulation type in the case of Autumn at SLP (1958-2000). Only the stat. signif. ones at a level 0.05 are marked

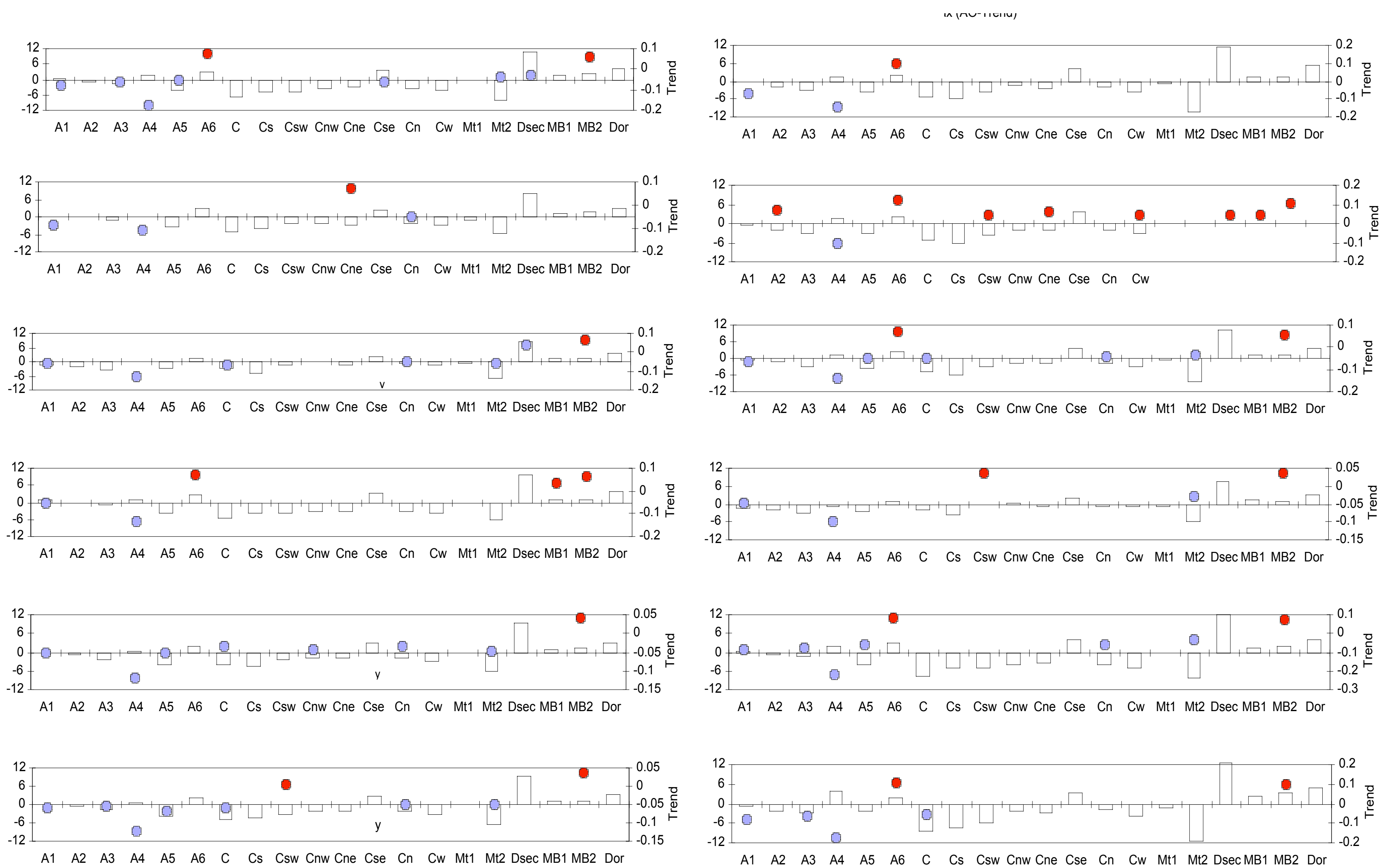

Figure 12e. Anomalies (__-bars) and trend of maximum Temperature (positive trends with red circles and negative trends with blue circles) by circulation type in the case of Year at SLP (1958-2000). Only the stat. signif. ones at a level 0.05 are marked

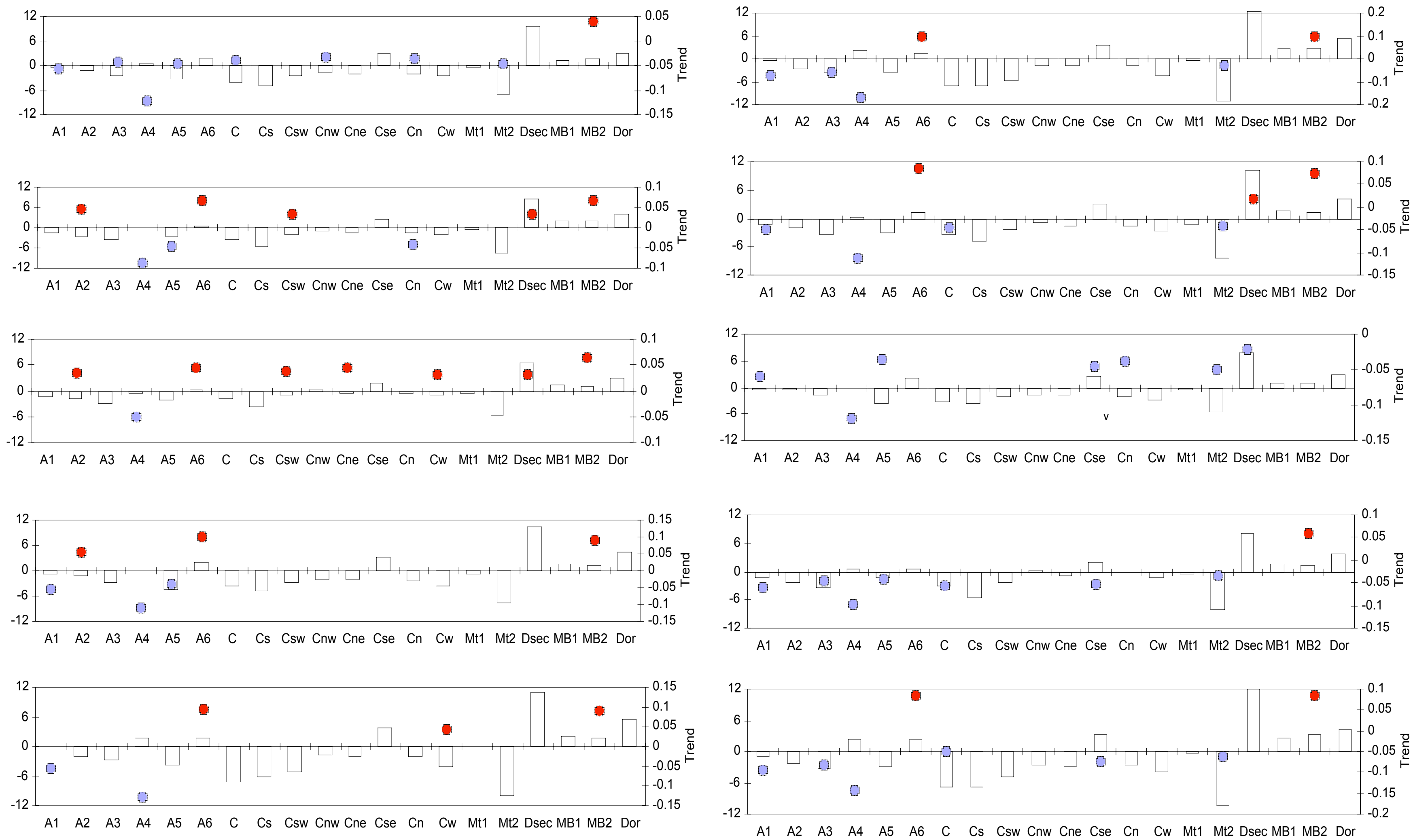

Figure 12e. Anomalies (__-bars) and trend of maximum Temperature (positive trends with red circles and negative trends with blue circles) by circulation type in the case of Year at SLP (1958-2000). Only the stat. signif. ones at a level 0.05 are marked

Table 1. Mean max cc between the precipitation amount and every isobaric surface and thickness

	Year		Winter		Spring		Summer		Autumn	
	Mean (+)	**Mean(-)**	**Mean (+)**	**Mean(-)**	**Mean (+)**	**Mean(-)**	**Mean (+)**	**Mean(-)**	**Mean (+)**	**Mean(-)**
300hPa	0.26	-0.47	0.39	-0.63	0.30	-0.55	0.39	-0.46	0.39	-0.34
500hPa	0.27	-0.49	0.39	-0.65	0.30	-0.54	0.40	-0.39	0.36	-0.35
700hPa	0.30	-0.48	0.36	-0.66	0.30	-0.51	0.41	-0.33	0.34	-0.35
850hPa	0.33	-0.47	0.36	-0.65	0.32	-0.45	0.41	-0.27	0.32	-0.34
1000hPa	0.36	-0.51	0.37	-0.65	0.35	-0.42	0.42	-0.27	0.32	-0.36
SLP	0.35	-0.51	0.37	-0.65	0.36	-0.42	0.42	-0.27	0.32	-0.36
1000-700hPa	0.44	-0.48	0.52	-0.50	0.38	-0.50	0.39	-0.44	0.39	-0.34
1000-500hPa	0.40	-0.47	0.50	-0.52	0.35	-0.51	0.38	-0.46	0.38	-0.31
700-500hPa	0.38	-0.46	0.47	-0.54	0.31	-0.51	0.38	-0.47	0.38	-0.32
500-300hPa	0.32	-0.39	0.38	-0.53	0.32	-0.49	0.36	-0.43	0.36	-0.29

Table 2. Mean max cc between the minimum temperature and every isobaric surface and thickness

	Year		Winter		Spring		Summer		Autumn	
	Mean (+)	Mean(-)	Mean (+)	Mean(-)	Mean (+)	Mean(-)	Mean (+)	Mean(-)	Mean (+)	Mean(-)
300hPa	0.47	-0.42	0.58	-0.57	0.58	-0.38	0.60	-0.26	0.57	-0.47
500hPa	0.41	-0.44	0.59	-0.58	0.55	-0.38	0.55	-0.27	0.53	-0.48
700hPa	0.38	-0.46	0.54	-0.59	0.47	-0.38	0.44	-0.29	0.47	-0.50
850hPa	0.38	-0.48	0.45	-0.59	0.37	-0.39	0.32	-0.34	0.45	-0.52
1000hPa	0.35	-0.52	0.40	-0.60	0.33	-0.42	0.31	-0.42	0.47	-0.54
SLP	0.36	-0.52	0.40	-0.60	0.33	-0.43	0.34	-0.44	0.47	-0.55
1000-700hPa	0.63	-0.30	0.72	-0.48	0.68	-0.38	0.66	-0.26	0.73	-0.44
1000-500hPa	0.61	-0.35	0.70	-0.51	0.67	-0.38	0.66	-0.26	0.69	-0.44
700-500hPa	0.58	-0.40	0.66	-0.52	0.66	-0.38	0.62	-0.27	0.60	-0.42
500-300hPa	0.55	-0.40	0.57	-0.53	0.59	-0.36	0.55	-0.29	0.61	-0.42

Table 3. Mean max cc between the maximum temperature and every isobaric surface and thickness

	Year		Winter		Spring		Summer		Autumn	
	Mean (+)	Mean(-)	Mean (+)	Mean(-)	Mean (+)	Mean(-)	Mean (+)	Mean(-)	Mean (+)	Mean(-)
300hPa	0.51	-0.49	0.62	-0.54	0.71	-0.45	0.67	-0.43	0.61	-0.54
500hPa	0.39	-0.51	0.58	-0.56	0.72	-0.46	0.60	-0.44	0.55	-0.56
700hPa	0.32	-0.53	0.49	-0.58	0.66	-0.47	0.45	-0.46	0.46	-0.57
850hPa	0.28	-0.55	0.36	-0.60	0.54	-0.50	0.34	-0.48	0.41	-0.58
1000hPa	0.25	-0.57	0.34	-0.62	0.42	-0.53	0.32	-0.49	0.40	-0.60
SLP	0.25	-0.58	0.34	-0.62	0.40	-0.54	0.34	-0.50	0.40	-0.60
1000-700hPa	0.71	-0.29	0.77	-0.46	0.79	-0.44	0.75	-0.40	0.79	-0.50
1000-500hPa	0.68	-0.37	0.75	-0.47	0.77	-0.44	0.75	-0.41	0.74	-0.50
700-500hPa	0.63	-0.44	0.71	-0.49	0.73	-0.42	0.69	-0.42	0.65	-0.49
500-300hPa	0.62	-0.43	0.68	-0.49	0.68	-0.39	0.63	-0.44	0.65	-0.49